Removal of N,N-dimethylacetamide from Water by Adsorption

by

Bo Qiu

A thesis

presented to University of Waterloo

in fulfilment of the

thesis requirement for the degree of

Master of Applied Science

in

Chemical Engineering

Waterloo, Ontario, Canada, 2017

©Bo Qiu 2017

Author's Declaration

I hereby declare that I am the sole author of this thesis. This is a true copy of the thesis, including any required final revisions, as accepted by my examiner.

I understand that my thesis may be made electronically available to the public.

Abstract

Discharge of untreated industrial effluents containing N,N-dimethylacetamide (DMAc) is hazardous to the environment. This study explores the separation of DMAc from wastewater using adsorption on activated carbons.

In total, three types of activated carbons were investigated. The adsorption characteristics of activated carbons for the removal of DMAc from aqueous solutions were investigated through a batch sorption study. The effects of DMAc concentration in the feed, contact time and temperature on the adsorption performance were investigated. The adsorption equilibrium was described by the Langmuir isotherm. A thermodynamic evaluation of the process showed that the DMAc adsorption on activated carbon was a spontaneous exothermic process.

For the kinetic data analysis, pseudo-second-order equation was modified since the term Q_e in the kinetic equation should be the equilibrium uptake corresponding to the instantaneous DMAc concentration in the solution. In order to evaluate the rate constant k_2, sorption kinetic data was fitted with the modified pseudo-second-order equation. The calculated values of rate constant k_2, for the adsorption of DMAc on all three types of carbons, were used to the modified pseudo-second-order model to predict the kinetic data. A good comparison was observed between the experimental data and model calculations. The kinetic data was also fitted with the pseudo-first-order model and the intraparticle diffusion model which both did not show clear conformity. There were at least five adsorption-

desorption cycles, using ethanol with heating and vacuum. The uptake capacity of DMAc and adsorption/desorption kinetics remained almost the same during and after the five cycles. The rate constants were also calculated by fitting the kinetic data with the modified pseudo-second-order model.

The dynamic adsorption was studied in a packed bed column packed (using two types of activated carbon, while the third type was not viable for column operation). Experiments were performed to study the effect of the influent flow rate (0.5, 1.0 and 1.5ml/min) and regeneration of carbon bed (up to five cycles). Whereas the bed height, column diameter and amount of adsorbent packed were kept constant during this study. Carbons in the column saturated with DMAc were taken out and regenerated effectively by extracting with ethanol and the by heating and vacuum. After three consecutive cycles of adsorption and desorption, no change in the uptake capacity was observed. The bed depth service time model, the Thomas model and the Yoon-Nelson model were used to analyse the breakthrough data. The calculated values of Yoon-Nelson constants were used to predict the breakthrough curves. A good comparison was observed between experimental data and the Yoon-Nelson model calculations.

An investigation was conducted to check if the novel hollow fibre contactors could fully utilise the potential of the third type of activated carbon on adsorption of DMAc. Four types of hollow fibre contactors were made, each had some variations or modifications to the former one. Experiments were performed to study the effect of the influent flow rate (0.5 and 1.0 ml/min) while the bed height, the column diameter and the weight of activated carbon packed were kept constant during this study. The

fourth design (the last type) of the contactors had three configurations regarding the geometric arrangement of the hollow fibres. Through these different types of modules, a clear direction for further design of the hollow fibre contactors was developed.

Acknowledgements

First and foremost, my deepest gratitude and appreciation to my supervisor, Professor Dr. Xianshe Feng, for all his encouragement, valuable time and guidance for me. It was never possible to accomplish this thesis without his continuous support, attention in detail and personal involvement in all the phases of this research which enables me to develop an understanding of the subject.

I am heartily grateful to my father and mother, for their profound care and support for me. I would not be able to complete these studies without their uncompromising encouragement.

I also want to thank my grandparents, for the beliefs and enthusiasms they spread to me. Though passed away, they were among the most important people in my life who helped me to reach this stage.

There are also great gratefulness to my group colleagues and lab mates, Dihua Wu, Boya Zhang, Shuixiu Lai, Elnaz Halakoo, Henry Manston, Silu Chen, Michael Celarek, Xiao Wang and Yifeng Huang, for their selfless and memorable friendships. Best wishes for them all to have bright futures.

Dedication

I am dedicating my whole master's work to those whom I love and those who love me, to the improvement of the environment and the prosperity of mankind.

Table of Contents

List of Figures xi

List of Tables xv

Nomenclature xvii

Chapter 1: Introduction 1

1.1 Motivation and objectives 2

1.2 Thesis Outline 3

Chapter 2: A literature Review 5

2.1 Dimethylacetamide and its impact as pollutant 5

2.2 Treatment of Wastewater 7

2.2.1 Removal of DMAc from Water 7

2.2.2 Adsorption, Effective for Contaminant Removal 9

2.3 Equilibrium and Kinetic Models of Adsorption 10

2.3.1 Equilibrium Study 11

2.3.2 Kinetic Study 14

2.4 Adsorption Columns 16

2.4.1 Modelling of Column Study 19

2.5 Hollow Fibre Contactors 23

Chapter 3: DMAc Adsorption on Activated Carbons 27

3.1 Introduction 27

3.2 Thermodynamic Parameters of Adsorption 28

3.3 Experimental 30

3.3.1 Materials 30

3.3.2 Adsorption Experiments 31
3.4 Results and Discussion 34
3.4.1 Adsorption Equilibrium 34
3.4.2 Kinetic Studies 41
3.4.3 Adsorption-desorption Cycle Study 59
3.5 Conclusions 62
Chapter 4: Packed Bed Column Adsorption 63
4.1 Introduction 63
4.2 Experimental 64
4.3 Results and Discussion 66
4.3.1 Effects of Flow Rate 68
4.4 Conclusions 73
Chapter 5: Hollow Fibre Contactor for DMAc Adsorption on Activated Carbons 75
5.1 Introduction 75
5.2 Experimental 76
5.2.1 Diffusion Through Hollow Fibre Walls 76
5.2.2 Direct Flow Through the Hollow Fibre Walls 80
5.2.3 Asher Configuration 83
5.3 Results and Discussion 86
5.3.1 Diffusion Through Hollow Fibre Walls 86
5.3.2 Direct Flow Through Hollow Fibre Walls 86
5.3.3 Asher Configuration 92
5.4 Conclusions 95
Chapter 6: General Conclusions and Recommendations 96

6.1 Conclusions 96

6.2 Recommendations for Future Studies 98

References 100

Appendix A 106

Appendix B 107

Appendix C 114

Appendix D 116

Appendix E 118

List of Figures

Figure 2.1 (a) Chemical formula and (b)3D model of N,N-dimethylacetamide 5

Figure 3.1 Photographs of the three types of activated carbons used in this work 30

Figure 3.2 The setup for kinetic study and sampling: (A) activated carbons, (B) mechanical stirrer, (C) DMAc solution, (D) 2L beaker, (E) beaker lid preventing evaporation, (F) connection to motor, (G) vent for sampling, (H) cellulose acetate microfiltration membrane (0.22μm, ϕ=25mm), (I) injection filter head, (J) 5ml glass syringe, (K) water bath 32

Figure 3.3 Equilibrium profiles of DMAc adsorption on AC01, AC02 and AC03 at different temperatures 35

Figure 3.4 Linearized Langmuir isotherms for the adsorption of DMAc on AC01, AC02 and AC03 at various temperatures. 37

Figure 3.5 Van't Hoff plot of Kl vs 1/T for entropy and enthalpy change calculations of DMAc adsorption on AC01, AC02 and AC03. 40

Figure 3.6 The experimental data of DMAc adsorption kinetics on three types of activated carbon at different temperatures..... 43

Figure 3.7 The pseudo-second-order model fitting for the kinetic adsorption of DMAc on activated carbons at different temperatures 46

Figure 3.8 Fitting of the Arrhenius equation for the kinetic adsorption of DMAc on activated carbons at different temperatures 48

Figure 3.9 The experimental kinetic data of adsorbing DMAc of different initial concentrations on three types of activated carbons at 40℃ 50

Figure 3.10 Patterns of data fitted into the linear form of pseudo-second order model for the kinetic adsorption of DMAc on activated carbons at 40℃ of different initial concentrations 51

Figure 3.11 Values of the kinetic rate constant $k2$ using traditional pseudo-second order model of three types of carbon adsorbent at five different initial concentrations 56

Figure 3.12 Values of the kinetic rate constant $k2'$ using modified kinetic model (equation 3.30) of three types of carbon adsorbent at five different initial concentrations 56

Figure 3.13 Patterns of fitting curves of the modified pseudo-second order model (equation 3.30) for the kinetic adsorption of DMAc on activated carbons at 40℃ of different initial concentrations using average values of kinetic rate constant $k2'$ and comparing to the experimental data..... 58

Figure 3.14 Equilibrium adsorption uptake of DMAc on AC01, AC02 and AC03 over five cycles of regeneration at 22℃, and the fitting of Langmuir model..... 60

Figure 3.15 Kinetic profiles of DMAc adsorption on AC01, AC02 and AC03 after the first, third and fifth cycle of regeneration at 22℃, and the fitting of the modified kinetic model (equation 3.30)..... 61

Figure 4.1 The setup for column study and sampling: (A) reservoir of DMAc aqueous solution (source of feed), (B) sample/test vial, (C) packed bed of activated carbons, (D) glass cylinder column, (E) fluid flow rate controlling unit, (F) glass fibre, (G) rubber stopper, (H) valves no.1, no.2 and no.3, (I) reservoir of pure water, (X) altitude difference between the liquid levels of the reservoirs and the entrance of the adsorbent bed, (Y) bed height H, (Z) column inner diameter Ø=3/8inches. 65

Figure 4.2 Breakthrough curves for adsorption of DMAc in packed bed columns of AC01 and AC02 at different flow rates. Data fitting with the Yoon-Nelson model is also shown. 70

Figure 4.3 Breakthrough data fitting with the Yoon-Nelson model for removing DMAc from effluent exiting the packed bed columns of AC01 and AC02 at different flow rates..... 72

Figure 5.1 Setup of experimental hollow fibre contactors: (A)reservoir for pure water, (B) reservoir for DMAc solutions, (C) peristaltic pump, (D) valves no.1, no.2 and no.3. As well as three types of hollow fibre modules and the numbering of their gates..... 77

Figure 5.2 Schematic of activated carbon adsorber (a) shell side packing and (b) tube side packing 78

Figure 5.3 Schematic of how substances flow and diffuse inside a type-I hollow fibre contactor module 80

Figure 5.4 Schematic structure of hollow fibre contactor module type-II .. 81

Figure 5.5 Schematic of hollow fibre contactor module type-III 83

Figure 5.6 Schematics of (a) the sealing configurations of the hollow fibres as well as the module, (b) the flow pattern of the streams within the module, (c) the detailed structures and the sectional views of the three configurations of contactor module type-IV 85

Figure 5.7 Breakthrough curves for the removal of DMAc using hollow fibre module type-II packed with AC03 in the shell side at different flow rates . 87

Figure 5.8 Monochromatic chronologic evolution chart showing how the ink flowed through hollow fibre module type-II packed with white chalk powders in the shell side at the flow rate of 1.0ml/min 89

Figure 5.9 Breakthrough curves for the removal of DMAc monitored at the openings no.2, no.3, no.4, no.5 and no.6 of the hollow fibre module type-III packed with AC03 in the shell side at the overall flow rate of 1.0ml/min .. 90

Figure 5.10 Schematics of how the fine carbon powder AC03 packed inside the hollow fibre contactor module type-II and type-III was not fully utilised and the overall DMAc uptake was low 92

Figure 5.11 Breakthrough curves for DMAc removal using hollow fibre module type-IV (with square, triangular and spiral configuration) packed with AC03 in the shell side at various flow rates 93

Figure A.1 Calibration curve used to determine DMAc concentration in water 106

Figure B.1 Data fitting with the linearized form of the Freundlich equilibrium adsorption model for DMAc adsorption on AC01, AC02 and AC03 at different temperatures 107

Figure B.2 Data fitting with the linearized form of the pseudo-first order kinetic model for DMAc adsorption on AC01, AC02 and AC03 at different temperatures 108

Figure B.3 Data fitted to the linear form of the intraparticle diffusion kinetic model for DMAc adsorption on AC01, AC02 and AC03 at different temperatures 109

Figure B.4 Data fitting with the linearized form of the pseudo-first order kinetic model for AC01, AC02 and AC03 adsorbing DMAc solution of different initial concentrations at 40℃ 111

Figure B.5 Data fitting with the linearized form of the intraparticle diffusion kinetic model for AC01, AC02 and AC03 adsorbing DMAc solution of different initial concentrations at 40℃ 112

Figure D.1 Breakthrough data fitting to BDST model for removing DMAc from effluent exiting the packed bed columns of AC01 and AC02 at different flow rates 116

Figure D.2 Breakthrough data fitting to Thomas model for removing DMAc from effluent exiting the packed bed columns of AC01 and AC02 at different flow rates. 117

Figure E.1 Illustration of how the hollow fibre contactor modules were constructed, (a) using adhesives, (b) using tees. 118

List of Tables

Table 2.1 Advantages and disadvantages of organic pollutant removal methods 8

Table 3.1 Three types of activated carbons 30

Table 3.2 Parameters of the Langmuir adsorption model and Gibbs free energy (ΔG) for the adsorption of DMAc on three types of activated carbons at different temperatures. 38

Table 3.3 ΔH and ΔS, calculated from the Van't Hoff equation with a temperature range of 22~60℃ for the adsorption of DMAc on all types of activated carbons. 40

Table 3.4 Experimental data and parameters calculated from pseudo-second order kinetic model for the adsorption of DMAc on activated carbons at an initial DMAc concentration of 1000mg/L 47

Table 3.5 Activation energy for DMAc adsorption on activated carbon .. 48

Table 3.6 Parameters of pseudo-second-order kinetic model for the adsorption of DMAc on activated carbons. Temperature 40℃ 52

Table 3.7 Values of modified kinetic rate constant $k2$ calculated from data fitting to equation 3.30 for the adsorption of DMAc on all activated carbons with different initial solution concentrations. (T, V, m, $Qmax$ and Kl are also presented) 55

Table 3.8 The Langmuir model parameters ($Qmax$ and Kl) and modified pseudo-second-order model parameters ($k2'$) of DMAc adsorption on activated carbons. 59

Table 4.1 Maximum saturation capacity of activated carbon packed bed column at different influent flow rate with constant DMAc concentration (1000mg/L). (Bed height = 10cm, Diameter = 0.35cm, mass of carbon = 0.8g) 69

Table 4.2 Parameters of Thomas model, BDST model and Yoon-Nelson model calculated from breakthrough data fitting. 73

Table 5.1 DMAc uptakes at saturation in hollow fibre contactor modules type-II and type-III packed with AC03 when DMAc in effluent were completely broken through, at inflow rate of 1.0ml/min 94

Table B.1 Correlation coefficients R^2 of the fitting kinetic experimental data with the pseudo-first order model 110

Table B.2 Correlation coefficients R^2 of the fitting kinetic experimental data with the intraparticle diffusion model 110

Table B.3 Correlation coefficients R^2 of the fitting kinetic experimental data with the pseudo-first order model 113

Table B.4 Correlation coefficients R^2 of the fitting kinetic experimental data with the intraparticle diffusion model 113

Table C.1 Checklist of the coefficients for calculating superficial velocity ε in packed bed column operations [62] 114

Nomenclature

A	Adsorbance
b	Langmuir adsorption constant, (L/mol)
C	Sampled concentration of adsorbate in solution, (mol/L)
C_0	Initial concentration of adsorbate in solution, (mol/L) or (mg/g)
C_e	Equilibrium concentration of adsorbate in solution, (mol/L) or (mg/g)
C_b	Effluent concentration at breakthrough, (mol/L)
C_s	Concentration of standard reference solution, (mol/L)
C_m	Maximum equilibrium capacity in bed, (mol/g)
c	Boundary layer effect, (mol/g)
F	Effluent Flow rate, (L/min)
ΔG	Gibbs free energy, (kJ/mol)
h	Bed height in adsorption column, (cm)
ΔH	Enthalpy change of adsorption, (kJ/mol)
ΔS	Entropy change of adsorption, (J/mol·K)
E_a	Activation energy, (kJ/mol)
K_f	Freundlich adsorption constant, (L/mol$^{1-\frac{1}{n}}$·g)
K_l	Langmuir adsorption constant, (L/mol)
k_A	Adsorption rate constant for Adams-Bohart model, (L/mol·min)
k_B	Adsorption rate constant for BDST model, (L/mol·min)
k_{Th}	Adsorption rate constant for Thomas model, (L/mol·min)
k_{YN}	Adsorption rate constant for Yoon-nelson model, (min^{-1})
k_d	Kinetic rate constant for desorption, (g/mol·min)
k_i	Intraparticle diffusion rate constant, (mol/g·min$^{1/2}$) or (mg/g·min$^{1/2}$)
k_1	Pseudo-first order rate constant, (min^{-1})
k_2	Pseudo-second order rate constant, (g/mol·min)
m	Mass of adsorbent, (g)
N_0	Saturation concentration of effluent, (mol/L)

$1/n$	Heterogeneity factor
θ_e	Fraction of surface of adsorbent covered at equilibrium
a_e	Activity of the adsorbate in solution at equilibrium
Q_e	Adsorbate uptake at adsorption equilibrium, (mol/g) or (mg/g)
Q_m	Adsorbate uptake at adsorption saturation, (mol/g) or (mg/g)
Q_t	Adsorbate uptake at time of sampling, (mol/g) or (mg/g)
Q_0	Maximum solid phase concentration for Thomas model, (mol/g)
R	Universal gas constant, (J/mol·K)
S_c	Cross sectional area of adsorption column, (cm^2)
T	Temperature, (K) or (°C)
t	Time, (min)
t_b	Service time at breakthrough, (min)
u	Linear flow rate of effluent, (cm/min)
V	Volume of effluent solution in adsorption process, (L) or (ml)

Greek symbols

β	Kinetic coefficient of external mass transfer, (L/min)
γ_e	Activity coefficient at adsorption equilibrium

Abbreviations

DMAc	N,N-Dimethylacetamide
AC	Activated carbon
BDST	Bed depth service time model
HF	Hollow fibre
TOC	Total organic carbon
YN	Yoon-Nelson model

Chapter 1: Introduction

Chemistry and pharmacy have been playing important roles in the development of our modern civilisation during the past centuries, while on the other hand, they may have caused some problems to our habitable environment as well. Humans are actually pouring a tremendous amount of hazardous organic chemicals into our surroundings while trying to make better living. The life cycle of organic compounds often begins in chemical and pharmaceutical industry and ends with wastewater disposal into natural water systems.

If these hazardous substances are sufficient to environmental pollution, it is a serious challenge to eliminate them. N,N-dimethylacetamide (DMA or DMAc) is one of the chemicals extensively used for various applications. The concentration of DMAc in the environment must be under a certain level, appropriate for the physical condition of the organisms in our environment. However, people around the world have not been paying enough attention to the discharge and emission of DMAc comparing to other toxic chemicals. As a consequence, the measures taken to control DMAc pollution are very limited. Adsorption is one of the most promising methods for processing wastewater containing DMAc.

1.1 Motivation and objectives

In recent studies, DMAc has been found to possess complicated toxicity to living organisms, and a mature process has not yet been developed to eliminate this threat. Protection of ground water and marine water is a complex issue and a vital public concern. Once contaminated, it will be technically difficult and enormously expensive to purify. One way to protect these waters from contamination is through the control of industrial discharges. Often, though, pollution control processes are not adequate in treating high flow rates or those with relatively low contaminant concentrations. This project deals with an adsorption process for removing DMAc from industrial wastewater. The proposed adsorption process has several advantages: eco-friendly activated carbon was used as an adsorbent, continuous adsorption-desorption cycles, and a high efficiency for DMAc removal from water.

Activated carbons are excellent adsorbents for a large number of pollutants. Their industrial applications involve the adsorptive removal of colour, odour, taste and other undesirable organics and inorganics from drinking water and wastewater. Numerous physicochemical factors affect adsorption process, including the interaction between the adsorbate and adsorbent, activated carbon surface area and pore structure, activated carbon surface chemistry, the effect of other components, characteristics of the dye molecule, activated carbon particle size, pH, temperature, contact time etc. Due to its unique molecular structure, activated carbon has an extremely high affinity for organic molecules, including DMAc.

The unit operation of fluid-particle contact and interaction is the basis of many adsorption separations. The mass transfer rate for adsorption, and pressure drop of the fluids in the contactor are critical to the process performance. Among the different fluid-particle contactor configurations, hollow fibre contactors, which are derived from module development in

membrane separation technology, have been recently developed as an alternative to the conventional designs of fluid-particle contactors. These novel contactors allow the use of minuteparticles (e.g. activated carbon powders) to enhance mass transfer without giving rise to a high pressure drop for the fluids.

In this project, three representative activated carbons were chosen for separating DMAc from water. These activated carbons are widely utilised in wastewater treatment research. The kinetic and equilibrium studies of DMAc adsorption on activated carbons were carried out, and the information generated would prove activated carbon as a potential adsorbent for practical application. A variety of architectures of hollow fibre arrangements were tested to find out the optimal design of the adsorption module. The major objectives of this research were:

- To investigate the sorption isotherm and kinetics involved in the removal of DMAc by activated carbons, and to identify appropriate adsorption kinetics and equilibrium models for these systems.
- To examine the reusability of activated carbon for adsorption of the DMAc after regeneration of the sorbent exhausted with the DMAc adsorbate.
- In order to scale up the adsorption process, column study was conducted to determine the dynamic parameters related to breakthrough.
- To investigate the performance of hollow fibre contactors and to find out their best configuration for capturing DMAc on activated carbon.

1.2 Thesis Outline

The first chapter is an introduction to and background about DMAc as a chemical solvent and its impacts on the environment if discharged as a

hazardous material. The sorbents that can be used for the separation of DMAc from waste water was also discussed.

The literature relevant to this research was reviewed in Chapter 2. It involved a critical review of the adsorbents commonly used for organic compound removal, adsorption models, experimental procedures and analytical techniques reported in the literature by different researchers.

In the Chapter 3, several types of activated carbons were selected in adsorption studies, and the equilibrium and kinetics of the DMAc adsorption on activated carbon were investigated. Chemical regeneration of the activated carbon was also carried out by using methanol. Once it was found that activated carbon worked well for the adsorption of DMAc particles and could also be regenerated for the following cycles of adsorption, the work continued with dynamic column adsorption, which was described in the fourth chapter. Breakthrough curves were determined experimentally and the breakthrough data were fitted to empirical models.

In the Chapter 5, hollow fibre contactors were studied to take advantages of the powder-form carbons efficiently. Four different designs of hollow fibre contactor modules were tested, and their performance was analysed and evaluated.

Chapter 2: A literature Review

N,N-Dimethylacetamide (DMAc) is an organic compound with the formula $CH_3C(O)N(CH_3)_2$. Its structure is shown in Figure 2. This colourless, water-miscible, high boiling liquid is commonly used as a polar solvent in organic synthesis. DMAc is miscible with most other solvents, although it is poorly soluble in aliphatic hydrocarbons.[1]

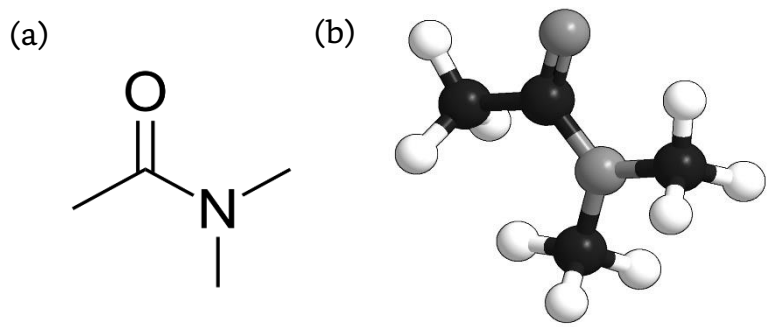

Figure 2.1 *(a) Chemical formula and (b)3D model of N,N-dimethylacetamide*

2.1 Dimethylacetamide and its impact as pollutant

DMAc is prepared by the reaction of dimethylamine with acetic anhydride and esters of acetic acid. Dehydration of the salt of dimethylamine and acetic acid also furnishes this compound[2]:

$$CH_3CO_2H{\cdot}HN(CH_3)_2 \rightarrow H_2O + CH_3CON(CH_3)_2$$

The chemical reactions of dimethylacetamide are typical of N,N-disubstituted amides. It will hydrolyse in the presence of acids:

$$CH_3CON(CH_3)_2 + H_2O + HCl \rightarrow CH_3COOH + (CH_3)_2NH_2 + Cl^-$$

DMAc reacts with acids, but is resistant to bases. For this reason, DMAc is a useful solvent for reactions involving such strong bases as sodium hydroxide. DMAc is commonly used as a solvent for fibres and membranes (e.g., polyacrylonitrile, spandex, etc.) or in the adhesive industry. It is also employed as a reaction medium in the production of pharmaceuticals and plasticisers. DMAc is also widely used as an excipient in drugs, e.g. in Vumon (teniposide), Busulfex (busulfan) or Amsidine (amsacrine).[3] In some special circumstances, DMAc is applied as high-performance refrigerant adsorbent.[4]

In many cases, the waste streams containing DMAc from different applications are disposed directly into the environment without any treatment, mainly because of the lack of corresponding regulations and laws about DMAc disposal. The first regulation on DMAc emission formally became effective in 2014[5], and the first in the USA was put into force by FDA in 2015, with both of them requiring further detailed amendments.

With regards to its toxicity, DMAc is a medium potency reproductive toxicant, classified by the European Chemical Agency as “toxic for reproduction, category 1B”.[5] The presence of DMAc in drinking water may damage fertility or the unborn child. It is also harmful to inhale or to contact with skin, and serious eye irritations may result if exposed to DMAc. DMAc is able to penetrate human skin and gastrointestinal mucosa very easily.[6]

Despite its toxic effects, DMAc has been used widely for a broad scope of applications. However proper treatment of DMAc-containing wastewater has attracted significant attention more recently, partly because some earlier studies falsely showed that DMAc toxicity was somehow negligible, and this issue is being revisited carefully.[7]

2.2 Treatment of Wastewater

There are numerous methods to treat DMAc bearing effluents. In spite of the availability of many techniques to remove organic contaminants from wastewaters (e.g. coagulation, chemical oxidation, membrane separation, electrochemical and aerobic and anaerobic microbial degradation), all these methods have inherent limitations.[8]

2.2.1 Removal of DMAc from Water

In general, many technologies are available to remove organic pollutants. Some of which are very mature and have been applied for decades, while some others are still under development. These technologies can be divided into three general categories: physical, chemical and biological. These methods have their own advantages and disadvantages as illustrated in Table 2.1, where various methods for organic pollutant removal are compared.[9][10]

Table 2.1 Advantages and disadvantages of organic pollutant removal methods

	Advantages	Disadvantages
Chemical treatments		
Oxidative process	Simplicity of application	Needs to be activated by some special agents
H_2O_2 + Fe(II) salts (Fenton's reagent)	Fenton's reagent is a suitable chemical means	Sludge generation
Ozonation	Ozone can be applied in its gaseous state and does not increase the volume of wastewater and sludge	Short half-life (20 min)
Photochemical	No sludge is produced and foul odours are greatly reduced	Formation of by-products
Sodium hypochlorite (NaOCl)	Initiates and accelerates azo-bond cleavage	Release of aromatic amines
Electrochemical destruction	No consumption of chemicals and no sludge build-up	Relatively high flow rates cause a direct decrease in DMAc removal
Biological treatment		
Destruction by fungi	Some species of fungi can degrade DMAc using enzymes	Enzyme production has also been shown to be unreliable
Other microbial cultures (mixed bacterial)	Decolourised in 24-30h	Under aerobic conditions, DMAc is not readily metabolised
Adsorption by living/dead microbial biomass	Certain microbial species have a particular affinity for binding with DMAc molecules	The performance is not stable under different conditions
Physical treatments		
Adsorption	Good removal by a wide variety of adsorbents	Some adsorbents are expensive
Membrane filtration	Highly controllable	Concentrated sludge production
Irradiation	Effective oxidation at lab scale	Requires a lot of dissolved oxygen
Electrokinetic coagulation	Economically feasible	High sludge production

2.2.2 Adsorption, Effective for Contaminant Removal

The term "adsorption" refers to the accumulation of a substance onto a solid surface from liquid or gas. The substance that accumulates at the liquid-solid or gas-solid interface is called adsorbate, and the solid on which adsorption occurs is adsorbent. Adsorption can be classified into two types: chemical sorption and physical sorption. Chemical adsorption or chemisorption is characterised by the formation of strong chemical associations between the molecules (or ions) of the adsorbate to the adsorbent surface, due to the exchange of electrons, and thus chemical sorption is generally irreversible in many cases. Physical adsorption or physisorption is characterised by weak Van der Waals bonds between adsorbate and adsorbent, thus the sorption-desorption process is reversible in most cases. The main forces inducing adsorption are Van der Waals forces, hydrogen bonds, polarity, dipole-dipole π-π interaction. Adsorption is attractive for the treatment of polluted water, especially if the sorbent is inexpensive and does not require an additional pre-treatment before use.[11] For environmental remediation purposes, adsorption techniques are widely used to remove various chemical contaminants from water, especially those that are ineffective with conventional biological treatments. Adsorption competes favourably with other techniques in terms of process flexibility, simplicity of design, capital cost, insensitivity to toxic pollutants and easiness of operation. Factors that influence adsorption efficiency include adsorbate–adsorbent interaction, adsorbent surface area, adsorbent to adsorbate ratio, adsorbent particle size, operating temperature, effluent pH (if liquid) and liquid-adsorbent contact time.[12]

Among the various adsorbents, activated carbons (ACs) are of particular interest. For a long time, activated carbons have been used as an adsorbent processing textile and dye wastewater. activated carbon is probably the most versatile adsorbent because of its large surface area,

polymodal porous structure, high adsorption capacity and variable surface chemical composition. In addition, activated carbons have also been used as supports in catalytic reactions, and their use as catalysts on their own (especially due to their surface oxygen groups) is growing quickly, even in dye removal processes. What furthermore makes activated carbons attractive to facilitate wastewater treatment is the possibility of tailoring their physical and/or chemical properties in order to optimise their performance.[13]

Activated carbons (ACs) themselves are excellent adsorbents for a large number of contaminants. Their industrial applications involve the adsorptive removal of colour, odour, taste due to undesirable organics and inorganics from drinking water and wastewater. Due to its unique molecular structure, activated carbon has an extremely high affinity to organic compounds.[14]

2.3 Equilibrium and Kinetic Models of Adsorption

Adsorption equilibrium studies are important to determine the efficacy of adsorption. In addition, it is also necessary to identify the adsorption mechanism. Kinetic models can be exploited to investigate the mechanism of adsorption and its potential rate-controlling steps Adsorption kinetics is expressed as the solute removal rate. In practice, kinetic studies are often carried out in batch systems at various initial sorbate concentrations, sorbent doses, particle sizes, agitation speeds, pH values and temperatures along with different sorbent and sorbate types. Then data regression is used to determine the best-fitting kinetic rate equation. The linear least-square method is usually applied to the linearly-transformed kinetic rate equations for fitting to the experimental data to determine the rate constant. To understand the adsorption kinetics and rate-limiting step, several kinetic models have been proposed in the

literature. Examples include the pseudo-first-order and pseudo-second-order rate models, the Weber and Morris sorption kinetic model, the Adam–Bohart-Thomas relation, the first-order reversible reaction model, the external mass transfer model, the first-order equation of Bhattacharya and Venkobachar Elovich's model and Ritchie's equation. The pseudo-first-order and pseudo-second-order kinetic models are the most widely accepted models to study the adsorption kinetics of compounds.

2.3.1 Equilibrium Study

Adsorption is considered to be a fast physical or chemical process, and its rate is governed by the type of the process. It can be defined as a general term for a number of processes for passive accumulation, which in any particular case may include ion exchange, coordination, complexation, chelation, adsorption and micro-precipitation. Proper analysis and design of an adsorption separation process requires relevant knowledge of adsorption equilibria. In equilibrium, there is a certain relationship between the solute concentration in the solution and the adsorbed state (i.e., the amount of solute adsorbed per unit mass of adsorbent). The sorption equilibrium is a function of temperature. The adsorption equilibrium relationship at a given temperature is referred as adsorption isotherm. Several models for adsorption isotherms originally used for gas adsorption are available, and they may be readily adopted to correlate the adsorption equilibria for DMAc adsorption. Some important examples are Freundlich, Langmuir, Redlich–Paterson and Sips equations. The most commonly used among them are the Freundlich and the Langmuir equations. The application of these isotherm equations on adsorbent-assisted DMAc removal from water and wastewater will be discussed later.

2.3.1.1 Freundlich Model

The Freundlich isotherm model is an empirical equation. That is able to describe the adsorption of organic and inorganic compounds on a large variety of adsorbents. This equation is in the form of:

$$Q_e = K_f C_e^n \tag{2.1}$$

which can also be expressed in the linearized form:

$$lnQ_e = lnK_f + nlnC_e \tag{2.2}$$

where Q_e (mol/g) is the adsorbate uptake at adsorption equilibrium, K_f ($\mathrm{L/mol^{1-\frac{1}{n}} \cdot g}$) is the Freundlich adsorption constant, C_e (mol/L) is the equilibrium concentration of adsorbate in solution, n is the adjustment constant for a given pair of adsorbate and adsorbent.

A plot of lnQ_e versus lnC_e has a slope equal to 1/n and an intercept of lnK_f. lnK_f is equivalent to lnQ_e when C_e equals to unity. The value of K_f depends on the units of Q_e and C_e used. On average, a favourable adsorption tends to have Freundlich constant n between 1 and 10. A larger value of n (that is, a smaller value of $1/n$) indicates stronger interaction between adsorbent and the adsorbate, while $1/n$ equal to 1 indicates a special case of linear adsorption where there are identical adsorption energies for all sites. The Freundlich isotherm has the ability to fit to many experimental adsorption–desorption data, and is especially excellent to fit to the data for highly heterogeneous sorbent systems. However, in some cases the Freundlich isotherm is not suitable for adsorption.

2.3.1.2 Langmuir Model

Another commonly used model for adsorption equilibrium is the Langmuir model. The Langmuir equation describes the relationship of the coverage of molecules on a solid surface and the concentration of a sorbate at a given temperature. This isotherm is based on three assumptions: (1) the adsorption is limited to monolayer coverage on the adsorbent surface, (2) all surface sites are alike and each site can only accommodate one adsorbed molecule, and (3) the ability of a molecule to be adsorbed on a given site is independent of whether its neighbouring sites are occupied or not. At adsorption equilibrium, the rates of adsorption to the solid surface and

desorption from the surface are equal. The Langmuir equation can be written as:

$$Q_e = Q_{max} \frac{C_e K_l}{C_e K_l + 1} \tag{2.3}$$

where Q_{max} (mol/g) is DMAc uptake at adsorption saturation, and K_l (L/mol) is the Langmuir adsorption constant.

The equation can also be written in different linear forms ($\frac{1}{Q_e}$ vs $\frac{1}{C_e}$ and Q_e vs $\frac{Q_e}{C_e}$):

$$\frac{1}{Q_e} = \frac{1}{Q_{max}} + \frac{1}{C_e Q_{max} K_l} \tag{2.4}$$

$$Q_e = Q_{max} - \frac{1}{K_l} \frac{Q_e}{C_e} \tag{2.5}$$

In adsorption, the saturation limits for various adsorbates are affected by the number of sites in the adsorbent material, the accessibility of the adsorption sites, the chemical state of the sites (i.e., availability), and the affinity between the sites and sorbate molecule (i.e., binding strength). In the case of covalent bonding, supposing that an occupied site is available, the extent to which the site is to be dwelled upon by a given substance depends on the binding strength and concentration of that substance relative to the molecules already occupying that site.

A decrease in K_l value with an increase in temperature signifies exothermicity of the adsorption process (physical adsorption), while the opposite trend indicates that the process needs thermal energy (endothermic), which is often relevant to chemisorption. In physical adsorption, the bonding between the sorbate molecules and the active sites of the adsorbent becomes weaker at higher temperatures, in contrast to chemisorption bonding which becomes stronger. The exothermicity or endothermicity of the adsorption is a thermodynamic property commonly determined using the Van't Hoff equation, which relates the equilibrium adsorption constant to the temperature.

2.3.2 Kinetic Study

Adsorption is not a single step process. It involves the transport of the adsorbate molecules from the aqueous phase to the surface of the solid adsorbent, followed by the diffusion of these solute molecules into the interior of the adsorbent. The overall adsorption process may be controlled by one or more steps, such as film or external diffusion, pore diffusion, surface diffusion, and adsorption on the pore surface, or a combination of more than one steps. To understand the significance of diffusion mechanism, accurate estimates of the diffusivities of the sorbate molecules in sorbent must be determined using diffusion-controlled kinetic models based on the experimental data. Due to the porosity of the specific adsorbent, intraparticle diffusion is expected in the kinetics of an adsorption process. In order to the mechanisms and the rate controlling steps, the kinetic data may be fitted with the intraparticle diffusion model proposed by Weber and Morris in 1962.[15] The intraparticle diffusion model is commonly expressed by the following equation:

$$Q_t = k_i\sqrt{t} + c \tag{2.6}$$

where c (mol/g) is a constant that gives information about the boundary layer effect, and k_i (mol/g·min$^{1/2}$) is the intraparticle diffusion rate constant. If the intraparticle diffusion is dominant in the adsorption process, then a plot of the sorption uptake Q_t versus the square root of time will result in a straight line with an intercept c that reflects the boundary layer effect on adsorption. The larger the intercept is, the greater the contribution of the surface sorption will be in controlling the adsorption rate. If the line passes through the origin (i.e. $c = 0$), the intraparticle diffusion will be the dominating rate controlling step. The intraparticle rate constant k_i can be evaluated from the slope of the linear plot of Q_t versus $\sqrt{t}$. When the intraparticle diffusion model is fitted to the kinetic data, if the Q_t vs $\sqrt{t}$ plot exhibits multi-linear plots which do not pass through the origin, it is indicative of some degrees of boundary layer effects, and this further

shows that the intraparticle diffusion is not the only rate-controlling step, and other steps (e.g., surface reaction, external boundary layer effects) may also affect the rate of sorption significantly.[16]

In previous studies, the intraparticle diffusion model has been applied in three different forms:

1) Q_t (the amount of adsorption t) is plotted against $\sqrt{t}$ (the square root of time) to get a straight line that is forced to pass through the origin.
2) Multi-linearity in Q_t versus $\sqrt{t}$ plot is considered (that is, two or three steps are considered to be involved the whole adsorption process). In this form, the external surface adsorption or instantaneous adsorption occurs in the first step; the second step is the gradual adsorption step, where intraparticle diffusion is controlled; and the third step is the final equilibrium step, where the solute moves slowly from larger pores to micro pores causing a slow adsorption rate. The time required for the second step usually depends on the variations of the system (including solute concentration, temperature, and adsorbent particle size), and thus it is difficult to predict or control
3) Q_t is plotted against $\sqrt{t}$ to obtain a straight line but does not necessarily pass through the origin; that is, there is a non-zero intercept. Almost all the intercepts reported in the literature are positive, indicating that rapid adsorption occurs within a short period of time.

The experimental kinetics data can also be analysed by using other kinetic models. The most commonly used ones are the pseudo-first-order equation and the pseudo-second-order equation, in order to determine whether adsorption is limited by chemical complexation or not. The original form of pseudo-first order reaction model equation is:

$$\frac{dQ_t}{dt} = k_1(Q_e - Q_t) \tag{2.7}$$

and that of the pseudo-second order reaction model equation is:

$$\frac{dQ_t}{dt} = k_2(Q_e - Q_t)^2 \tag{2.8}$$

where t is the time (min), Q_t and Q_e (mol·g^{-1}) are the quantities of the sorbate on the adsorbent at time t and at equilibrium, respectively. k_1 (min^{-1}) and k_2 (g·mol^{-1}·min^{-1}) are the adsorption rate constants based on the pseudo-first-order and pseudo-second-order adsorption, respectively. To evaluate k_1, equation 2.6 can be rearranged as follows:

$$log(Q_e - Q_t) = logQ_e - \frac{k_1}{2.303}t \tag{2.9}$$

Thus, a plot of $log(Q_e - Q_t)$ vs t will be a straight line with a slope equal to $-\frac{k_1}{2.303}$ and an intercept equal to the $logQ_e$. However, if the intercept does not equal to the equilibrium uptake of the sorbate, the adsorption is not likely to obey pseudo-first-order kinetics even if this plot has a high correlation coefficient with the experimental data. For the pseudo-second-order, kinetics equation 2.7 can be transformed into:

$$\frac{t}{Q_t} = \frac{1}{k_2 Q_e^2} + \frac{t}{Q_e} \tag{2.10}$$

A plot of $\frac{t}{Q_t}$ vs t will be a straight line with a slope of $\frac{1}{Q_e}$ and an intercept of $\frac{1}{k_2 Q_e^2}$. Hence, we can obtain k_2 from the intercept and slope of the $\frac{t}{Q_t}$ vs t plot.

2.4 Adsorption Columns

Adsorption processes can be performed under a batch or continuous mode, and a continuous adsorption process is preferred for practical applications. The same adsorption column can be utilised for adsorption-desorption cycle studies.

There is little research on adsorption of DMAc by ACs, and very few closely related articles are available. Several papers reporting adsorption of other organic compounds on activated carbons are referenced in this case.

Spahn et al.[17] used activated carbons for dynamic adsorption of a variety of organic pollutants in wastewater, and the continuous adsorption column data were fitted with the fixed bed model and reduced lumped diffusion mode. By varying the column heights and the flow rates of effluent, the adsorption rate and the breakthrough curves were analysed based on the models. In the initial period of adsorption, the solute removal was fast. With the passage of time, the adsorption bed got saturated gradually and the removal rate gradually began to decrease. This was due to the decrease in the driving force for adsorption. The breakthrough data was evaluated using the fixed bed model and reduced lumped diffusion model, and the model predictions had a w agreement with the experimental data. It was observed that both models could predict the column dynamics well at high effluent flow rates.

Pond mud and other similar sediments have been employed as a sorbent for the removal of organic compounds.[18] Though most of the work has been carried out in batch mode in order to investigate the adsorption kinetics, the equilibrium and thermodynamics of the adsorption process and the column study part was very brief.

Han et al.[19] studied a column adsorption system using a fixed-bed column packed with phoenix tree leaf powders as adsorbent for the removal of methylene blue from aqueous solutions. The effects of flow rate, influent concentration and bed depth on the adsorption characteristics was investigated at pH 7.4. The breakthrough curves were shown to be dependent on the flow rate, the initial concentration of the dye and the bed depth. Four kinetic models, the Thomas, the Adams–Bohart, the Yoon–Nelson and the Clark models, were applied to describe the experimental data to predict the breakthrough curves. Nonlinear regression was used to determine the characteristic parameters of the packed column that are useful for process design and scale up. In addition, the bed-depth service time analysis (BDST) model was used to study the effects of bed depth on the

adsorption breakthrough and to predict the time needed for breakthrough at other conditions. The Thomas and Clark models were found satisfactory for the description of the whole breakthrough curve, while the Adams–Bohart model was only used to predict the initial part of the dynamic process. A in good agreement between the experimental data and the BDST model calculations was obtained. It was concluded that the leaf powder column can be used in wastewater treatment.

Zhang et al.[20] also studied the elimination of methylene blue in a fixed-bed column, packed with carboxymethyl straw as an adsorbent material. The straw based adsorbent showed a high methylene blue uptake in the packed column. Various column models were also employed to fit to the experimental data. Among these, the Thomas model was found to be the most suitable to describe the adsorption behaviour, which is based on the monolayer chemical adsorption mechanism. The effects of initial solution concentration and pH, bed height, temperature, and the flow rate on the column adsorption performance were studied in detail based on the Thomas model. It was found that these operating conditions greatly affect the breakthrough curves, except for temperature which had little influence on the adsorption of methylene blue on the modified straw.

Li et al.[21] used activated carbons treated with nitric acid as adsorbents for the removal of methylene blue from aqueous solutions. The adsorbents were characterised by N_2 adsorption-desorption isotherms, infrared spectroscopy, particle size, and zeta potential measurements. Batch adsorption experiments were carried out to study the effects of solution pH and contact time on the dye adsorption performance. The kinetics studies showed that the adsorption data followed a pseudo-second-order kinetic model, and equilibrium adsorption data followed the Langmuir isotherm model. Though this paper did not show details about column study, the features of both the isotherm and kinetic models of activated carbons adsorbing methylene blue matched with those reported by Han and Zhang

mentioned above. Those consistencies may provide helpful references for this project.

2.4.1 Modelling of Column Study

For a continuous process, a packed-bed adsorption column is usually used. The effectiveness of an adsorbent can be evaluated from the breakthrough curve of the effluent concentration (or the concentration–time profile). A typical S-shaped breakthrough curve is usually observed.[22] In order to predict the breakthrough curve of an adsorption process in a fixed bed, the Bohart–Adams, Thomas and Yoon-Nelson models have been often used. Moreover, the required bed height is an important parameter in designing an adsorption column. This can be determined from the breakthrough curve and the bed-depth service time (BDST) model. In the present study, the effectiveness of activated carbons as adsorbents for DMAc removal from water will be evaluated. The adsorption capacity of activated carbons in a continuous fixed-bed column will also be determined. For a proper design of an adsorption column, an accurate prediction of the breakthrough curve is needed. Therefore, the experimental results obtained from the continuous system will be fitted with the above-mentioned models for adsorption.[23]

Most of the earlier investigations on adsorption of organic contaminants were restricted to batch equilibrium sorption studies. The adsorption capacity of the adsorbents obtained from the batch equilibrium experiments is useful in providing fundamental information about the effectiveness of adsorbate-adsorbent system. However, this data cannot be taken for granted because in most of the treatment systems (such as column operations), the contact time is not sufficient to attain sorption equilibrium. Hence, there is a need to perform adsorption studies using adsorbent filled columns. Several investigators have identified packed columns as the most effective arrangement for cyclic adsorption-desorption as it makes the best use of concentration difference as a driving force for the adsorption. The

present laboratory-scale study will aim at investigating the effectiveness of activated carbons for removal of DMAc molecules from the aqueous solutions.[24]

The study was conducted in a fixed bed column with variable parameters including influent concentration and flow rate. The breakthrough curves for the adsorption of DMAc will be analysed by using the bed depth service time (BDST) model, Thomas model and Yoon-Nelson model, etc.

Among all available types of adsorption systems, packed bed columns offer several advantages, including simplicity to operate, high process yield, and easiness to scale-up.[25] Although adsorption studies dealing with fixed bed columns involving immobilised adsorbents is not totally new, immobilised adsorption bed has not been well studied, for DMAc removal. A literature search showed that there was no record of any column study of activated carbons adsorbing DMAc. Therefore, the present work also looked into the regeneration and reuse of activated carbons for in the adsorption of DMAc from water using packed bed. To analyse the performance of the column in the removal of the DMAc, several design and operating parameters, as outlined below, will be evaluated.

The breakthrough behaviour of the DMAc particles in the effluent exiting the packed bed is usually expressed in terms of the ratio of effluent to initial DMAc concentrations C/Co as a function of time (t) or volume (V) of the eluate for a given bed height, which is termed the breakthrough curve.

The maximum (equilibrium) capacity Q_m of a packed bed column in capturing DMAc is calculated from the area under the plot for adsorbed DMAc concentration versus time. This is more conveniently expressed as:

$$Q_m = F \int_0^t C\, dt \tag{2.11}$$

where C is the adsorbed DMAc concentration (mol/L) in the effluent exiting the column and F is the flow rate (L/min) at which the DMAc solution is passed through the column for a time period t until column bed get saturated.

The equation for breakthrough curve developed by Thomas[26] calculates the maximum amount of the solute on the adsorbent and the adsorption rate constant for a continuous adsorption process in the column. The linearized form of the model is given as:

$$ln\left(\frac{C_0}{C} - 1\right) = \frac{k_{Th}Q_m m}{F} - k_{Th}C_0 t \tag{2.12}$$

where k_{Th} is the Thomas rate constant (L/mol·min), Q_m is the maximum solid phase concentration (mol/g) and m is the amount of adsorbent (g) in the column, F is the volumetric flow rate (L/min) and V is the effluent volume (L). To determine the Thomas rate constant k_{Th} and maximum solid phase concentration Q_m the experimental data can be fitted by plotting versus time t.

Adams-Bohart developed the following equation 2.12 to describe the relationship between C/Co and t in a flowing system.

$$ln\frac{C}{C_0} = k_a C_0 t - k_a N_0 \frac{h}{u} \tag{2.13}$$

where h is the bed depth (cm), u (cm/min) is divided by as the superficial velocity that is equal to the volumetric flow rate F to the cross-sectional area A_0 (cm^2) of the column, k_a is the adsorption rate constant (L/mol·min), and N_o is the saturation concentration (mol/L).

For describing the concentration distribution in the bed for low concentration ranges (i.e., low C/C_o) in the breakthrough curve, the following relationship, first described by Wolborska[27], can be used:

$$ln\frac{C}{C_0} = \frac{\beta C_0}{N_0} t - \frac{\beta h}{u} \tag{2.14}$$

The Wolborska expression is equivalent to the Adams–Bohart relation if the constant k_a is equal to β/N_0. The parameters in these two models can be determined from a plot of $ln(C/C_0)$ against t for a given bed height and flow rate. Apparently, the terms k_a and N_0 are fixed only for particular values of h and F in a column.[28]

One of the most successful models used in analysing breakthrough data from column tests has been the bed-depth service time (BDST) model. It was originally proposed by Bohart and Adams[29], which shares a common basis with the Adams–Bohart model. Later, Hutchins[30] described the linear form of this model by the following equation:

$$t_b = \frac{N_0}{uC_0}h - \frac{1}{k_B C_0} ln\left(\frac{C_0}{C_b} - 1\right) \tag{2.15}$$

where t_b is the service time at breakthrough (min), and C_b is the effluent concentration at breakthrough (mol/L). A straight line obtained by plotting t_b versus h, which allows for determination of the values of saturation concentration of bed (N_0) and kinetic constant k_B from its slope and intercept, respectively. The value of N_0 can also be calculated in a more convenient way as follows: At 50% breakthrough (where C_b/C_0=0.5), C_0/C_b=2 and t_b=$t_{0.5}$, the final term in the BDST equation becomes zero resulting in the following relationship:

$$t_{0.5} = \frac{N_0}{uC_0}h \tag{2.16}$$

Thus, a plot of time at 50% breakthrough ($t_{0.5}$) against bed height (h) should be a straight line passing through the origin, allowing No to be calculated.

Another simple model developed by Yoon-Nelson[31] can also be used to investigate the dynamic breakthrough behaviour of solute adsorption in a column. The linearized form of the Yoon-Nelson Model for a single solute system is described by:

$$t = t_{\frac{1}{2}} + \frac{1}{k_{YN}} ln\frac{C}{C_0 - C} \tag{2.17}$$

where C_f is inlet concentration of solute (mol/L), C is the solute concentration in effluent (mol/L) at time t, k_{YN} is the Yoon-Nelson rate constant (min^{-1}), t is time (min) and $t_{\frac{1}{2}}$ (min) is the time when $C/C_o = 0.5$.

From the linear relationship between $ln\frac{C}{C_0-C}$ and time t, the model parameters k_{YN} and $t_{\frac{1}{2}}$ can be calculated for a given flow rate and initial concentration. In order to validate the model, the breakthrough curve can be regenerated using the calculated values of k_{YN} and $t_{\frac{1}{2}}$ determined from data fitting to Yoon-Nelson.

2.5 Hollow Fibre Contactors

Hollow fibre (HF) membranes are commonly produced from polymers. Originally developed in the 1960s for reverse osmosis applications, hollow fibre membranes have since become prevalent in water treatment, desalination, cell culture, medicine, and tissue engineering. Most commercial hollow fibre membranes are packed into cartridges which can be used for a variety of liquid and gaseous separations.[32]

Gas/liquid contacting operations are traditionally done using some type of tower, column or mixer–settler designs. Usually, the main challenge in designing and operating these devices is to maximise the mass transfer rate by providing as much interfacial area as possible. For packed columns this requires judicious selection of packing material and uniform distribution of fluids. Alternatively, for devices with mobilised adsorbents, the design challenge is to minimise the bubble or droplet size of the dispersed phase and maximise the number of bubbles or droplets.[33]

Although packed columns have been workhorses of the chemical industry for decades, an important disadvantage is the interdependence of the two fluid phases to be contacted, which sometimes leads to difficulties

such as emulsions, foaming, and flooding. An alternative technology that overcomes these disadvantages while substantially improving the interfacial area is non-dispersive contact by using a microporous membrane. Using a suitable membrane configuration such as hollow fibres, fluids on opposite sides of the membrane form the contact interface via the pores of the membranes. Mass transfer occurs by diffusion across the interface just as in traditional contacting equipment.[34]

However, unlike normal membrane operations, the membrane imparts no selectivity to the separation. Comparing to such conventional membrane technologies as microfiltration, ultrafiltration and reverse osmosis, the driving force for separation is the difference of concentration instead of pressure. Only a tiny pressure drop across the membrane is required to achieve the essential mass transfer in the pores.[35]

Comparing to columns and other conventional mass transfer equipment hollow fibre contactors possess many advantages[36]:

- The available surface area remains undisturbed at high and low flow rates because the two fluid flows are independent. This is useful in applications where the required solvent/feed ratio is very high or very low. In contrast, columns are subject to flooding at high flow rates and unloading at low flow rates.
- Emulsion formation does not occur, again because there is no fluid/fluid dispersion.
- Unlike traditional contactors, where the density difference is required between fluids is a concern; membrane contactors can accommodate fluids of identical density and can be operated in any orientation.
- Scale-up is more straightforward with membrane contactors. Membrane operations usually scale linearly, so that a predictable

increase in capacity is achieved simply by adding membrane modules (subject to the limitations of support equipment such as transfer pumps, piping). On the other hand, the scale-up with conventional equipment is not nearly as straightforward.

- Modular design also allows a membrane plant to operate over a wide range of capacities.
- Interfacial area is known and is constant, which allows performance to be predicted more easily than with conventional dispersed phase contactors.
- Substantially higher is achieved with membrane contactors than with dispersive contactors.
- The solvent holdup is low, an attractive feature when using expensive solvents.
- Unlike mechanically agitated dispersed phase columns, membrane contactors have no moving parts.

However, membranes also have disadvantages[37]:

- The hollow fibres themselves introduce another resistance to mass transfer not found in conventional operations. However, this resistance is not always important, and steps can be taken to minimise it.
- Membranes are subject to fouling, although this tends to be more of a problem with pressure-driven devices than with concentration-driven membrane contactors.

These disadvantages are often outweighed by the advantages mentioned above. For this reason, membrane contactors have attracted attention from both academia and industry for a diverse range of applications.

During the past decades, several new configurations of fluid-particle contactors have been developed. They are mainly based on microporous hollow fibres to provide uniform and efficient fluid-particle contact and yet still maintain an acceptable pressure drop through the entire contactor. The hollow fibres used are often highly porous, and there is essentially no selectivity in permeation through the fibres. The primary function of those membranes is to offer means for managing the fluid flow through the contactor to achieve an efficient fluid-particle contact and interaction without giving rise to an excessive pressure drop.[38]

In this thesis research, hollo fibre modulated packed bed of minute carbon powders will also be studied for DMAc removal from water.

Chapter 3: DMAc Adsorption on Activated Carbons

3.1 Introduction

In order to optimise the design of an adsorption system to remove DMAc from wastewater, it is important to establish the correlation between equilibrium uptake and solute concentration. An accurate mathematical description of equilibrium adsorption is essential to a reliable prediction of adsorption parameters as well as to the quantitative comparison of the adsorption performance of different adsorbents systems (or varied experimental conditions within any given system).[39]

Adsorption equilibrium is established when the rate of DMAc adsorbed onto the activated carbon is equal to the rate being desorbed. It is possible to depict the equilibrium adsorption isotherms by plotting the uptake of the DMAc in the solid phase versus DMAc concentration in the liquid phase. The distribution of DMAc between the two phases reflects the equilibrium in the adsorption process and can generally be expressed by isotherm models.[40]

The analysis of equilibrium adsorption data is important for comparing different activated carbons under different operating conditions, to help design and operate the adsorber. To determine the parameters of an equilibrium isotherm model, the experimental data of the adsorbed amount of uptake at different solute concentrations was fitted into the models.

Several adsorption isotherm models have been adopted to correlate adsorption equilibria adsorption of organic compounds on activated carbons. The Freundlich models and the Langmuir model have been widely used.[41]

3.2 Thermodynamic Parameters of Adsorption

The Langmuir isotherm is commonly used for the description of adsorption data at equilibrium:[42]

$$Q_e = Q_m \frac{C_e K_l}{C_e K_l + 1}$$

where Q_e is the adsorption uptake (mmol/g) of the adsorbent (i.e., DMAc in this study) at equilibrium and Q_m is the adsorption capacity (mmol/g) when the sorption sites are fully occupied. C_e is the equilibrium concentration of adsorbate in solution (mmol/L), K_l is the Langmuir equilibrium constant of adsorption with a unit of L/mmol. The Langmuir equilibrium constant has often been employed for calculation of the Gibbs free energy change (ΔG) using the following equation:[43][44]

$$\Delta G = -RTlnK_l \tag{3.1}$$

It should be noticed that the thermodynamic equilibrium constant in equation 3.1 is unit less, whereas the Langmuir equilibrium constant is dimensional. Therefore, a simple but rarely asked question in adsorption studies is whether the use of the Langmuir equilibrium constant for calculation of ΔG by equation 3.1 is reasonable. According to Langmuir[45], the adsorption process can be written as:

$$X + Y = XY \tag{3.2}$$

in which X represents free adsorptive solute molecules, Y is vacant sites on the adsorbent and XY is the occupied sites. For equation 3.4, the thermodynamic equilibrium constant K_f can be written as follows:

$$K_f = \frac{(activity\ of\ occupied\ sites)}{(activity\ of\ vaccant\ sites)\times(activity\ of\ solute\ in\ solution)} \quad (3.3)$$

Usually, the activity coefficients of the occupied and unoccupied sites are the same,[46] and thus equation 3.4 becomes:

$$K_f = \frac{\theta_e}{(1-\theta_e)\cdot a_e} \quad (3.4)$$

where θ_e is the fraction at surface of adsorbent covered by the sorbate molecules at equilibrium, and a_e is the activity of the adsorbate in solution at equilibrium. The activity of a substance is related to its concentration C_e by:

$$a_e = \gamma_e \frac{C_e}{C_s} \quad (3.5)$$

where γ_e is the activity coefficient of the adsorbate molecules in the solution at the adsorption equilibrium, and C_s is the molar concentration of the standard reference solution, which is defined to be 1 mol/L. Thus equation 3.6 can be rewritten as:

$$a_e = \gamma_e C_e\ (L/mol) \quad (3.6)$$

Combining equations 3.6 and 3.8 together, the following can be derived:

$$K_f = \frac{\theta_e}{(1-\theta_e)\gamma_e C_e}\ (L/mol) \quad (3.7)$$

On the other hand, since θ_e is equal to the ratio of Q_e and Q_m, the Langmuir isotherm (equation3.1) may be expressed as:

$$K_l = \frac{\theta_e}{(1-\theta_e)C_e} \quad (3.8)$$

Comparing equation 3.9 with equation 3.11:

$$K_f = \frac{K_l}{\gamma_e}\ (L/mol) \quad (3.9)$$

In this study, DMAc concentration in the solution is rather low, and it is reasonable to assume $\gamma_e = 1$. Therefore, the Langmuir equilibrium constant K_l with a unit of (L/mol) can be used directly to calculate ΔG.

Similar treatments have been used in the literature by others (see, for example, Annadurai[47] and Moreno-Castilla[48]).

3.3 Experimental

3.3.1 Materials

Three types of activated carbons were chosen to be the main adsorbents of this project, and they were all made from coir pith (coconut shells). Their autoignition temperature is 450°C, vapor pressure is lower than 0.1 mmHg and resistivity is 1375 μΩ·cm at 20°C. Their surface topography, the average pore size and pore size distribution have not been tested by either the distributer or the supplier, according to the technical service of Sigma-Aldrich®. The types and specifications of these activated carbons are listed in Table 3.1.

Table 3.1 *Three types of activated carbons*

AC no.	Supplier, product code, and basic classification
01	329428 (Sigma-Aldrich), NORIT® ROW 0.8 SUPRA, pellets (0.8mm)
02	C2889 (Sigma-Aldrich), untreated, granular, 8-20 mesh (0.8-2.4mm)
03	242276 (Sigma-Aldrich), DARCO®, −100 mesh, powder (0.15mm)

Figure 3.1 shows photographs of the activated carbons:

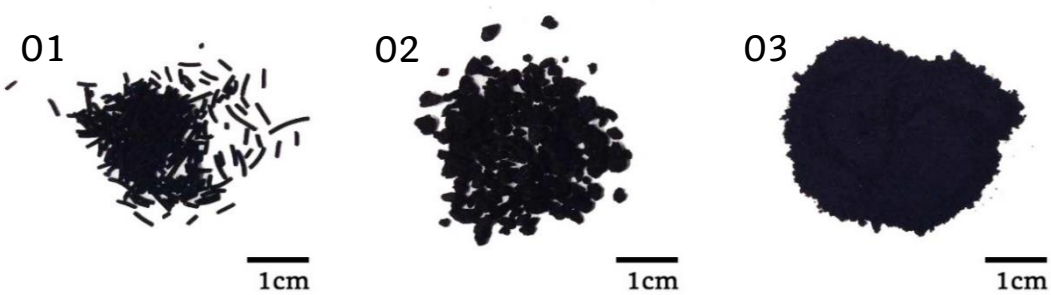

Figure 3.1 Photographs of the three types of activated carbons used in this work

All the activated carbons were washed with deionized water to remove soluble impurity substances before being used in the experiments. After the rinsing water was removed by filtration using filtration papers, the activated carbons were fully dried at 80°C in air for at least 120 hours.

DMAc was purchased from Sigma-Aldrich® (anhydrous 99.8%) and used directly without further purification. All the weighing operations were performed on a "METTLER PM200" analytical balance.

3.3.2 Adsorption Experiments

A 20000mg/L stock solution of DMAc was prepared in water. This stock solution was diluted with water to get desired DMAc concentrations. Three sets of 50ml Pyrex bottles were filled with 50ml of DMAc solutions at concentrations of 500, 800, 1000, 1500, 2000, 2500, 3000, 3500, 4000, 4500, 5000, 6000, 7000, 8000, 9000 and 10000mg/L. Activated carbon samples (2.5g each) were immersed into the DMAc solutions. The concentrations of DMAc were monitored until adsorption reached equilibrium. The sorption equilibrium was considered to have been reached when the DMAc concentration in the solution became constant. The sorption uptake Q_e of DMAc in activated carbons at equilibrium was determined using the following mass balance equation:

$$Q_e = \frac{C_0 - C_e}{m} V \tag{3.10}$$

where V is the volume of solution (L), m is the weight of adsorbent used (g), C_0 is the initial concentration of the solute (mol/L), and C_e is the concentration of the solute (mol/L) at equilibrium.

The equilibrium adsorption was carried out at different temperatures (22, 30, 40, 50 and 60°C). A water bath was used to maintain a constant temperature during the adsorption experiments, except for adsorption measurement at room temperature (22°C).

Experiments on adsorption kinetics were also carried out at temperatures (22, 30, 40, 50 and 60°C), using a much larger quantity of the DMAc solution to minimize experimental error due to sampling during the course of adsorption. The DMAc solution was put inside a 2L beaker, a mechanical impeller (pitched 45°, 4-blade) placed in the centre was used to provide agitation. The rotation speed was set at 150rpm. The timer started as soon as the activated carbons (100g each batch) was added into the DMAc solutions in the beakers. Samples were collected periodically using a syringe fitted with micro-filter head (diameter ϕ=25mm, installed with cellulose acetate microfiltration membrane of 0.22μm pore size) for concentration analysis using a Shimadzu total organic carbon analyser. The setup and the equipment were illustrated in Figure 3.2.

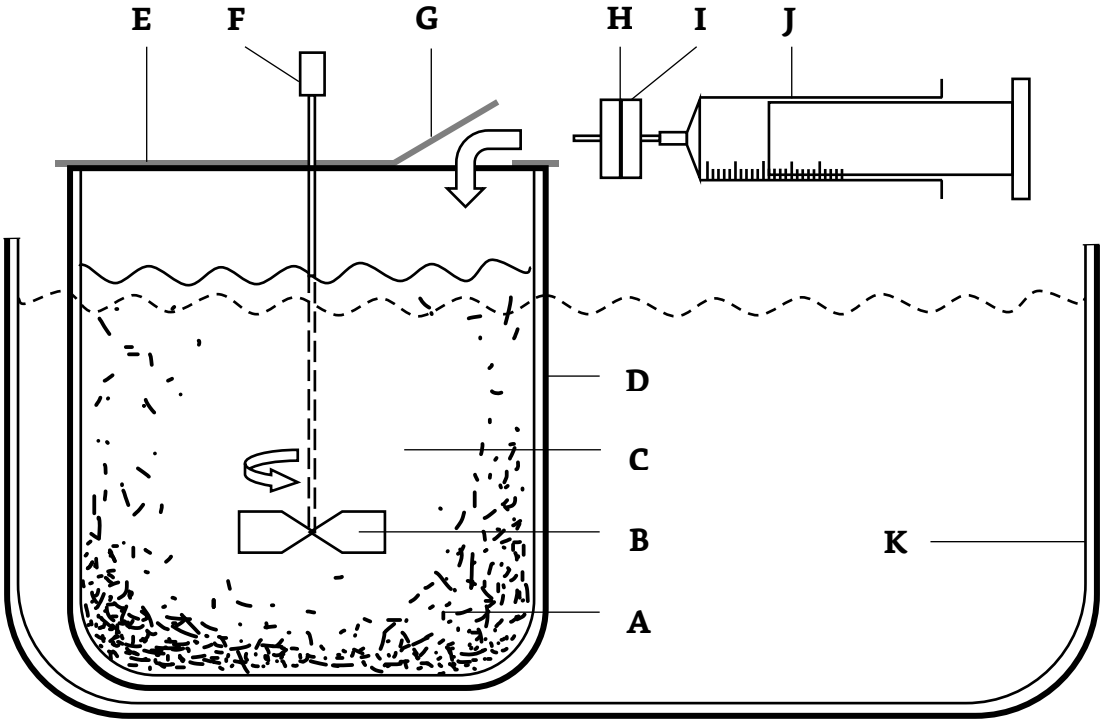

Figure 3.2 The setup for kinetic study and sampling: (A) activated carbons, (B) mechanical stirrer, (C) DMAc solution, (D) 2L beaker, (E) beaker lid preventing evaporation, (F) connection to motor, (G) vent for sampling, (H) cellulose acetate microfiltration membrane (0.22μm, ϕ=25mm), (I) injection filter head, (J) 5ml glass syringe, (K) water bath

The desorption of DMAc from activated carbon was also investigated for regeneration and reuse of the adsorbent. The idea is to replace the hard-to-remove DMAc adsorbed on the activated carbons with the easy-to-

remove ethanol. In addition, Ethanol is relatively inexpensive and has good affinity and solubility with DMAc. First, the retracted activated carbon was placed in an oven at 80°C for at least 120 hours to evaporate most of the DMAc and water that was trapped inside the activated carbon. Then 50g of activated carbon was submerged into 800ml of ethanol (98% purity) for 72 hours. The liquid phase was placed with a new batch of 800ml of ethanol, to keep contact with activated carbon for another 72 hours. The beaker was shaken occasionally to accelerate the desorption of DMAc from activated carbon. Finally, the activated carbon was moved out of the ethanol solution for drying in an vacuum oven "Isotemp Model 281A" at 115°C) for 96 hours. The regenerated activated carbon was fully ready for use in another cycle. A standard 1L suction flask paired with filter paper was used to separate activated carbon from the solution each time. At least 5 cycles of adsorption-desorption operations were performed to examine the reusability of the regenerated activated carbons. All the time length settings mentioned here was formulated based on preliminary tests.

Each adsorption run was repeated using the same equipment at the same conditions and configurations for at least three times to minimise the experimented error.

All the measurements of DMAc concentrations in aqueous solutions were performed using a "Shimadzu TOC-500" total organic carbon (TOC) analyser. The TOC analyser was operated a carrier gas flow rate of 150ml/min. In sample analysis, 3μl of liquid sample was injected into the TOC using a standard gas chromatography syringe. The TOC was calibrated using standard DMAc solutions of a variety of known concentrations, and the calibration curves are presented in Appendix A (Figure A.1). Before being injected into the TOC analyser, the DMAc solution samples were centrifuged using an Eppendorf Centrifuge (5810) at 11,000 rpm for 15 minutes to eliminate any carbon particles which would potentially influence the TOC reading. The centrifuge tube size was 10ml, and only 0.1ml of the

supernatant of the centrifuged solvent liquid was removed for TOC analysis. The TOC measurements were repeated at least five times, and the TOC readings were averaged to minimise the error.

3.4 Results and Discussion

3.4.1 Adsorption Equilibrium

The effects of temperature on the equilibrium adsorption of DMAc on the three activated carbons were determined in a temperature range of 22-60°C. Figure 3.3 represents the equilibrium uptake of DMAc on activated carbon at different temperatures and DMAc concentrations in the liquid phase.

The three types of carbons were labelled and abbreviated as *AC01*, *AC02* and *AC03*, for NORIT® ROW 0.8 SUPRA (pellets), granular (8-20 mesh), and DARCO® (−100 mesh, powder), respectively.

The curves of equilibrium profiles of DMAc adsorption on the three types of activated carbons are shown in Figure 3.3.

In general, the temperature effects on the sorption of DMAc in activated carbon are very consistent regardless of the type of carbon utilised. Figure 3.3 shows that a given DMAc concentration in the solution, there is a decrease in the sorption uptake of DMAc with an increase in the temperature for all the activated carbons studied here. It has been believed previously that the adsorption of organic compounds on activated carbon is primarily a physical process. A higher temperature will make the organic molecules move faster on carbon surfaces, making adsorption harder to accomplish. Recently, other theories have also been proposed to further explain the temperature influence, some of which focus on the interactions between the hybrid electron orbitals of the two substances.[49]

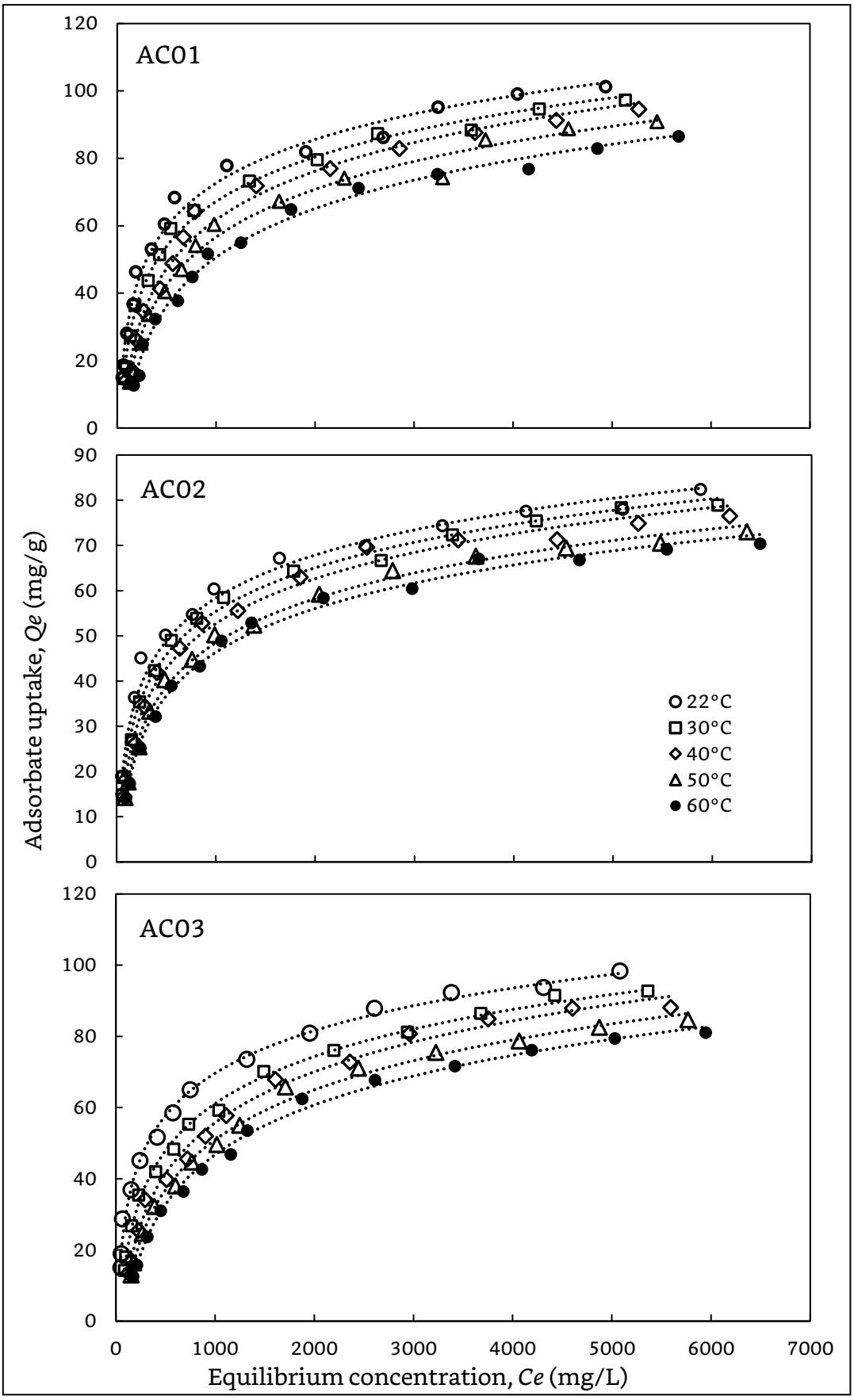

Figure 3.3 Equilibrium profiles of DMAc adsorption on *AC01*, *AC02* and *AC03* at different temperatures

Equilibrium adsorption data for the sorption of DMAc on activated carbons was fitted to the Langmuir adsorption model. The linearized form of Langmuir adsorption model is:

$$\frac{1}{Q_e} = \frac{1}{Q_m} + \frac{1}{C_e Q_m K_l} \tag{3.11}$$

where Q_e is equilibrium uptake of adsorbent (mg/g), C_e is DMAc concentration in solution (mol/L), Q_m is the maximum adsorption capacity of adsorbent (mol/g) and K_l is Langmuir adsorption constant (L/mg). Plotting $\frac{1}{Q_e}$ versus $\frac{1}{C_e}$ gives a straight line, as shown in Figure 4.5 with an intercept and a slope given by:

$$Intercept = \frac{1}{Q_m} \tag{3.12}$$

$$Slope = \frac{1}{Q_m K_l} \tag{3.13}$$

The Langmuir constants K_l and Q_m for each type of activated carbon are shown in Table 3.2. In all cases, the correlation coefficient (R^2) was close to unity, which shows that the adsorption equilibrium data corresponds well with the Langmuir adsorption model.

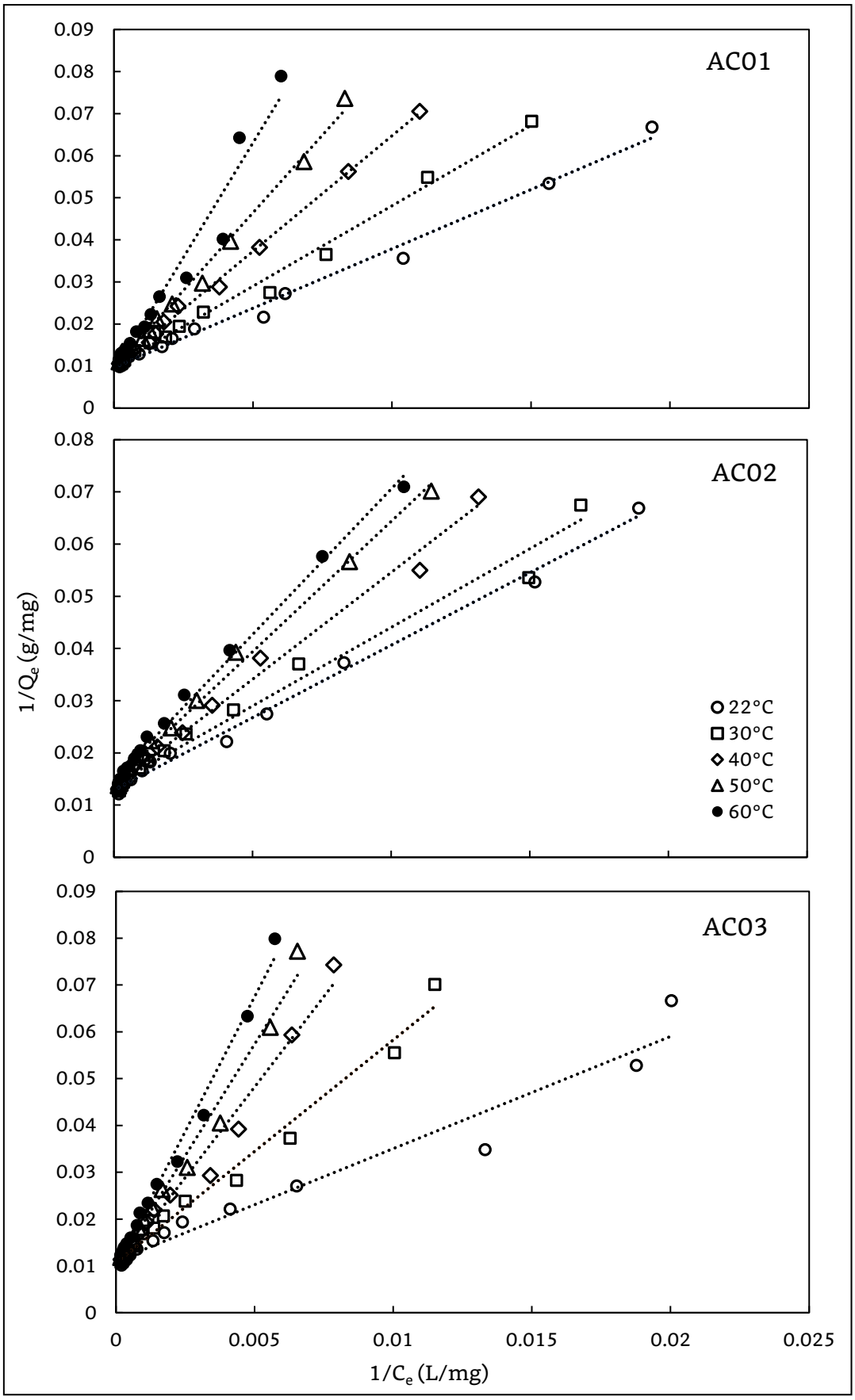

D

Figure 3.4 Linearized Langmuir isotherms for the adsorption of DMAc on AC01, AC02 and AC03 at various temperatures.

Using the adsorption equilibrium parameter k_l, the Gibbs free energy ΔG can be calculated by using equation 3.15, and the calculated ΔG is also shown in Table 3.2. The Langmuir constant K_l was expressed in a unit of L/mol to be thermodynamically consistent.

Table 3.2 Parameters of the Langmuir adsorption model and Gibbs free energy (ΔG) for the adsorption of DMAc on three types of activated carbons at different temperatures.

Adsorbent	Temperature (°C)	Q_m (mmol/g)	K_l (L/mmol)	R^2	ΔG (kJ/mol)
AC01	22	1.042	2965	0.9917	-19.6
	30	1.010	2257	0.9931	-19.3
	40	1.031	1428	0.9978	-19
	50	1.053	1121	0.9946	-18.6
	60	1.163	688	0.9577	-18.3
AC02	22	0.7246	4849	0.9939	-11
	30	0.7194	4020	0.9828	-10.9
	40	0.7353	2894	0.9913	-10.7
	50	0.6944	2511	0.9947	-10.6
	60	0.6757	2312	0.9941	-10.4
AC03	22	0.8929	3217	0.9608	-19.7
	30	0.9434	1939	0.9856	-19.3
	40	1.043	1071	0.9823	-18.8
	50	1.020	896	0.9864	-18.3
	60	1.010	749	0.9913	-17.8

(Note: $\Delta G = -RTlnK_l$, where K_l is in unit of L/mol)

As shown by data in Table 3.2, the equilibrium adsorption constant K_l decreased with an increase in adsorption temperature for all three type of activated carbons. Similarly, the maximum uptake capacity of DMAc Q_m in the activated carbon also tended to decline with an increase in temperature. These results are consistent with the speculations of some researchers that the -COOH and -OH groups attached on the edge of activated carbon may inhibit the adsorption for DMAc. An increase in the temperature will help

oxygen atoms bound electrons, and thus weaken the interaction between the C=O group of DMAc and the π system of the carbon structure.[50]

The adsorption equilibrium data clearly show that the adsorption of DMAc on activated carbon is an exothermic process.

The negative value of ΔG shows that the adsorption process is spontaneous. With an increase in temperature, the values of ΔG become slightly less negative. This indicates that the degree of spontaneity of the adsorption process decreased with the rise in adsorption temperature. The adsorption equilibrium constant K_l decreased when temperature increased.

Similar results were obtained by Amin et al.[51] and many other researchers mentioned in the literature review part, for the adsorption of a variety of organic compounds on various types of activated carbons.

For the calculation of the changes in enthalpy ΔH and entropy ΔS, equation 3.3 is applied. By plotting K_l vs $1/T$ (Van't Hoff relation), a straight line was obtained with:

$$Slope = -\frac{\Delta H}{R} \tag{3.14}$$

and

$$Intercept = \frac{\Delta S}{R} \tag{3.15}$$

This is shown in Figure 3.5. The ΔH and ΔS calculated from the slope and intercept are presented in Table 3.3. The correlation coefficient for the linear K_l versus $1/T$ relationship is also presented in the table.

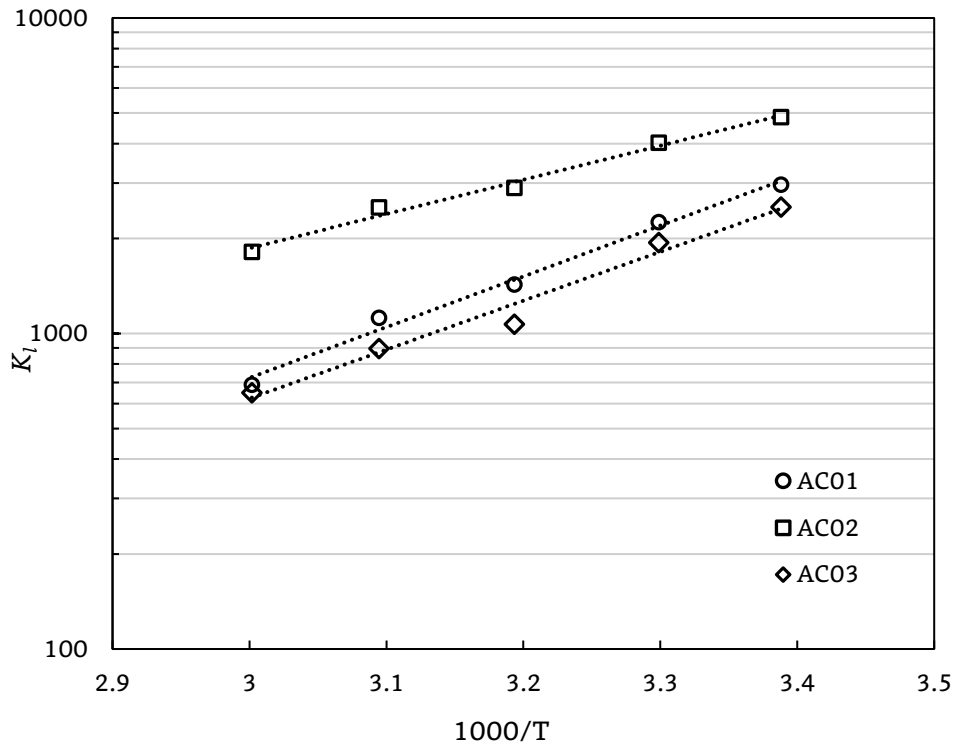

Figure 3.5 Van't Hoff plot of K_l vs *1/T* for entropy and enthalpy change calculations of DMAc adsorption on *AC01*, *AC02* and *AC03*.

Table 3.3 ΔH and ΔS, calculated from the Van't Hoff equation with a temperature range of 22~60°C for the adsorption of DMAc on all types of activated carbons.

Adsorbent	Enthalpy Change ΔH (kJ/mol)	Entropy Change ΔS (kJ/mol·K)	R^2
AC01	-29.32	-0.03307	0.989
AC02	-15.94	-0.01658	0.980
AC03	-34.72	-0.05071	0.970

The values of ΔS, for the adsorption by all three activated carbons are negative but small, which indicates that there is not much difference in the randomness of the adsorbate molecules on the solid surface and the DMAc in the liquid phase. The negative value of ΔH represents the heat effect of DMAc adsorption on activated carbon surface, which is exothermic. The heat evolved during physical adsorption generally falls into a range of 0.008-25kJ/mol, while the heat of chemical adsorption generally falls into a

range of 80-200kJ/mol.[52] It shows that the DMAc adsorption on activated carbon is basically a physical process.

Besides the Langmuir Isothermal model, the Freundlich model is also widely used to describe equilibrium. In many cases, this model is more suitable for the physical adsorption of organic compounds on activated carbons. The Freundlich model can be represented by the following equation[53]:

$$Q_e = K_f C_e^n \tag{3.16}$$

where Q_e is equilibrium uptake capacity of adsorbent (mg/g), C_e is equilibrium solution concentration (mol/L), n is empirical constants, and K_f is the Freundlich adsorption constant $((\frac{\mathrm{mg}}{\mathrm{g}})(\frac{\mathrm{L}}{\mathrm{mg}})^{1-\frac{1}{n}})$.

The Freundlich model can be rearranged into a linear form:

$$lnQ_e = lnK_f + nlnC_e \tag{3.17}$$

The same set data of DMAc adsorption on the three types of activated carbons at different temperatures was also examined using this model. When lnQ_e was plotted against lnC_e, no linear trend was observed, and the correlation coefficients (R^2) were below 0.95. This is shown in Appendix B (Figure B.1). Therefore, the Freundlich model was not inspected further.

3.4.2 Kinetic Studies

During adsorption, the contact time of the adsorbent with the adsorbate is vital. The adsorption kinetics of DMAc on different activated carbons was determined at different temperatures, and also at different initial DMAc concentrations. Generally, the adsorption kinetics can be considered in two phases, the first phase is the initial rapid adsorption of DMAc, followed by the second phase which involves a slow removal of DMAc molecules. In present study, the first phase (the 10min period since the start) was fast and most of the adsorption takes place within this period. At second phase, which is slow enough (the period after the 10min mark), the DMAc

removal rate slowed down and only small amounts of DMAc were adsorbed on the ACs. Eventually, an equilibrium was achieved around 150min mark of the contact time and the DMAc uptake did not change anymore.

The majority of adsorption kinetics studies related the initial rapid phase of sorption to the passive physical adsorption or substance exchange at the sorbent surface. However, the slower second phase of adsorption may imply other adsorption mechanisms such as microprecipitation or complexation.[54]

In order to gain an insight into the mechanism of adsorption such as mass transfer and micro interaction and to determine the kinetic parameters, the adsorption kinetic data was fitted with the pseudo-first-order, pseudo-second-order and Weber's intraparticle diffusion models. Though these kinetic and mass transfer models were discussed in Chapter 2 (Literature review), an overview is presented here for easy comparisons.

Firstly, the effects of temperature on adsorption kinetics was examined using an initial DMAc concentration of 1000mg/L. At a given temperature, the amount of DMAc adsorbed as a function of time was recorded. The raw experimental data are shown in Figure 3.6.

As expected, the equilibrium uptake of DMAc is consistent with the data obtained in previous equilibrium study, where the overall DMAc uptake decreased with an increase in temperature. In addition, the DMAc uptake rate increased noticeably as the temperature increased. This is because the adsorption is an activated process that the adsorption rate will be enhanced at higher temperatures. Additionally, *AC03* adsorbed DMAc much faster than the other two activated carbons, mainly because *AC03* has a much smaller particle size which leads to higher magnitude of specific surface area.

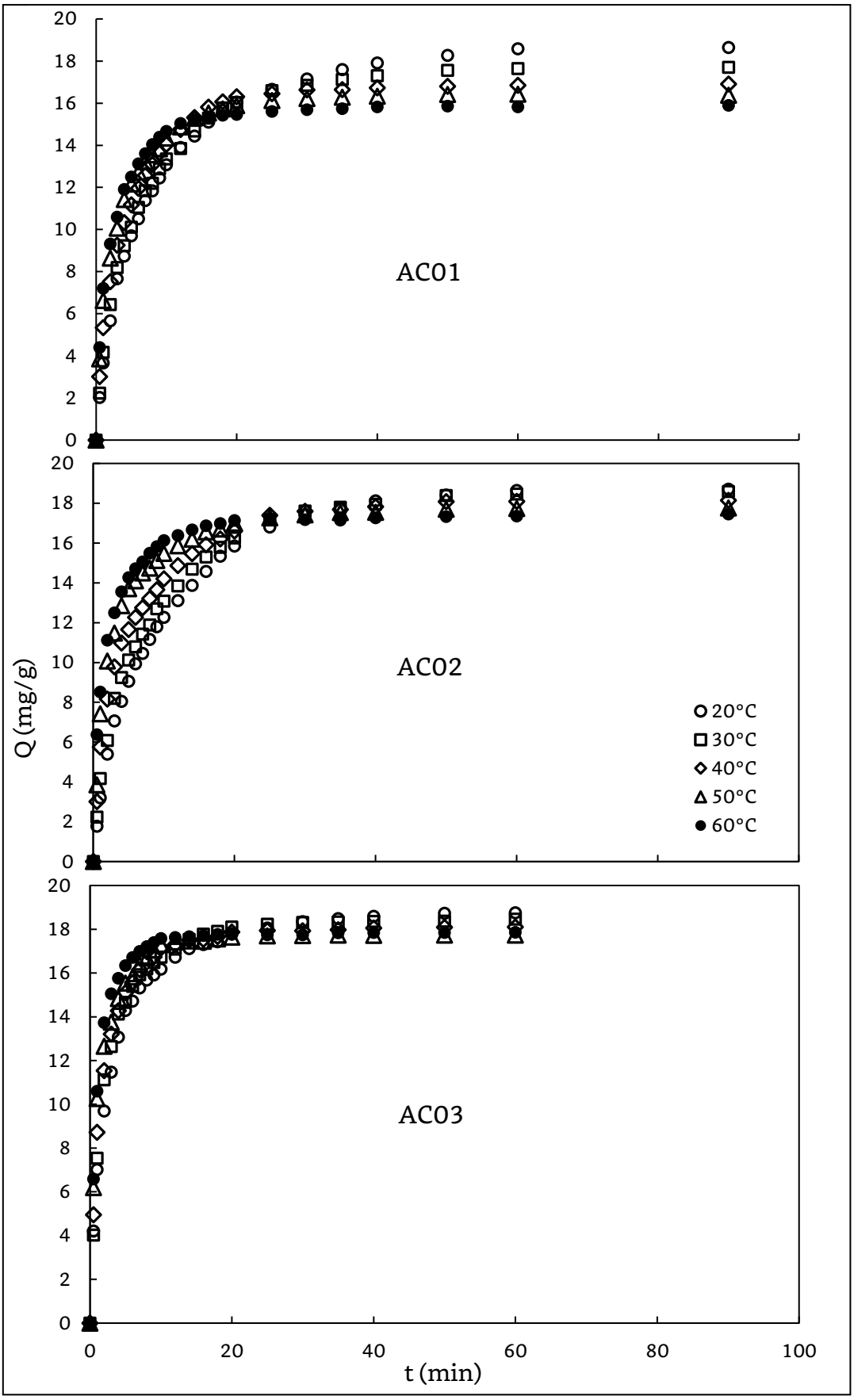

Figure 3.6 The experimental data of DMAc adsorption kinetics on three types of activated carbon at different temperatures

The pseudo-first-order kinetic model assumes that the rate of occupation of adsorption sites is proportional to the number of unoccupied sites, whereas the pseudo-second-order model assumes that the sorption capacity is determined by the number of active sites occupied on the adsorbent and that the adsorption may be the rate-limiting step involving valence forces through sharing or exchanging electrons between the adsorbent and the adsorbate.[54]

The original forms of the three widely applied kinetic adsorption models are represented mathematically:

Pseudo-first-order: $$\frac{dQ_t}{dt} = k_1(Q_e - Q_t) \quad (3.18)$$

Pseudo-second-order: $$\frac{dQ_t}{dt} = k_2(Q_e - Q_t)^2 \quad (3.19)$$

Intraparticle diffusion: $$Q_t = k_d t^{1/2} + C \quad (3.20)$$

where Q_t is the uptake of adsorbate at t, Q_e is the equilibrium uptake k_2 or k_1 or k_d are the kinetic rate constants based on the three models respectively.

The linearized pseudo-first-order and pseudo-second-order model can be expressed as:

Pseudo-first-order: $$log(Q_e - Q_t) = logQ_e - \frac{k_1}{2.303}t \quad (3.21)$$

Pseudo-second-order: $$\frac{t}{Q_t} = \frac{1}{k_2 Q_e^2} + \frac{t}{Q_e} \quad (3.22)$$

Intraparticle diffusion: $$Q_t = k_d t^{1/2} + C \quad (3.23)$$

By plotting $log(Q_e - Q_t)$ versus t and plotting $t^{1/2}$ versus Q_t, the fitting of the pseudo-first order model and Weber's intraparticle diffusion model to the experimental data can be investigated, respectively. The linear fitting patterns of the two models are shown in Appendix B (Figures B.2 and

B.3). The correlation coefficients (R^2) of the fittings are presented in Appendix B (Tables B.1 and B.2) too. Neither model is able to represent the adsorption kinetics better than the pseudo-second order model, which will be discussed in more detail later. This indicates that both the pseudo-first-order model and the intraparticle diffusion model are not suitable for describing kinetic adsorption behaviour of DMAc on these activated carbons.

By plotting $\frac{t}{Q_t}$ versus t, the pseudo-second-order model is fitted to the experimental data, and the results are shown in Figure 3.7.

The pseudo-second-order kinetic rate constant k_2 , the equilibrium adsorbent uptake Q_e, and the correlation coefficient of the fitting R^2 are obtained, and they are presented in Table 3.4.

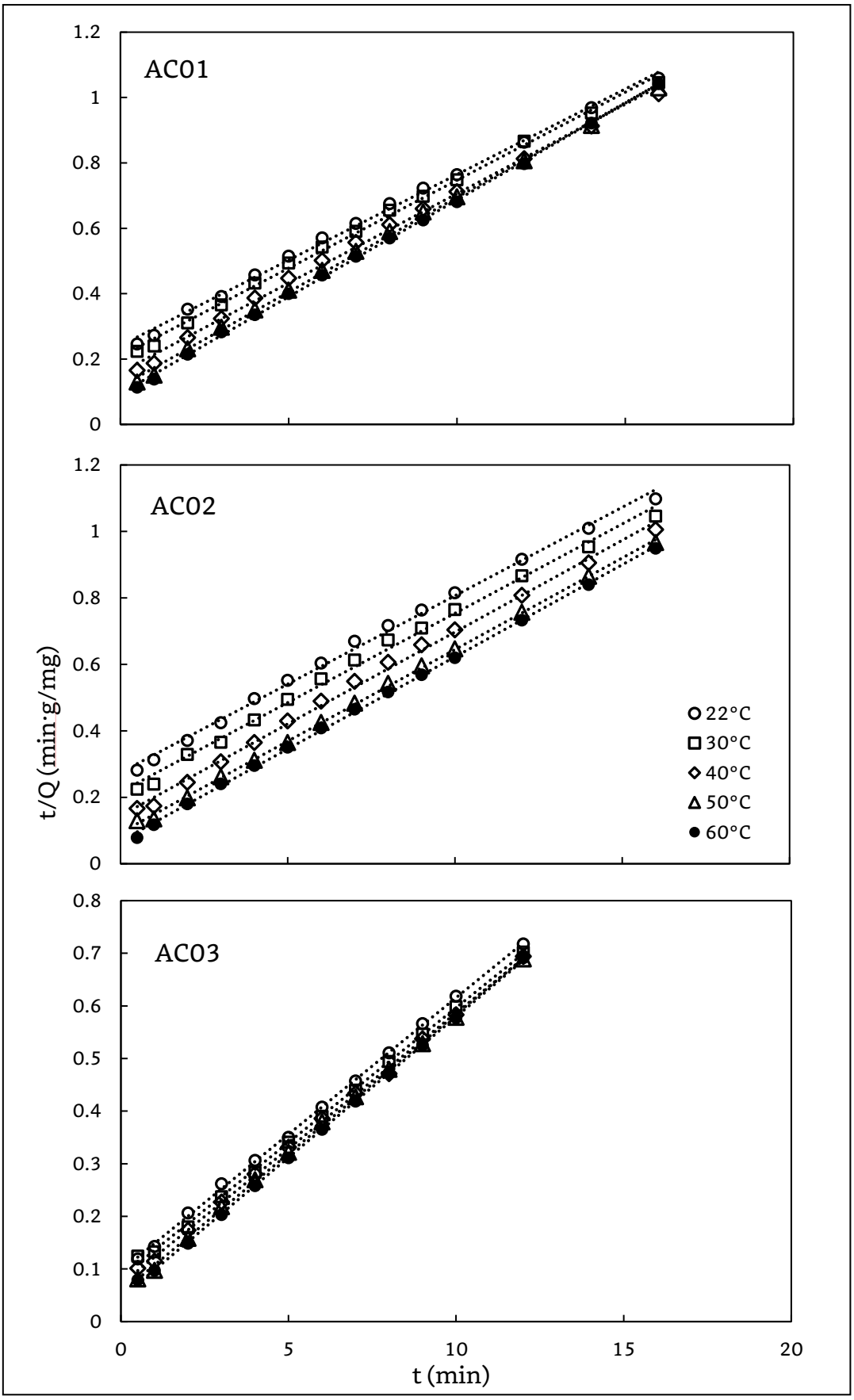

Figure 3.7 The pseudo-second-order model fitting for the kinetic adsorption of DMAc on activated carbons at different temperatures

Table 3.4 Experimental data and parameters calculated from pseudo-second order kinetic model for the adsorption of DMAc on activated carbons at an initial DMAc concentration of 1000mg/L

Adsorbent	Experimental Data				Calculated Data of Pseudo-Second Order		
	Temperature	Final Concentration (C_e)		DMAc uptake (Q_e)	DMAc uptake (Q_e)	Kinetic Rate Constant (k_2)	R^2
	(°C)	(mg/L)	(mmol/L)	(mmol/g)	(mmol/g)	(g/mmol·min)	
AC01	22	67.68	0.7769	0.214	0.228	8.838	0.999
	30	114.8	1.318	0.203	0.215	12.42	0.999
	40	154.4	1.772	0.194	0.201	21.48	0.999
	50	181.0	2.078	0.188	0.194	31.62	0.999
	60	205.0	2.353	0.182	0.186	45.89	0.999
AC02	22	64.75	0.7432	0.215	0.233	7.332	0.999
	30	70.73	0.8118	0.213	0.227	9.775	0.999
	40	93.09	1.069	0.208	0.217	15.92	0.999
	50	112.2	1.288	0.204	0.209	29.38	0.999
	60	127.5	1.463	0.200	0.203	45.67	0.999
AC03	22	62.53	0.7177	0.215	0.223	23.39	0.999
	30	77.65	0.8913	0.212	0.218	34.03	0.999
	40	94.48	1.084	0.208	0.212	48.20	0.999
	50	112.7	1.294	0.204	0.207	71.75	0.999
	60	120.0	1.377	0.205	0.205	98.27	0.999

Apparently, the experimental data for all types of activated carbons seem to fit very well with the pseudo-second-order kinetic model, with correlation coefficients R^2 all greater than 0.998. The calculated Q_e values from the pseudo-second-order model fitting have a very good agreement with the experimental Q_e values determined from equilibrium adsorption uptake at all temperatures. As presented in Table 3.4, the rate constants k_2 show a clear temperature dependence. The effects of temperature on the rate constant k_2 can be measured using the activation energy of adsorption, which can be evaluated using Arrhenius equation:[55]

$$k_2 = k_2^o exp\left(-\frac{E}{RT}\right) \tag{3.24}$$

where k_2 is the kinetic rate constant (in this case it is the second-order kinetic rate constant k_2), R is the universal gas constant, T is temperature, and k_2^o is the pre-exponential coefficient.

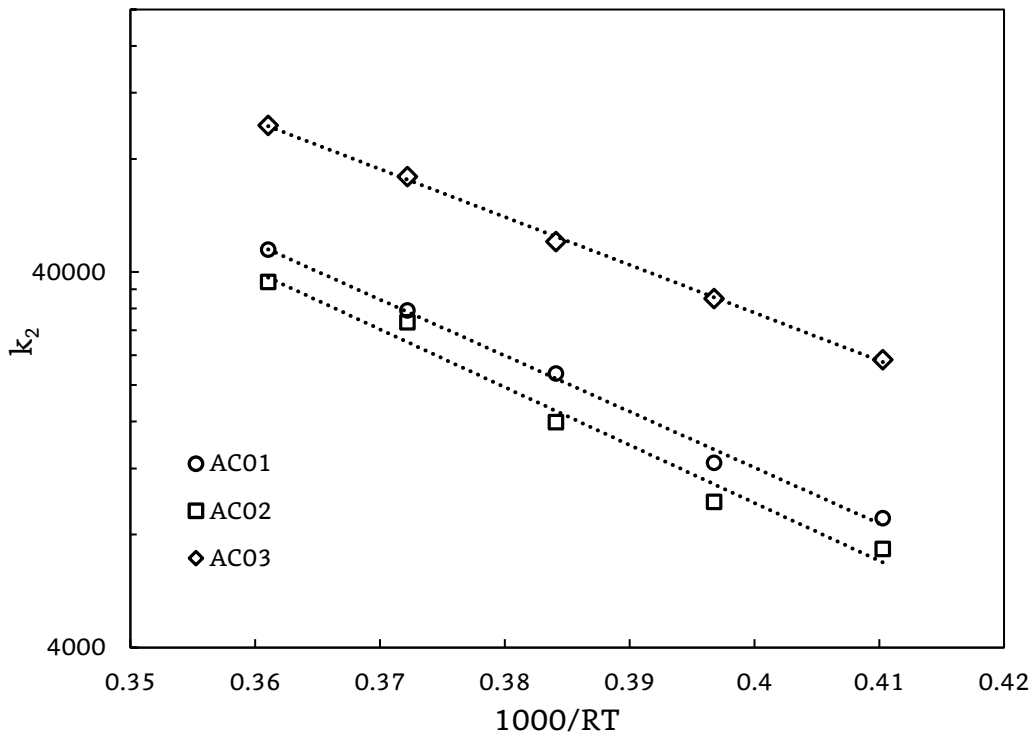

Figure 3.8 Fitting of the Arrhenius equation for the kinetic adsorption of DMAc on activated carbons at different temperatures

The Arrhenius plot is shown in Figure 3.8, and the activation energies (E) of adsorbing DMAc on activated carbons were calculated from the slopes of the plots. Table 3.5 shows the activation energy of DMAc adsorption on activated carbon; the correlation coefficients of the data fitting are also shown in the table. The negative values of activation energy mean the adsorption of DMAc on activated carbon is a typically barrierless process.

Table 3.5 Activation energy for DMAc adsorption on activated carbon

Adsorbent	Activation energy E (kJ/mol)	R^2
AC01	-19.6	0.995
AC02	-11.0	0.988
AC03	-19.7	0.998

For the second series of the adsorption experiments, the impact of initial DMAc concentration on adsorption kinetics was examined. Operating at temperature 40°C, aqueous DMAc solutions of various concentrations (1000, 2000, 3000, 4000 and 5000mg/L) were treated by three types of ACs. The amount of DMAc adsorbed as a function of time was recorded. The results are shown in Figure 3.9.

Again, the agreement of the experimental data with the classic empirical models was examined. The pseudo-first-order and intraparticle diffusion models were found not as good as the pseudo-second-order model. The model fitting to the experimental data are presented in Appendix B (Figure B.4 for the pseudo-first-order model and Figure B.5 for the intraparticle diffusion model; their correlation coefficients are shown in Tables B.3 and B.4, respectively). As shown by Figure 3.10, where $\frac{t}{Q_t}$ is plotted versus t, the pseudo-second-order model works well in all cases. The model parameters determined from the data fitting are shown in Table 3.6.

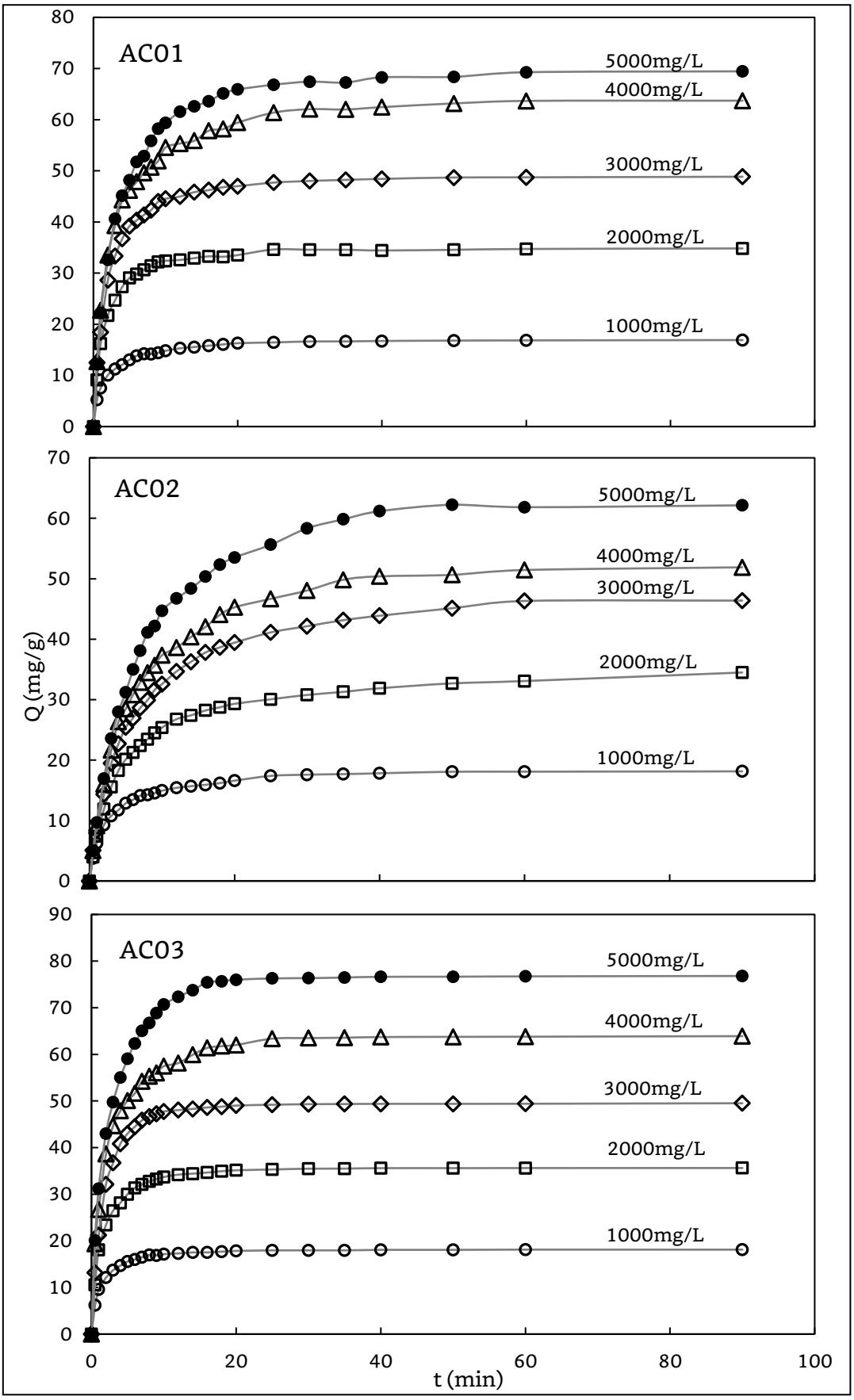

Figure 3.9 The experimental kinetic data of adsorbing DMAc of different initial concentrations on three types of activated carbons at 40°C

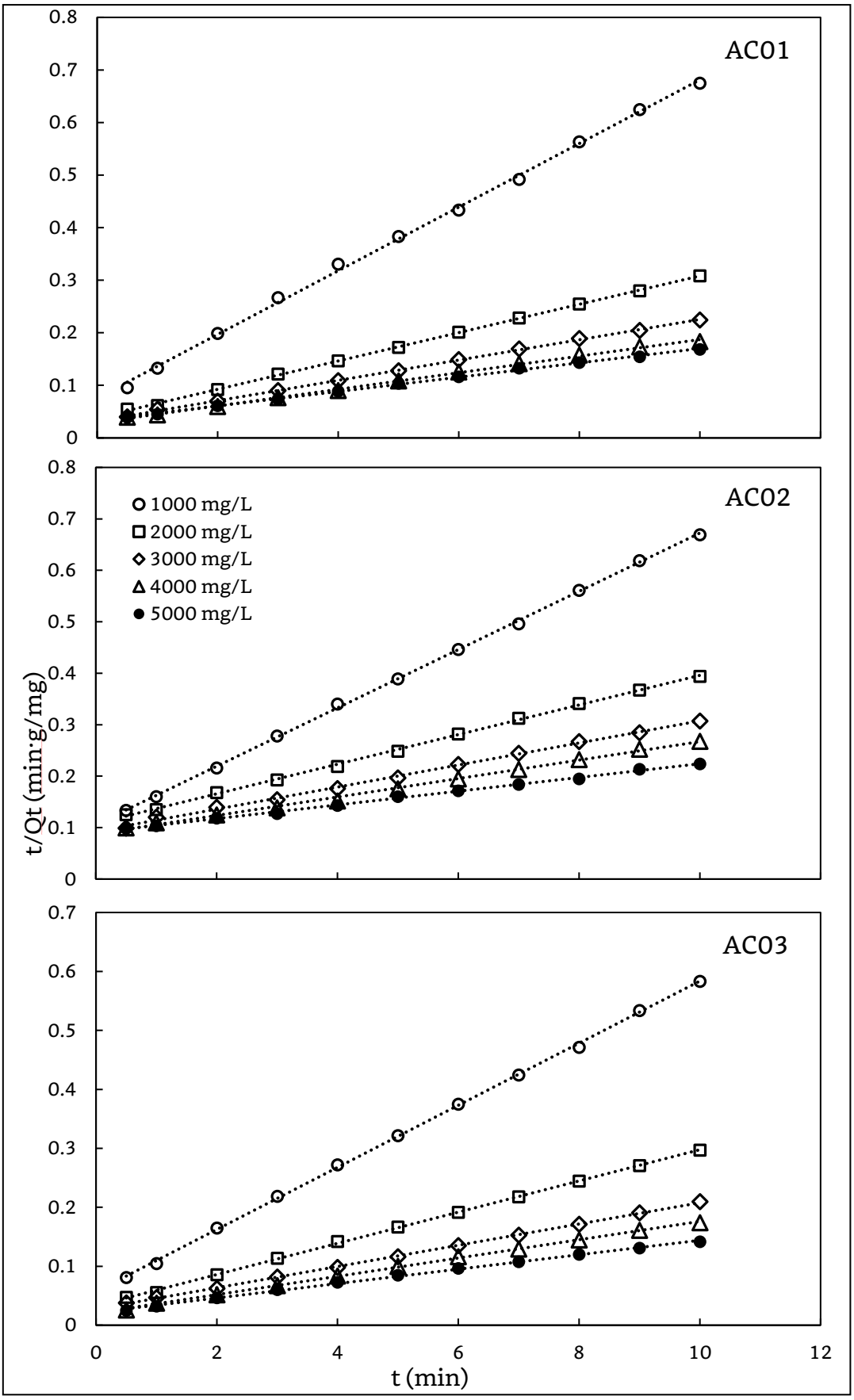

Figure 3.10 Patterns of data fitted into the linear form of pseudo-second order model for the kinetic adsorption of DMAc on activated carbons at 40°C of different initial concentrations

Table 3.6 Parameters of pseudo-second-order kinetic model for the adsorption of DMAc on activated carbons. Temperature 40°C

Adsor-bent	Experimental Data					Calculated Data of Pseudo-Second Order		
	Initial Concentration		Final Concentration (C_e)		DMAc uptake (Q_e)	DMAc uptake (Q_e)	Kinetic Rate Constant (k_2)	R^2
	(mg/L)	(mmol/L)	(mg/L)	(mmol/L)	(mmol/g)	(mmol/g)	(g/mmol·min)	
AC01	1000	11.47	154.4	1.773	0.174	0.172	29.47	0.999
	2000	22.95	258.9	2.975	0.370	0.353	23.69	0.999
	3000	34.43	557.8	6.403	0.511	0.498	13.23	0.999
	4000	45.91	814.4	9.349	0.701	0.654	6.474	0.999
	5000	57.39	1527.	17.53	0.727	0.714	5.730	0.999
AC02	1000	11.47	93.09	1.069	0.198	0.187	15.92	0.999
	2000	22.95	275.5	3.162	0.366	0.356	5.910	0.999
	3000	34.43	680.7	7.814	0.502	0.493	3.637	0.999
	4000	45.91	1405	16.13	0.566	0.553	3.346	0.999
	5000	57.39	1892	21.73	0.683	0.671	2.442	0.999
AC03	1000	11.47	94.47	1.084	0.198	0.184	48.20	0.999
	2000	22.95	219.1	2.515	0.379	0.361	28.57	0.999
	3000	34.43	524.7	6.023	0.528	0.503	22.85	0.999
	4000	45.91	805.1	9.241	0.673	0.654	10.46	0.999
	5000	57.39	1160	13.32	0.812	0.787	8.950	0.999

As shown in Table 3.6, the rate constant also varies with the initial DMAc concentration. This is against the general perception that the adsorption rate constant k_2 should only depend on temperature. This motivated us to look into the model fitting in more depth. It may be pointed out that in many previous studies, the kinetic rate constant was simply determined from the data fitting based on the pseudo-second-order model in the same manner without any questioning.[56]

For the adsorption of organic compounds on activated carbons, similar trends were reported with regard to the model parameters based on the pseudo-second-order kinetic model.[57][58] They found that the values the

rate constant k_2 so evaluated varied when changing the initial concentration of organic adsorbates.

The calculated values of kinetic rate constant k_2 and DMAc uptake at equilibrium Q_e from pseudo-second-order model seems to be good based on data fitting, and most previous work on adsorption kinetics reported in the literature was done in the same manner. However, further investigation reveals there are some issues. In the pseudo-second-order rate equation, Q_e is the equilibrium adsorption uptake, and the difference between Q_e and Q at a given time determines the adsorption rate at that moment. However, during the batch adsorption experiments, the DMAc uptake increases as adsorption proceeds. The Q_e in the kinetics equation should be the equilibrium uptake corresponding to the instantaneous DMAc concentration in the solution. Thus, the data fitting equation should be modified.

The pseudo-second-order reaction equation is:

$$\frac{dQ_t}{dt} = k_2(Q_e - Q_t)^{\,2} \tag{3.25}$$

With the Langmuir adsorption model for adsorption equilibrium, the adsorption uptake at solute concentration C_t will be given by the following equation if the adsorption would reach equilibrium:

$$Q_e = Q_{max}\frac{C_t K_l}{C_t K_l + 1} \tag{3.26}$$

For a batch adsorption process, a simple mass balance equation gives:

$$mQ_t = C_0 V - C_t V \tag{3.27}$$

where m is the mass of adsorbent (g), Q_t is DMAc uptake at time t, C_0 is the initial DMAc concentration, C_t is the DMAc concentration in the solution at time t, and V is the volume of solution (L). Rearranging equation 3.27 gives:

$$C_t = C_0 - \frac{mQ_t}{V} \tag{3.28}$$

Substituting equation 3.28 into equation 3.26 makes:

$$Q_e = Q_m \frac{K_l}{K_l + \frac{1}{C_0 - \frac{mQ_t}{V}}} \tag{3.29}$$

Then the pseudo-second order kinetic equation may be represented as:

$$\frac{dQ_t}{dt} = k_2' \left(Q_m \frac{K_l}{K_l + \frac{1}{C_0 - \frac{mQ_t}{V}}} - Q_t \right)^2 \tag{3.30}$$

Equation 3.30 is derived to explain the kinetics of an adsorption process in which equilibrium uptake Q_t is not constant during the course of adsorption, but is varying with time if the equilibrium follows the Langmuir model.

The modified kinetic rate constant k_2' (g/mmol·min) can be evaluated by fitting Equation 3.30 to the experimental kinetic data. Numerical solutions derived in Matlab® software (the original code is shown in Appendix C) was used in this study. For the data fitting, the values of Q_m, K_l, C_0, m and V, which are used in equation 3.30, are presented in Table 3.7, along with the calculated values of modified rate constant k_2.

The values of modified rate constant k_2' seem independent of the initial concentrations. As shown in Table 3.7, the modified values of rate constant k_2' of all three types of activated carbons do not fluctuate much at different initial DMAc concentrations. The evolving trends of rate constant k_2 from the traditional pseudo-second-order kinetic model are shown in Figure 3.11 as comparison, while the trends of the values of rate constant k_2' from the modified kinetic model are shown in Figure 3.12.

Table 3.7 Values of modified kinetic rate constant k_2 calculated from data fitting to equation 3.30 for the adsorption of DMAc on all activated carbons with different initial solution concentrations. (T, V, m, Q_{max} and K_l are also presented)

T=40°C		V=2L		m=100g	
K_l	Q_{max}	Initial Concentration C_0		Modified Rate Constant k_2'	Correlation Coefficient R^2
(L/mmol)	(mmol/g)	(mg/L)	(mmol/L)	(g/mmol·min)	
AC01					
0.1428	1.183	1000	11.48	0.268	0.997
		2000	22.96	0.277	0.989
		3000	34.44	0.266	0.997
		4000	45.91	0.273	0.994
		5000	57.39	0.275	0.984
				Average k_2': 0.270	
AC02					
0.2894	0.8390	1000	11.48	0.1665	0.997
		2000	22.96	0.1634	0.998
		3000	34.44	0.1784	0.994
		4000	45.91	0.1781	0.995
		5000	57.39	0.1768	0.990
				Average k_2': 0.1716	
AC03					
0.1070	1.208	1000	11.48	0.4726	0.991
		2000	22.96	0.4709	0.988
		3000	34.44	0.4895	0.979
		4000	45.91	0.4908	0.987
		5000	57.39	0.4953	0.933
				Average k_2': 0.4898	

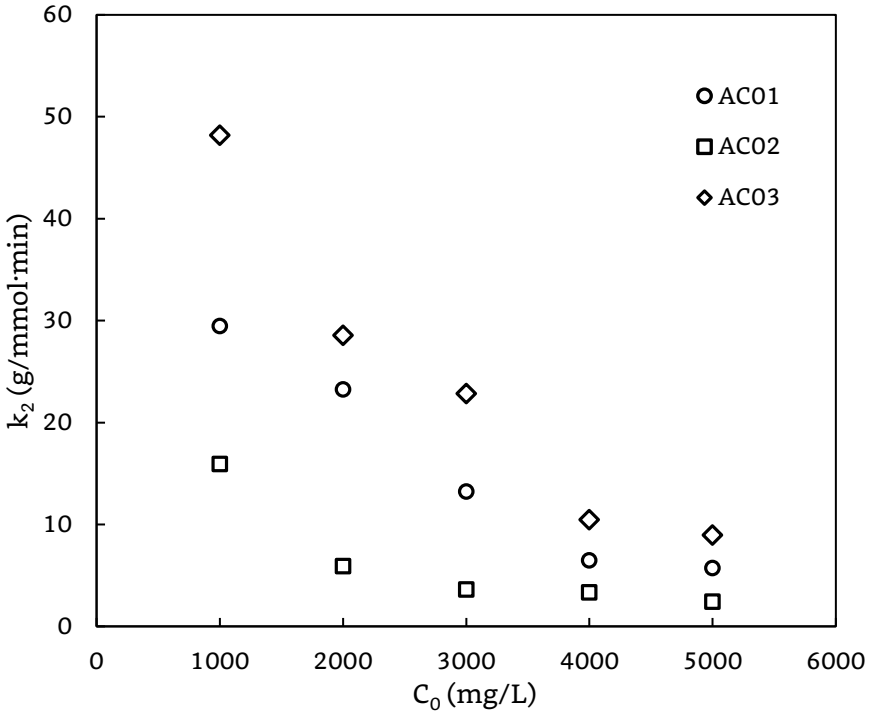

Figure 3.11 Values of the kinetic rate constant k_2 using traditional pseudo-second order model of three types of carbon adsorbent at five different initial concentrations

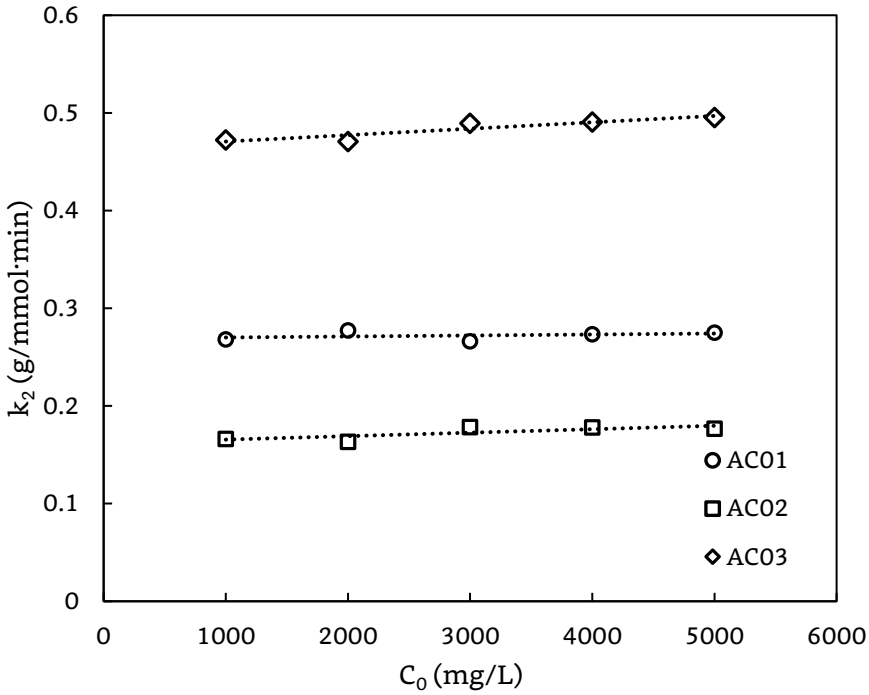

Figure 3.12 Values of the kinetic rate constant k_2' using modified kinetic model (equation 3.30) of three types of carbon adsorbent at five different initial concentrations

As it is apparently indicating in the figures, the rate constant k_2 obtained by traditional pseudo-second-order model shifts enormously as the initial adsorbate concentration changes, which is contrary to the

common knowledge. Whereas the rate constant k_2' obtained by the modified model are almost constant regardless how the initial adsorbate concentration changes, which expectedly further proves the feasibility of the modified model.

To check whether the newly calculated values of rate constant k_2' are adequate, the adsorption kinetics profile was calculated based on averages of the modified k_2'. The results are presented in Figure 3.13 for comparison with the experimental data. In general, the modified kinetic model works well to describe the experimental adsorption kinetics for DMAc adsorption on activated carbon.

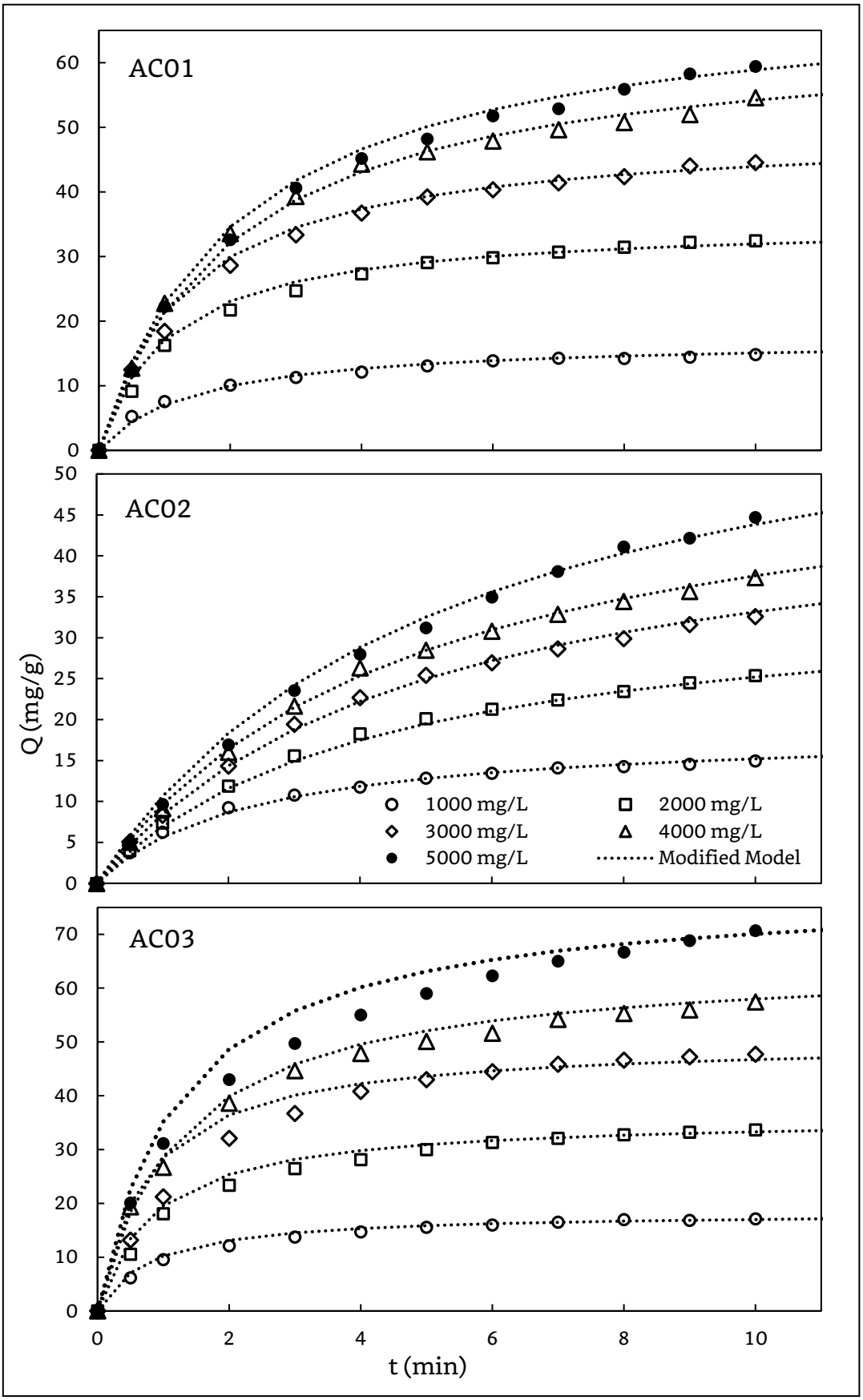

Figure 3.13 Patterns of fitting curves of the modified pseudo-second order model (equation 3.30) for the kinetic adsorption of DMAc on activated carbons at 40°C of different initial

concentrations using average values of kinetic rate constant k_2' and comparing to the experimental data

3.4.3 Adsorption-desorption Cycle Study

The adsorption-desorption study was carried out to investigate regeneration and reuse of the spent activated carbons. Ethanol was selected as the extracting agent for the desorption of DMAc from activated carbons. Ethanol is cheap and widely available solvent that has good solubility to many organic substances. DMAc is readily miscible with ethanol, and ethanol should be a strong extracting agent for stripping DMAc off the carbon surface. Tanthapanichakoon et al.[59] also found ethanol to be a viable extracting agent for desorption of phenol from activated carbon.

In the present study, two main parameters for adsorption-desorption cycles were considered: the overall equilibrium adsorption and the kinetic behaviour of adsorption after each cycle of regeneration All the adsorption processes in this recovery study were operated at room temperature (22°C). The equilibrium adsorption data of all activated carbons over five cycles of regeneration is shown in Figure 3.14, and the kinetic adsorption data of for the first, third and fifth cycle of regeneration are shown in Figure 3.15. Overall, there is no change in the adsorption characteristics after regeneration. The thermodynamic and kinetic parameters for DMAc adsorption on the activated carbon (pristine and regenerated) are presented in Table 3.8, based on the Langmuir model and the modified pseudo-second-order adsorption model, respectively.

Table 3.8 The Langmuir model parameters (Q_{max} and K_l) and modified pseudo-second-order model parameters (k_2') of DMAc adsorption on activated carbons.

	Q_{max} (mg/g)	K_l (L/mmol)	k_2' (g/mmol·min)
AC01	1.183	0.1428	0.2701
AC02	0.8390	0.2839	0.1706
AC03	1.208	0.1070	0.4898

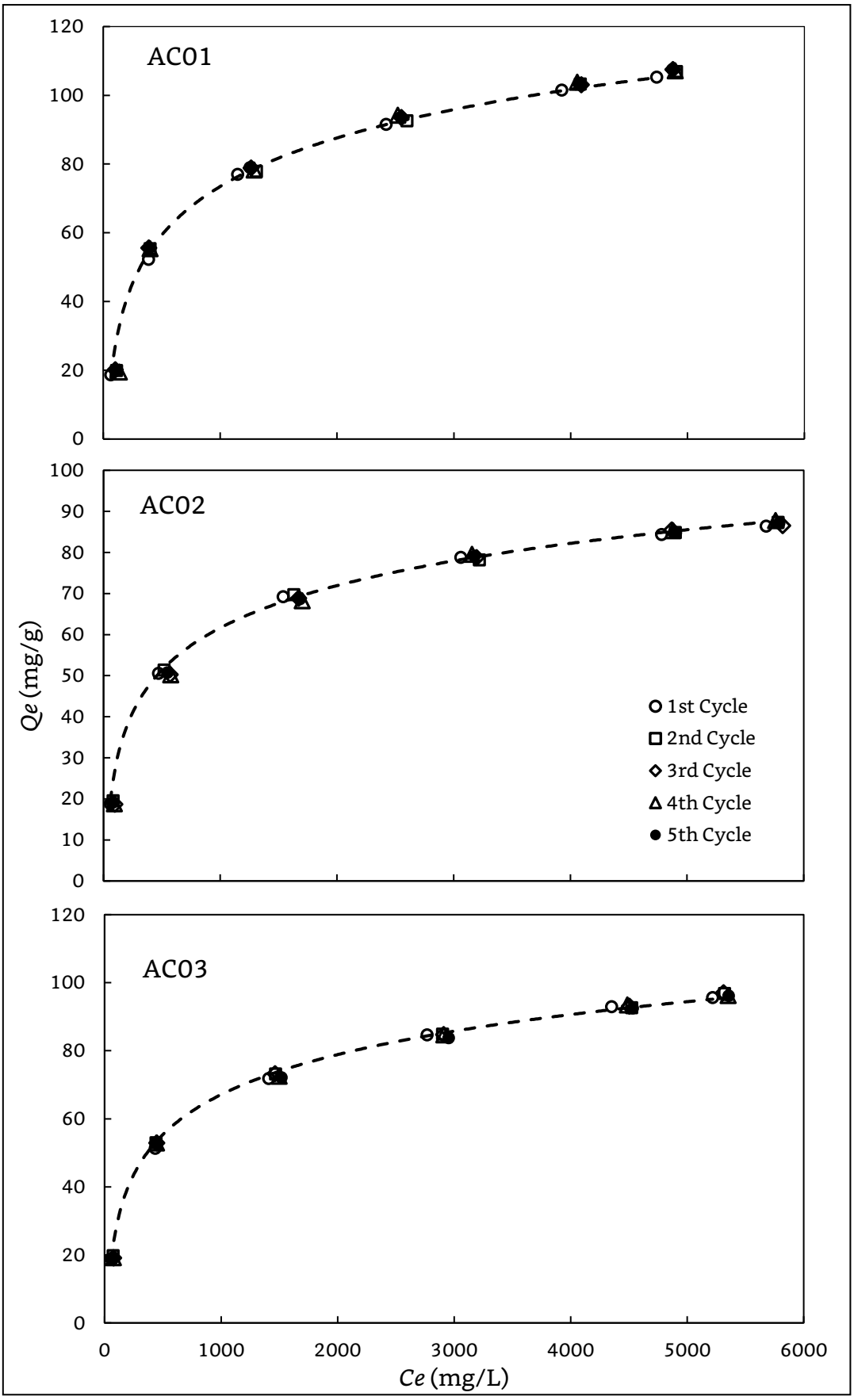

Figure 3.14 Equilibrium adsorption uptake of DMAc on *AC01*, *AC02* and *AC03* over five cycles of regeneration at 22°C, and the fitting of Langmuir model

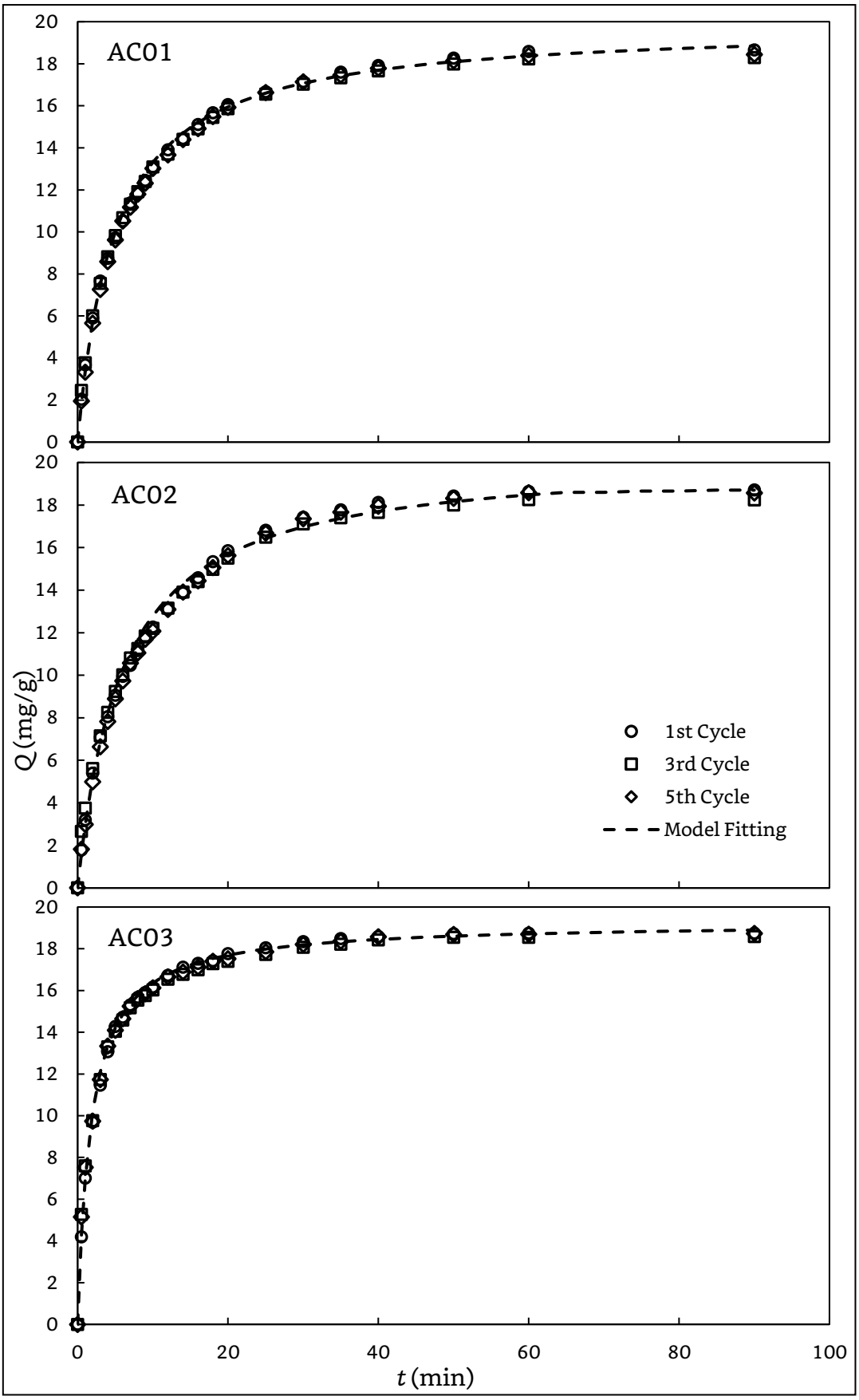

Figure 3.15 Kinetic profiles of DMAc adsorption on *AC01*, *AC02* and *AC03* after the first, third and fifth cycle of regeneration at 22°C, and the fitting of the modified kinetic model (equation 3.30)

The overall outcome of the adsorption-desorption cycle study was very pleasing. The outstanding performance of those recycles as well as the considerably low cost of ethanol as desorbent are favourable for practical applications of removing DMAc from water using activated carbons.

3.5 Conclusions

Batch adsorption experiments for the removal of DMAc from aqueous solutions were carried out using three activated carbons as adsorbents. The adsorption equilibrium, kinetics and adsorbent regeneration for reuse were investigated, and the following conclusions can be drawn:

- The adsorption of DMAc from aqueous solution to activated carbons followed the Langmuir isotherm.
- The thermodynamic study of the adsorption process indicated that the adsorption was spontaneous and exothermic.
- The adsorption kinetics was shown to follow the widely used pseudo-second-order adsorption model mathematically. However, the rate constant k_2 based on the traditional pseudo-second order kinetic model varied with initial adsorbate concentration which contradicted the assumption of constant rate constant in the model development.
- There was an oversight in using the model for data fitting, which was rectified to yield rate constant k_2' that was concentration independent.
- After the adsorbent was exhausted with DMAc, the exhausted activated carbons can be regenerated with the use of ethanol, and there was no change in adsorption characteristics after regeneration.

Chapter 4: Packed Bed Column Adsorption

4.1 Introduction

Column studies are necessary to assess dynamics of the adsorption system since mass transport occurs with the flow of liquid along the length of the column. The dynamic behaviour of adsorption in a column involves saturation of the adsorbent along the column in relation to time, and column length. In an adsorption column, the adsorbent is packed uniformly; as the liquid flows through the adsorber, the adsorbent will absorb DMAc before approaching local equilibrium.[60] Once the adsorbent is saturated with the adsorbate, no additional DMAc can be retained locally and thus there exists a mass transfer zone in the column that moves along the column length towards the effluent outlet. As a result, there is a concentration front that moves along the column length, there is always a contact with the fresh adsorbent before DMAc begins to appear in the liquid stream exiting the column.

For the removal of DMAc, the kinetics and equilibrium of adsorption have been explored in a batch system. These results are relevant to column adsorption where the activated carbons are packed in columns. The parameters derived from this study are useful for engineering design of industrial applications.

4.2 Experimental

The experimental setup for a continuous adsorption system consisted of a 35cm long glass column (inside diameter of 3/8" or 9.53mm). Activated carbons were packed uniformly and firmly into the column. The reservoirs of pure water and DMAc solution were more than three metres higher than column entrance, to provide the driving force for the fluid flow through the column under gravity. The height of carbon bed in the column was 265mm. A schematic of the column arrangement is shown in Figure 4.1. During the column study, the height of the packed bed (265mm), diameter (9.53mm) and the mass of adsorbent (depends on the type of the carbon used) were kept constant. Before feeding the DMAc solution into the column, the packed bed was filled with pure water by opening valve no.1 and no.2, then valve no.2 was closed and valve no.3 was opened to start the adsorption process. The flow rate was controlled by the special controlling unit on the feeding pipe. During the operation, 2ml of effluent fluid was collected by sample vials at specific times (every five minutes from starting). The effects of adsorbate concentration in the feed solution, feed flow rate and the performance of the fixed bed column after regeneration were studied. (Note: Height of column and height of packed bed are different; the height of packed bed, i.e., 265mm, was used in all calculations.)

The effects of feed flow rate on the performance of the adsorption column were studied by varying the feed flow rate (0.5, 1.0 and 2.0ml/min) while maintaining a constant DMAc concentration in the feed (1000mg/L).

The feed flow through the column was controlled using the controlling valve, and the actual flow rate was monitored during entire experiments by measuring the quantity of effluent exiting the column over a given period of time.

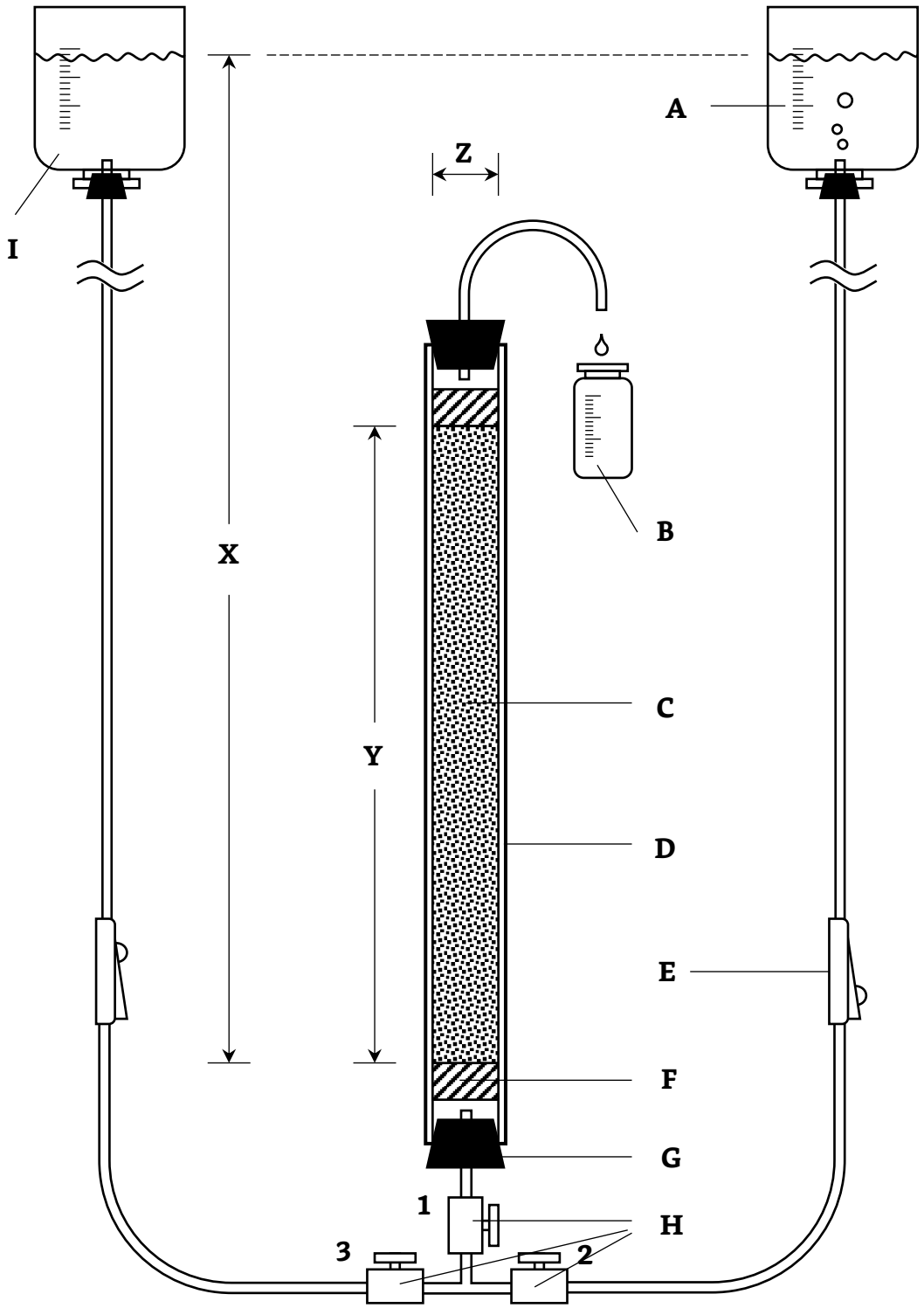

Figure 4.1 The setup for column study and sampling: (A) reservoir of DMAc aqueous solution (source of feed), (B) sample/test vial, (C) packed bed of activated carbons, (D) glass cylinder column, (E) fluid flow rate controlling unit, (F) glass fibre, (G) rubber stopper, (H) valves no.1, no.2 and no.3, (I) reservoir of pure water, (X) altitude difference between the liquid levels of the reservoirs and the entrance of the adsorbent bed, (Y) bed height *H*, (Z) column inner diameter Ø=3/8inches.

4.3 Results and Discussion

Only adsorbents *AC01* and *AC02* were used in this part of the thesis work. During preliminary tests, it was discovered that the packed column with *AC03* fine powders had a very large resistance to the fluid flow; the liquid solution could not penetrate the packed bed even under a pressure of 5-atm with the aid of a pump. As a matter of fact, even when the packed bed was shortened to 5cm long, the liquid solution was still unable to flow through the packed bed even under 5 atm. The solution to this issue will be elaborated in Chapter 5.

The breakthrough time and the shape of the breakthrough curve are important characteristics for determining the operation and the dynamic response of adsorption column. The adsorption breakthrough curve along the time axis depends on the capacity of the column with respect to the feed concentration, bed height and the flow rate.[61]

The breakthrough curves for DMAc adsorption are represented by plotting the ratio of adsorbate concentration in effluent (C) exiting the column at any time and the adsorbate concentration in the feed entering the column (C_0) versus time (t). The ratio (C/C_0) varies from 0 to 1 as the time lapses until the bed is completely saturated at which time the DMAc concentration in the feed becomes the same as the DMAc concentration exiting the column (i.e., $C = C_0$). The amount of DMAc adsorbed in the column can be determined from the area above the breakthrough curve constructed from (C/C_0) versus time.

The maximum uptake (equilibrium) capacity Q_m of activated carbons (mmol/g) packed in the adsorption column is calculated by the area under the plot of adsorbed DMAc concentration versus time (i.e., $1 - C/C_0$ vs t). It may be expressed by the mass balance equation:

$$Q_m = \frac{C_0 \cdot F}{1000m} \int_0^t \left(1 - \frac{C}{C_0}\right) dt \tag{4.1}$$

where C_0 and C are the DMAc concentrations in the feed and effluent, respectively (mmol/L), F is the volumetric flow rate at which the effluent solution is passed through the column (L/min), and m is the mass of adsorbent packed into the column (g).

To determine the amount of DMAc adsorbed, the time required to get the bed saturated with DMAc, the height of the bed, the flow rate and the breakthrough data were analysed using dynamic adsorption models. Three empirical models (i.e., the Yoon-Nelson model, the bed depth service time (BDST) model, and the Thomas model), are used in the data fitting. These models have been discussed in Chapter 2 (Literature review), and the model fitting to the breakthrough data is presented here.

The Yoon-Nelson model is described by:

$$ln\frac{C}{C_0 - C} = k_{YN}t - t_{\frac{1}{2}}k_{YN} \tag{4.2}$$

The Yoon-Nelson model was fitted to experimental data, $ln\left(\frac{C}{C_0-C}\right)$ versus t is plotted, which gives a straight line. The parameters $t_{\frac{1}{2}}$ (which are usually expressed as τ) and k_{YN} in this model can be calculated from its intercept and slope.

When the BDST model is used for data fitting, the following mathematical form may be used:

$$ln\left(\frac{C_0}{C} - 1\right) = ln\left[exp\left(k_B Q_m \frac{h}{u}\right) - 1\right] - k_B C_0 t \tag{4.3}$$

When $exp\left(k_B Q_m \frac{H}{u}\right)$ is much larger than 1, the BDST model can be reduced and rearranged as:

$$t = \frac{N_0}{uC_0}h + \frac{1}{k_B C_0} ln\left(\frac{C_0}{C} - 1\right) \tag{4.4}$$

which is similar to the Thomas equation, where N_0 also represents the adsorption capacity in the bed, similar to Q_m. The values of k_B and N_0 can

be calculated from the slope and intercept of the $ln\left(\frac{C_0}{C}-1\right)$ vs t plot. While most researchers[23] calculated the superficial flow velocity (u) here by simply dividing the volumetric flow rate (F) by the interior sectional area of the column ($A_0 = \frac{\pi D^2}{4}$), it might be better to take the bed porosity (ε) into consideration. There are several empirical correlations for evaluating ε, the one proposed by Pushno[62] was employed in this project due to its simplicity:

$$\varepsilon = \frac{A}{(D/d)^n} + B \tag{4.5}$$

where D is the inner diameter of the column, d is the average diameter of the carbon granules, A, B, and n are constants depending on the shape of the granules (for the values of A, B, and n, check Table C.1 in Appendix C). Therefore, the modified flow velocity (u) can be further obtained by:

$$u = \frac{F}{\varepsilon \cdot \frac{\pi D^2}{4}} \tag{4.6}$$

The linearized form of the Thomas model is given as:

$$ln\left(\frac{C_0}{C}-1\right) = \frac{k_{Th} m Q_m}{F} - k_{Th} C_0 t \tag{4.7}$$

or

$$F \cdot ln\left(\frac{C_0}{C}-1\right) = k_{Th} m Q_m - k_{Th} C_0 V \tag{4.8}$$

The Thomas rate constant (k_{Th}) and maximum solid phase concentration (Q_m) can be evaluated by plotting $ln\left(\frac{C_0}{C}-1\right)$ versus V, which yields a straight line. Here V is the volume of effluent exiting the column. The slope of this straight line is used for the calculation of k_t and the intercept is used to determine the maximum solid phase concentration Q_m.

4.3.1 Effects of Flow Rate

The adsorption performance of fixed bed activated carbon column was tested at various flow rates ranging from 0.5 to 1.5ml/min. The breakthrough curves for adsorption in *AC01* and *AC02* packed columns are

presented in Figures 4.2. As expected, at a higher influent flow rate, the breakthrough was achieved earlier.

The change in flow rate affected the column performance. The time to achieve adsorption breakthrough decreased with an increase in the flow rate. This is because that at a higher flow rate, the binding sites available on the surface of the carbon granules become occupied more quickly by DMAc molecules which caused the adsorbent to exhaust more rapidly. By increasing the flow rate, the maximum uptake capacity of activated carbons Q_m maintained stable.

Table 4.1 Maximum saturation capacity of activated carbon packed bed column at different influent flow rate with constant DMAc concentration (1000mg/L). (Bed height = 10cm, Diameter = 0.35cm, mass of carbon = 0.8g)

Flow Rate (ml/min)	0.5	1.0	1.5
Adsorbent	Uptake at saturation (mmol/g)		
AC01	1.17	1. 17	1. 17
AC02	0.76	0.76	0.76

The values of maximum uptake capacity of activated carbon packed bed column Q_m at different flow rates are calculated using equation 4.1, and they are presented in Table 4.1. Apparently, the values of Q_m at different influent flow rates are almost constant. This is easy to understand because Q_m corresponds to the uptake when DMAc in the adsorbent bed was in equilibrium with influent liquid.

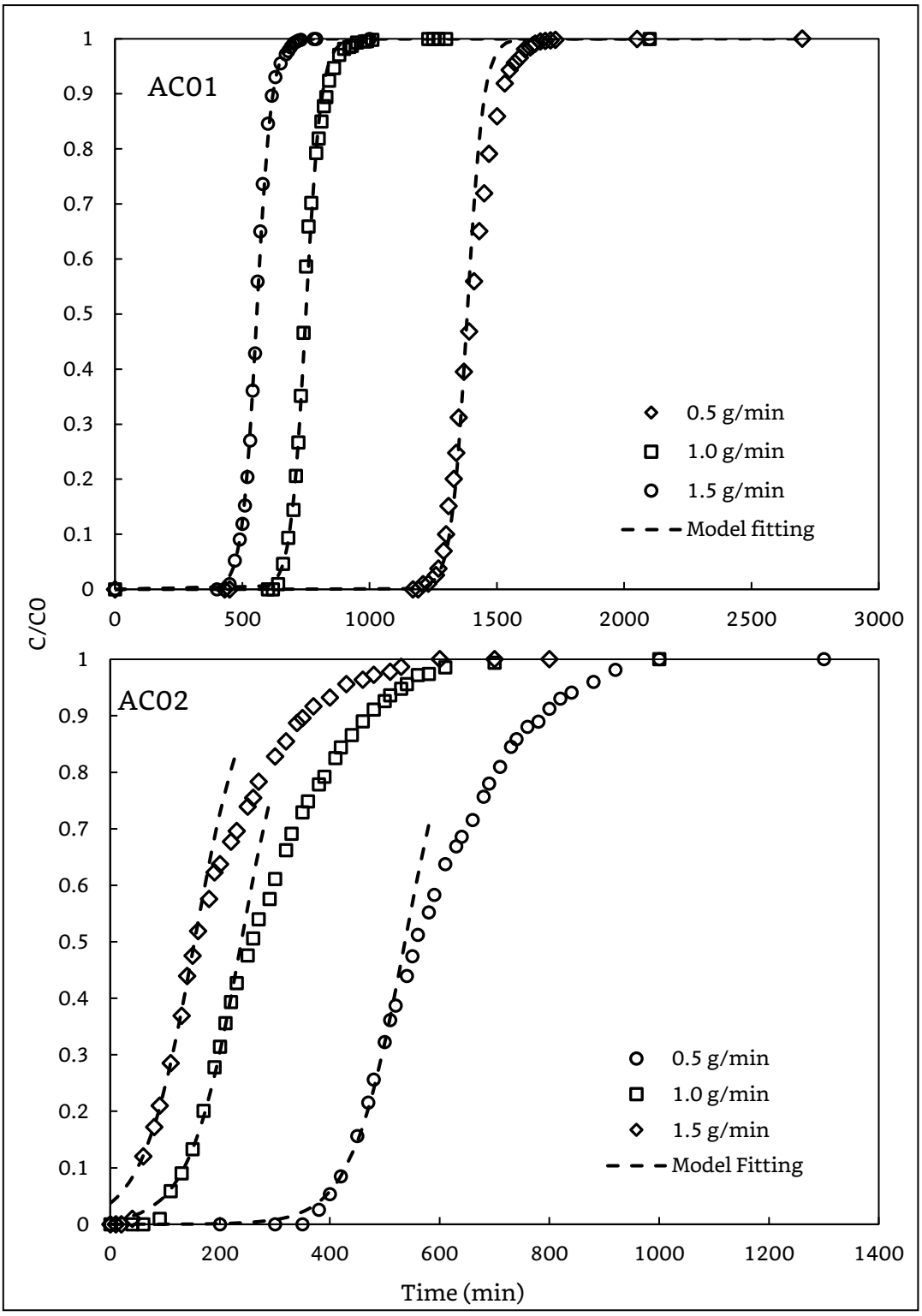

Figure 4.2 Breakthrough curves for adsorption of DMAc in packed bed columns of *AC01* and *AC02* at different flow rates. Data fitting with the Yoon-Nelson model is also shown.

The breakthrough data in Figure 4.2 was fitted with the Yoon-Nelson model, the BDST model, and the Thomas model. Data fitting with the Yoon-Nelson model is presented in Figure 4.3, and the calculated parameters of Yoon-Nelson model are presented in Table 4.2. The

correlation coefficients R^2 for the data fitting are very close to 1, indicating a good fit of experimental data to the model. The values of τ, time to achieve 50% breakthrough decreases with an increase in the flow rate for both adsorbents studied. For both adsorbents, the Yoon-Nelson rate constant k_{YN} for the adsorption of DMAc tend to remain constant, not affected by the flow rate.

Using the parameters k_{YN} and τ obtained, the breakthrough curves can be predicted using the model. For this purpose, the Yoon-Nelson model equation is rearranged as follows:

$$\frac{C}{C_0} = \frac{C_0 \cdot exp[k_{YN}(t-\tau)]}{1 + exp[k_{YN}(t-\tau)]C_0} \tag{4.9}$$

The breakthrough curves predicted based on equation 4.9 is also shown in Figures 4.2 (dash lines). There is a good agreement between experimental data and model calculations, although a deviation was observed for *AC02* when the DMAc concentration in effluent is high enough.

Furthermore, the breakthrough data is fitted to the bed depth service time (DBST) model, and the data fitting is presented in Appendix D (Figure D.1). The values of characteristic parameters of the model, i.e., maximum solid phase concentration (Q_m) and dynamic rate constant (k_B), are presented in Table 4.2 as well. A correlation coefficient R^2 close to 1 was obtained for the data fitting. With an increase in initial DMAc concentration in the feed, the values of N_0 also increased, and the rate constant k_B decreased. Increasing the initial DMAc concentration resulted in a reduction in the dynamic rate constant k_B of the BDST model.

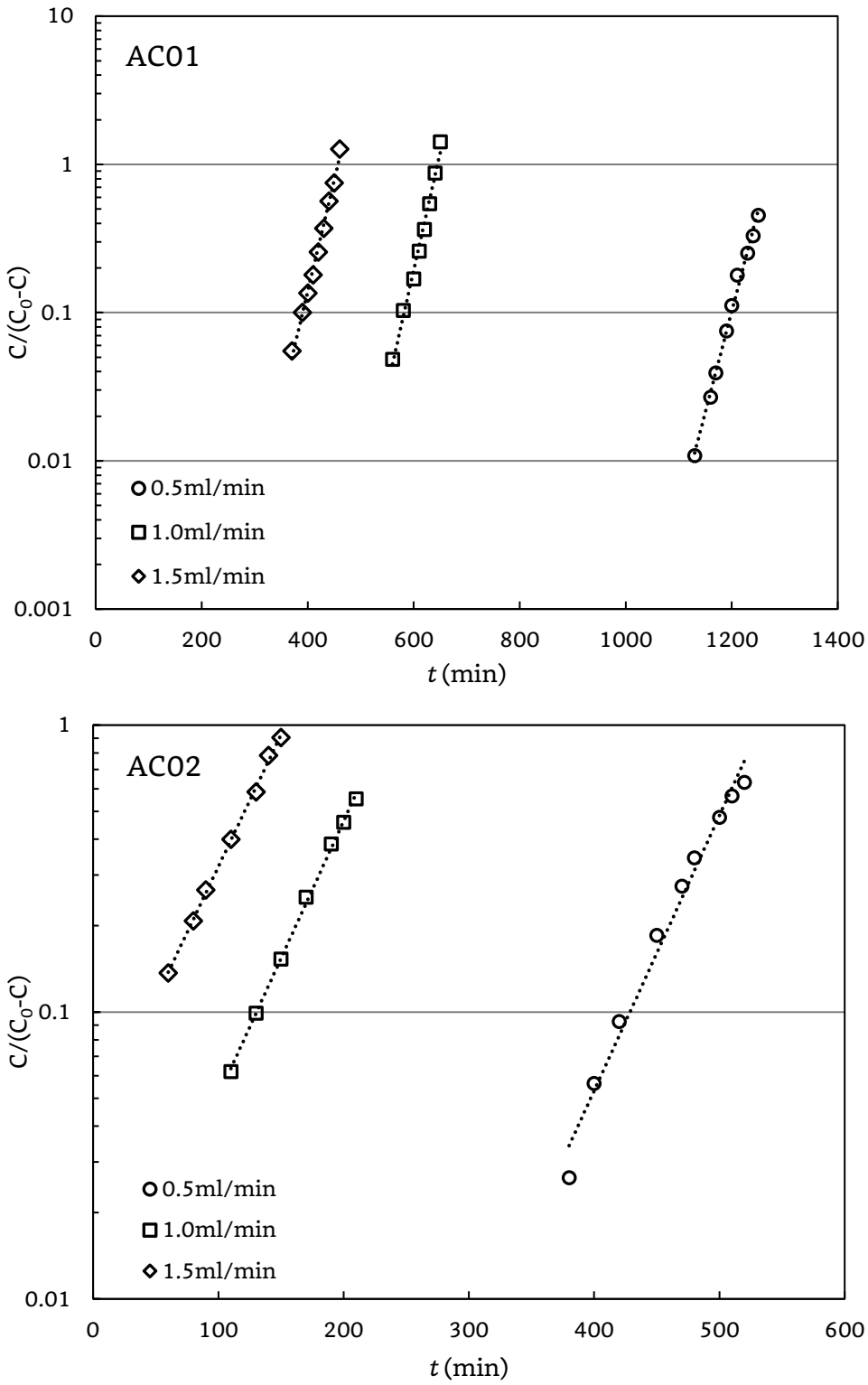

Figure 4.3 Breakthrough data fitting with the Yoon-Nelson model for removing DMAc from effluent exiting the packed bed columns of *AC01* and *AC02* at different flow rates.

Similarly, the Thomas model was also tested for fitting to the experimental data for the adsorption of DMAc flowing through the activated carbon packed bed column at different effluent concentrations. This is

shown in Appendix D (Figure D.2). The model parameters, dynamic rate constant (k_{Th}) and maximum solid phase concentration (Q_m), are evaluated and are presented in Table 4.2. The Thomas model also gave a good fit to the breakthrough data. The calculated Thomas rate constant (k_{Th}) decreased with an increase in the influent DMAc concentration, while the maximum solid phase concentration (Q_m) increased.

Table 4.2 Parameters of Thomas model, BDST model and Yoon-Nelson model calculated from breakthrough data fitting.

Adsorbent	Flow Rate (ml/min)	Yoon-Nelson Model			Thomas Model			BDST Model		
		τ (min)	k_{YN} (min^{-1})	R^2	Q_m (mmol/g)	k_{Th} (L/mmol·min)	R^2	N_0 (mmol/L)	k_B (L/mmol·min)	R^2
AC01	0.5	1270	0.0345	0.99	4.108	1.820	0.99	67.99	3.361	0.99
	1.0	644	0.0346	0.99	3.929	1.906	0.99	69.90	3.214	0.99
	1.5	456	0.0345	0.99	3.672	1.991	0.99	73.28	3.023	0.99
AC02	0.5	532	0.0221	0.99	9.625	0.5264	0.99	36.17	2.224	0.99
	1.0	235	0.0221	0.99	9.717	0.4826	0.99	37.91	2.194	0.99
	1.5	153	0.0220	0.99	11.12	0.4277	0.99	38.42	2.045	0.99

Ahmad et al.[63] found similar results while performing the dynamic adsorption of azo dye solution flowing through a packed bed of activated carbons. With an increase in the flow rate, an increase in the uptake and a decrease in the breakthrough time were reported. The breakthrough data followed the BDST model, Yoon-Nelson model and the Thomas model; they reported similar effects of flow rate on the model parameters.

4.4 Conclusions

In this chapter, adsorption of DMAc in a fixed bed column packed with two types of activated carbons was studied; the following conclusions can be drawn:

- The saturation capacity of the activated carbon bed was independent of the feed flow rate.
- All the three models (i.e., Yoon-Nelson model, BDST model and Thomas model) fit well to the experimental data; the bed depth service time model and Thomas model, which are essentially equivalent common basis, described the adsorption breakthrough equally well.
- *AC01* has better performance than *AC02* in terms of uptake capacity, column operation duration and packing density.

Chapter 5: Hollow Fibre Contactor for DMAc Adsorption on Activated Carbons

5.1 Introduction

Activated carbons have proved themselves as potential adsorbents for removing DMAc, and the column studies have proved that a packed bed design worked well when the activated carbon particle size is not very small. However, an important issue was encountered. *AC03*, which showed the best adsorption performance during the earlier equilibrium and kinetic studies among all three types of ACs, was unsuitable for use in the regular packed columns due to its fine powder form which resulted in an excessively large pressure drop through the packed bed. Therefore, alternative contactor design was required to utilise *AC03* as adsorbent while overcoming the large resistance to fluid penetration.

The idea was to use hollow fibre (HF) membrane contactors, which can lower the overall fluid resistance substantially. With different purposes, the contactors can be constructed into various configurations, each having advantages and disadvantages. Several typical configurations of HF contactors were built and tested, and some of them showed great prospects.

The structure of the HF contactors employed in this project could be scaled-up easily with predictable efficiency and capacity by just extending the length of the modules or increase the number of hollow fibres. It can also

minimise the loss of the adsorbents packed inside because the fine powders were immobilised by the hollow fibre themselves, lowering the cost of maintenance and eliminating the potential secondary water contamination.

The experiments for this part were not exhaustive, due to time limitation and the incalculable amount of possibilities of the structural design of the contactors. This chapter was just to discuss the features of the HF contactors, in order to reveal the tip of the iceberg and provide an inspiration for further research in future.

5.2 Experimental

The powdered activated carbons confined with microfiltration hollow fibre membranes for water treatment are relatively less developed, and there are very few existing reports on the topic. Consequently, this part of the experiment was carried out step by step, with each step using a new contactor module modified based on the outcome of preliminary tests carried out prior, just like *crossing the river by feeling the stones.* The modification on the setup and the procedures were mainly on the detailed structures of the hollow fibre modules.

5.2.1 Diffusion Through Hollow Fibre Walls

The setup resembles that in the column study (reported in Chapter 4), except that a peristaltic pump was used to supply the feed liquid to the hollow fibre modulated carbon bed, as shown in figure 5.1. There were two reservoirs, one was for pure water, the other for 1000 mg/L DMAc solution. Both reservoirs were connected to a peristaltic pump (Model 7553-80 Cole-Parmer Instrument Co.) for forcing the solutions to penetrate the adsorber modules. All the hollow fibre modules were positioned vertically with the feeding stream entering the module from the bottom.

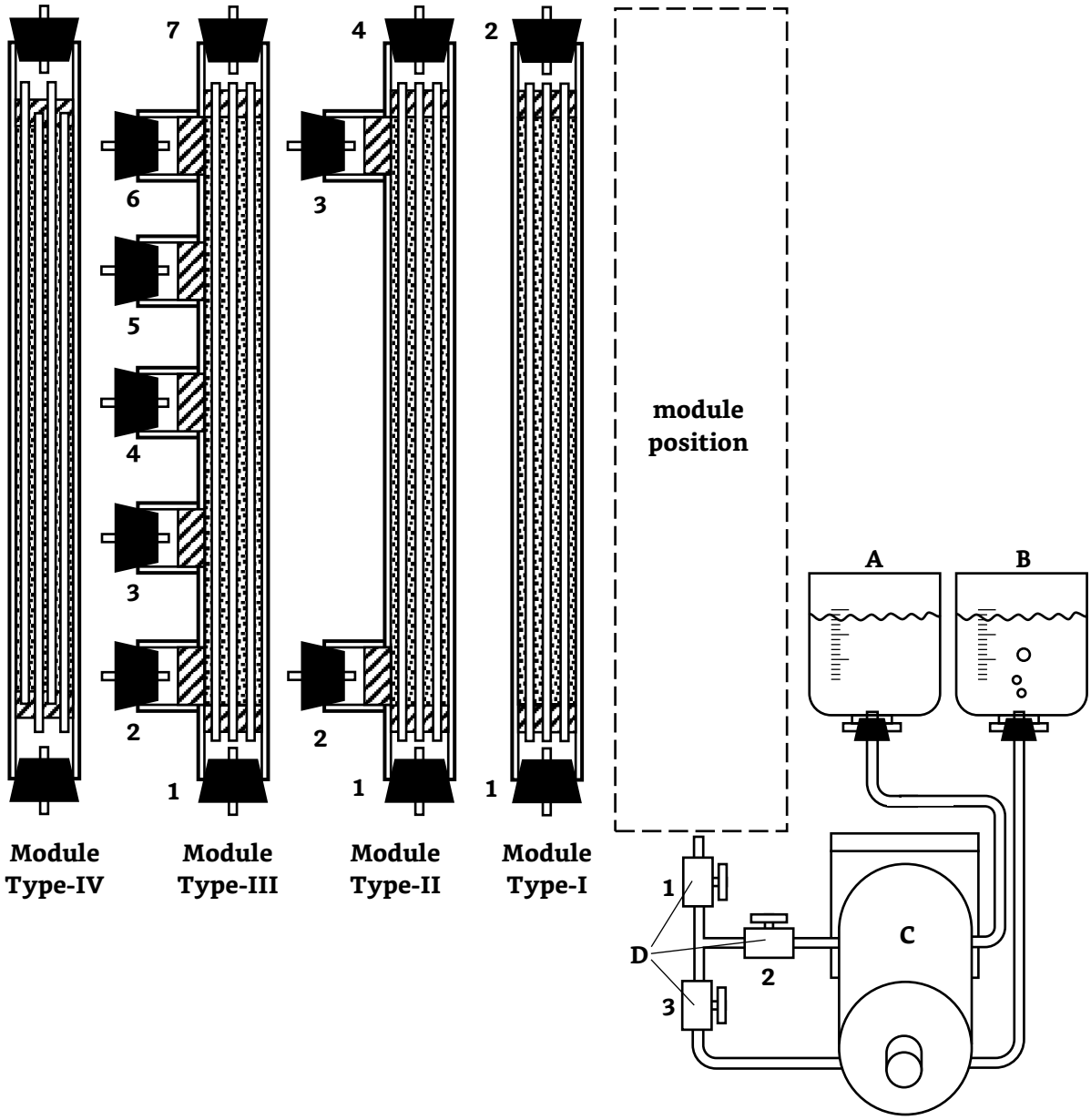

Figure 5.1 Setup of experimental hollow fibre contactors: (A)reservoir for pure water, (B) reservoir for DMAc solutions, (C) peristaltic pump, (D) valves no.1, no.2 and no.3. As well as three types of hollow fibre modules and the numbering of their gates.

All the modules consisted the following basic opponents: semi-translucent polyethene tubes with 3/8" diameter which was used as the hollow fibre housing, hollow fibres (product of Hoechst Celanese©, Celgard™, serial number 6545-41-01-05, inner diameter = 0.6mm, pore diameter = 0.22μm, wall thickness = 300 μm), epoxy seals (2 Ton™ Clear Epoxy, Devcon©), glass-fibre cotton filters, and activated carbon powder adsorbents. Due to the limitation of the diameter (3/8") of the chamber, the

quantities of the hollow fibres in each module were set to 60, making the volumetric ratio of the interior and exterior of the hollow fibres 1:1.

Inspired by Pan and MacMinis[64], two forms of adsorbent packing were tested: one was to pack the activated carbon outside the hollow fibres (shell side, shown in Figure 5.2(a)), sealing both ends of the fibres to confine the activated carbons and leaving the hollow fibre bores open to allow for fluid flow; the other was to pack the activated carbons inside the hollow fibres (tube side, shown in figure 5.2(b)), sealing the fibres to immobilise the activated carbons in the fibre lumens. Unlike the traditional membrane modules for fluid separation where the separation is based on selective permeation through the membrane, the porous hollow fibre membranes used in the contactors cause no separation for DMAc solute.

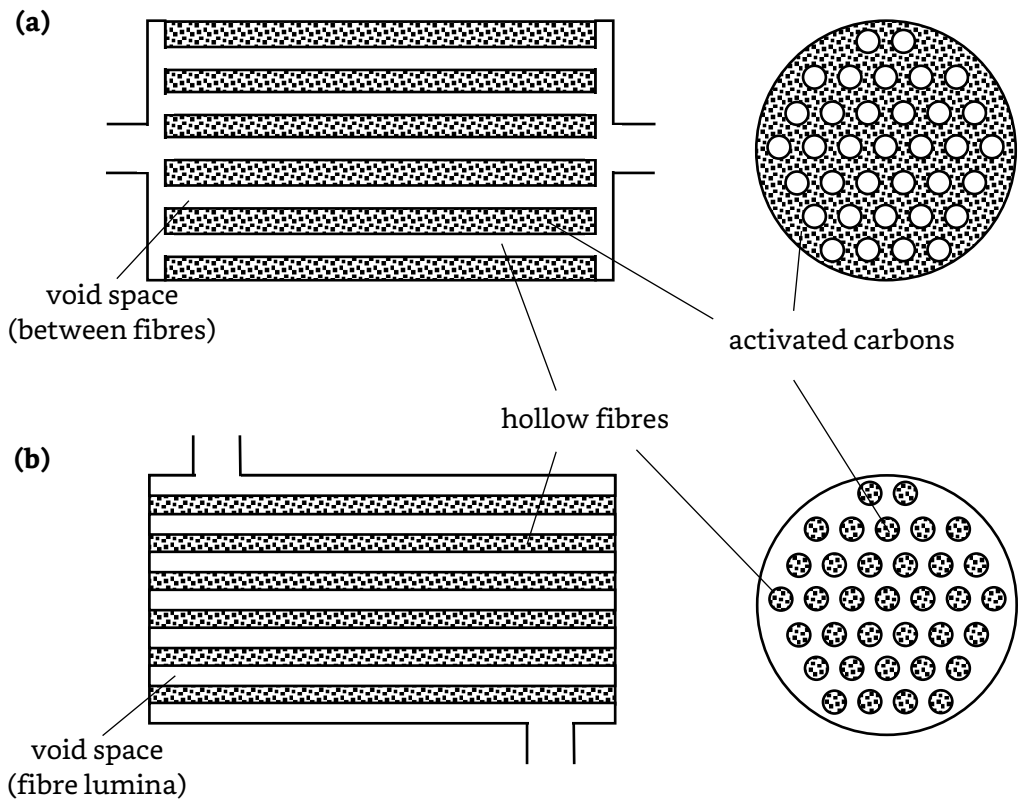

Figure 5.2 Schematic of activated carbon adsorber (a) shell side packing and (b) tube side packing

It was found out soon afterwards, when under manual operating conditions, the inner diameter of the hollow fibres was so tiny that it was extremely difficult to pack the *AC03* powder in the fibre lumen, and this

design [illustrated in figure 5.2(b)] was not studied further, and all the modules reported in this thesis fall into the category shown in Figure 5.2(a).

Among the prototype series of hollow fibre modules built in this project, module type-I has the simplest structure. It could be regarded as a type-II design with side opening no.2 and no.4 sealed. 60 hollow fibres with a length of 320mm were inserted into a 340mm-long tube, and one end of the shell side was sealed with epoxy. It took about 48 hours for the epoxy to fully harden. 4.5g of *AC03* powder was loaded to shell side densely and carefully, leading to a carbon packing length of 265mm. The remaining end of the shell side was sealed with epoxy to completely confine the carbon powders within the module.

When being tested, module type-I was incorporated into the experimental setup, shown in Figure 5.1. Valves no.1 and no.2 were opened while the valve no.3 was closed. The pump was turned on to let pure water flow into the module until it was clearly observed that all void spaces in the module were filled with water and that water began to exit the module from the top outlet. After waiting for about an hour for the activated carbon to be fully water wet, valves no.1 and no.3 were opened and no.2 was closed so that the DMAc solution began to enter the module, and the timer was started instantly. The liquid flow rate was controlled by the pumping rate. During the operation, 2ml of effluent fluid was collected in sample vials atdifferent instant during the course of the adsorption process.

It has been reported[37] that the solute could move through the membrane towards the adsorbent due to concentration difference between the two sides of the membrane, where one side was at the high concentration (in the feeding stream) and the other side was at a much lower concentration (in the adsorbent). This experiment was designed to study this diffusion behaviour through the hollow fibres without any pressure difference added to the two sides of the membrane. Figure 5.3 shows the

ideal pattern of the fluid path in this type of hollow fibre modulated carbon adsorbers.

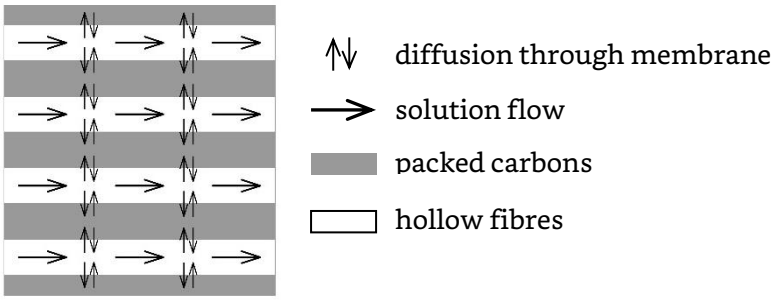

Figure 5.3 Schematic of how substances flow and diffuse inside a type-I hollow fibre contactor module

The breakthrough curves for DMAc adsorption were obtained by measuring the concentration of DMAc in the effluent during the course of adsorption process.

5.2.2 Direct Flow Through the Hollow Fibre Walls

In the aforementioned hollow fibre contactors, the fluid flowed through an unobstructed passageway and the fluid/particle contact is primarily due to diffusion through the porous hollow fibre walls.

The module was modified and upgraded to type-II, by adding two side openings (no.2 and no.3 shown in Figure 5.1) at the ends of the module. Two short tubes were installed to the main tube using super glue or tees (illustrated in Figure E.1, appendix E). The two new opening tubes were filled with abundant fibre-glass wools to keep the carbon powders immobilised and prevent adsorbent loss.

The interior of hollow fibre module type-II replicated that of type-I, with 60 random positioned hollow fibres and 4.5g of *AC03* powders densely packed around the fibres with the height of 265mm. The detailed structure and flow directions during adsorption are illustrated in Figure 5.4.

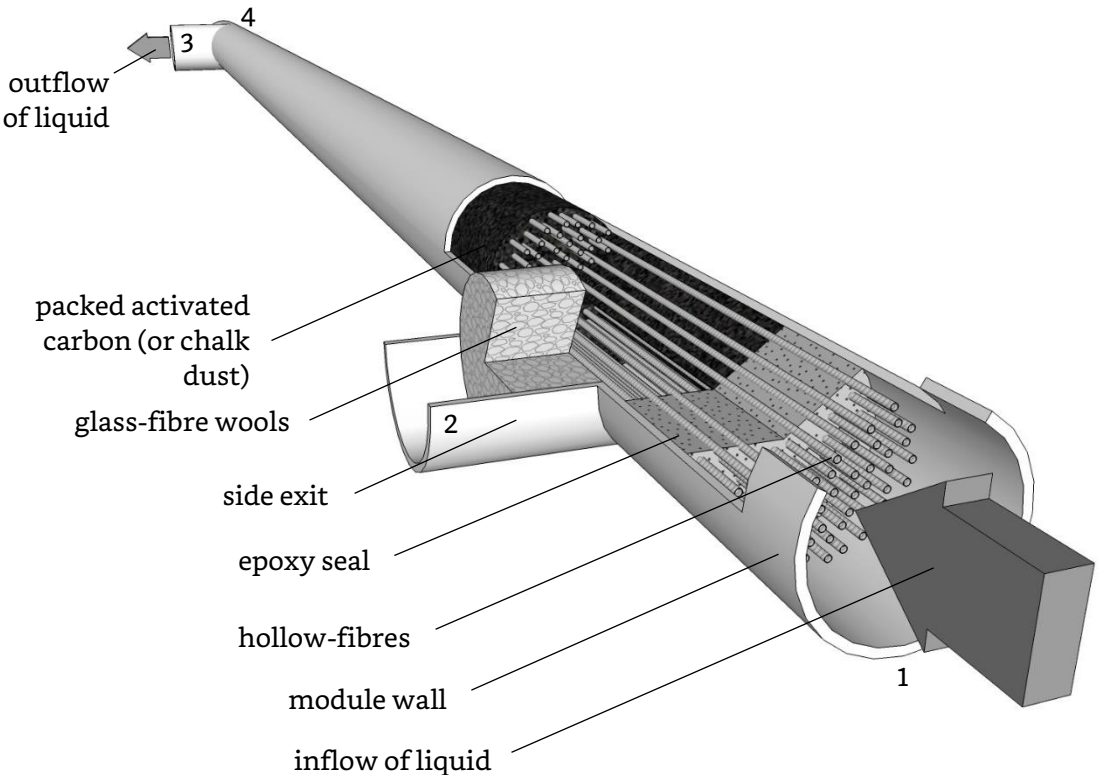

Figure 5.4 Schematic structure of hollow fibre contactor module type-II

When the module position was secured in place, opening no.3 was used as the only exit for effluent, opening no.1 was connected to the pump, and openings no.2 and no.4 were sealed. The feed entered the module straight to the interior of the hollow fibres and was forced to go through fibre walls to directly contact the adsorbent powders before flowing out from the side outlet. Obviously, forcing the fluid to flow through the packed particles was the major difference from the Pan and McMinis configuration.

Inflow rates of 0.5 and 1.0ml/min were examined, which were controlled by the rotational speed of the pump. During the operation, 2ml of fluid effluent was collected in sample vials periodically (every five minutes from start). The effect of flow rate and the overall DMAc removal efficiency of this design was studied. Another setting (sealing openings no.1 and no.3, feed stream entering through opening no.2 to the packed shell side and exiting from no.4) should yield identical results, but in order to maintain the same flow rates, the pump has to endure a much higher pressure, because

the carbon powders could block the micropores on the membrane easily when pressurised from the packing side.

An additional test was run at 0.5ml/min, while *AC03* was replaced with white chalk powders and the DMAc solution was replaced with standard black 'Parker' ink, respectively. This allowed us to investigate how the liquid streams flowed through the packed adsorbent, since the actual flow of the black ink running through the packed white chalk powder could be clearly observed and recorded by a time-lapse camera. All other configurations and operation procedures remained unchanged.

Then three more identical side openings were added to the module, with the same distance between each other, turning it into the new hollow fibre contactor module type-III. When module type-III was used, opening no.1 was connected to the pump, and opening no.7 was sealed. Openings nos. 2-6 were used as effluent outlets. The inlet flow rate was set to 1.0ml/min. The DMAc solution was forced to penetrate the membrane from the tube side to the shell side to contact with the activated carbon and flowed out of the module through the five side outlets. During the operation, 1ml of effluent fluid was collected in sample vials periodically (every ten minutes) at all five exits. This allowed to further investigate to what extent the number of effluent exits would affect the overall performance of the adsorbers.

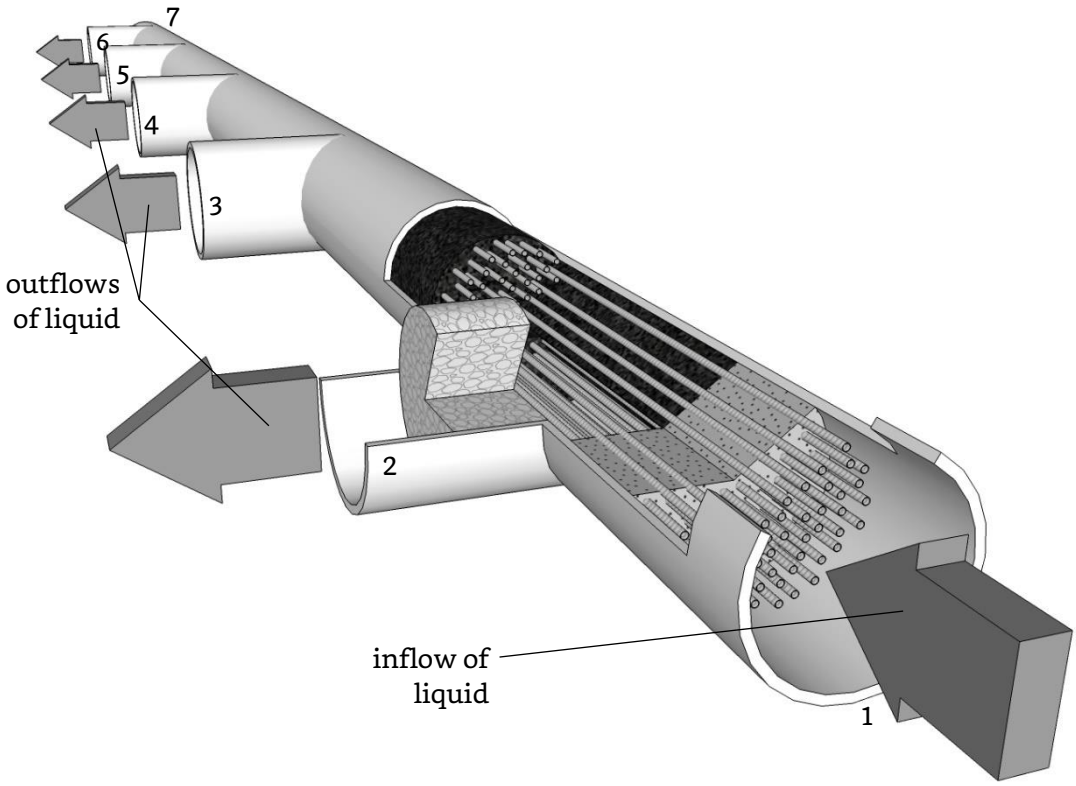

Figure 5.5 Schematic of hollow fibre contactor module type-III

5.2.3 Asher Configuration

In the aforementioned hollow fibre contactors, the fluid could hardly reach the entire packed adsorbents. As further improvements, Asher[65] proposed an alternative configuration for the case of packing the particles on the shell side, namely module type-IV in this project. In this case, the hollow fibres were divided into two groups; one was for receiving and distributing the fluid to be treated (inflow fibres), and the other was for collecting and discharging the treated fluid (outflow fibres). All the hollow fibres were sealed at one end and an individual fibre could only be used as an entrance to the module or an exit. The detailed structure is described in Figure 5.6. The spaces between the hollow fibres were packed with the adsorbents (shell side). Similar to modules type-II and III, as the fluid flowed in the lumen of the inflow fibres towards the sealed end, the liquid stream was compelled to penetrate through the walls of the inflow fibres to directly contact the carbon adsorbents before entering the lumen of the outflow fibres to exit the contactor, as shown in Figure 5.6(b).

There are usually two different configurations for shell side packing, regarding flow direction, as shown in Figure 5.6(a). One is that the open ends of inflow and outflow fibres in opposite direction (ii), and the other configuration is that they are in the same direction (i). Considering the simplicity of operation, it is always easier to feed and discharge in separate ends of the module, so the configuration in Figure 5.6(a)(i) was used in this project.

During the production of module type-IV, it is important to maintain an even spacing between the inflow and outflow fibres to ensure a relatively uniform thickness of the packed particle layer. Otherwise, an uneven flow path through the packed adsorbent will result, causing uneven contacts and undermining the efficiency of the contactor. Preferably, the inlet and outlet hollow fibres are spaced alternately and evenly.

Usually, weaving fabrics or threads can be used to achieve an even distribution of the hollow fibres inside the module. However, in this project, due to the limitation of the module's inner diameter, there was not enough room to place weaving fabrics, and the relatively short modules used here did not make fabrics essential. In this project, the hollow fibres in all the modules were kept tightened so that all fibres were kept straight in shape and did not need additional fabric supports.

Modules of three cross-sectional configurations (the sectional view showing different forms of patterns that two neighbouring hollow fibres having different hydrodynamic relationships) were produced and tested in this project, as a result of three different assembling techniques. The three configurations were named as square, triangular, and spiral, as shown in Figure 5.6(c). All these configurations used 60 hollow fibres in total, 30 for inflow and 30 for outflow purposes.

The spiral configuration was tested at flow rates of 0.5 and 10ml/min; the square and spiral configurations were tested at a flow rate of 0.5ml/min.

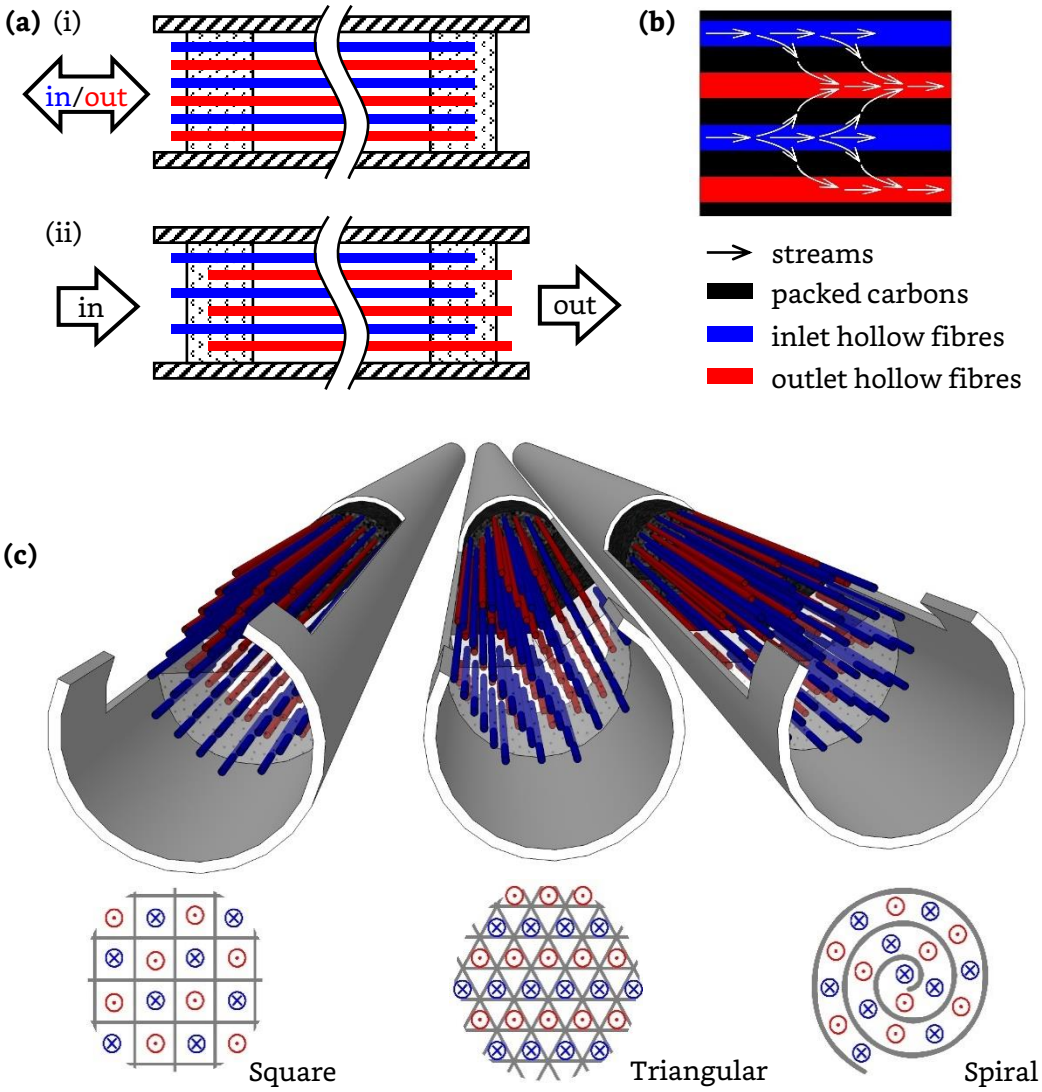

Figure 5.6 Schematics of (a) the sealing configurations of the hollow fibres as well as the module, (b) the flow pattern of the streams within the module, (c) the detailed structures and the sectional views of the three configurations of contactor module type-IV

Every time a new hollow fibre contactor module was installed, a new sequence of operation was carried out. In the laboratory condition, it is extremely difficult to regenerate the adsorbent packed inside the contactor without disassembling or destroying the module. As a result, the regeneration of exhausted adsorbent in the various types of contactor modules were not performed. Nonetheless, previous studies on the

regeneration of activated carbons showed that DMAc-loaded activated carbons can be regenerated readily.

5.3 Results and Discussion

5.3.1 Diffusion Through Hollow Fibre Walls

The results of this part of the experiment were discouraging. The breakthrough curves for the adsorption of DMAc monitored at opening no.2 of the hollow fibre module type-I at different flow rates is shown in Figure E.1 (see Appendix E). It was soon after the process started that the adsorption breakthrough occurred, indicating there was little adsorption happening inside the module and the DMAc solution essentially flowed through the hollow fibre lumens without significant adsorption uptake by the activated carbon powders.

It can be considered that the diffusion rate between the two sides of the hollow fibre walls was too low, comparing to flow rates of the liquid along the fibres. The speed of the DMAc molecules moving across the fibre walls was so slow that the DMAc removal efficiency of module type-I was trivial to for practical applications. This motivated us to look into other types of hollow fibre adsorber designs for improved performance.

5.3.2 Direct Flow Through Hollow Fibre Walls

After upgrading the module to type-II, the breakthrough curves for the removal of DMAc monitored at the opening no.3 of at different flow rates is transformed into the form shown in Figure 5.7. The shape and the trend were very similar to that of the regular packed bed column adsorptions, only the time points of the breakthroughs were significantly earlier, with the breakthrough point of 400min at the flow rate of 0.5ml/min and 220min at 1.0ml/min. In another way, the breakthrough uptakes of DMAc were much lower than the expectations for hollow fibre contactor modules, reaching

only about 20% of the comparing packed columns' uptakes at corresponding flow rates.

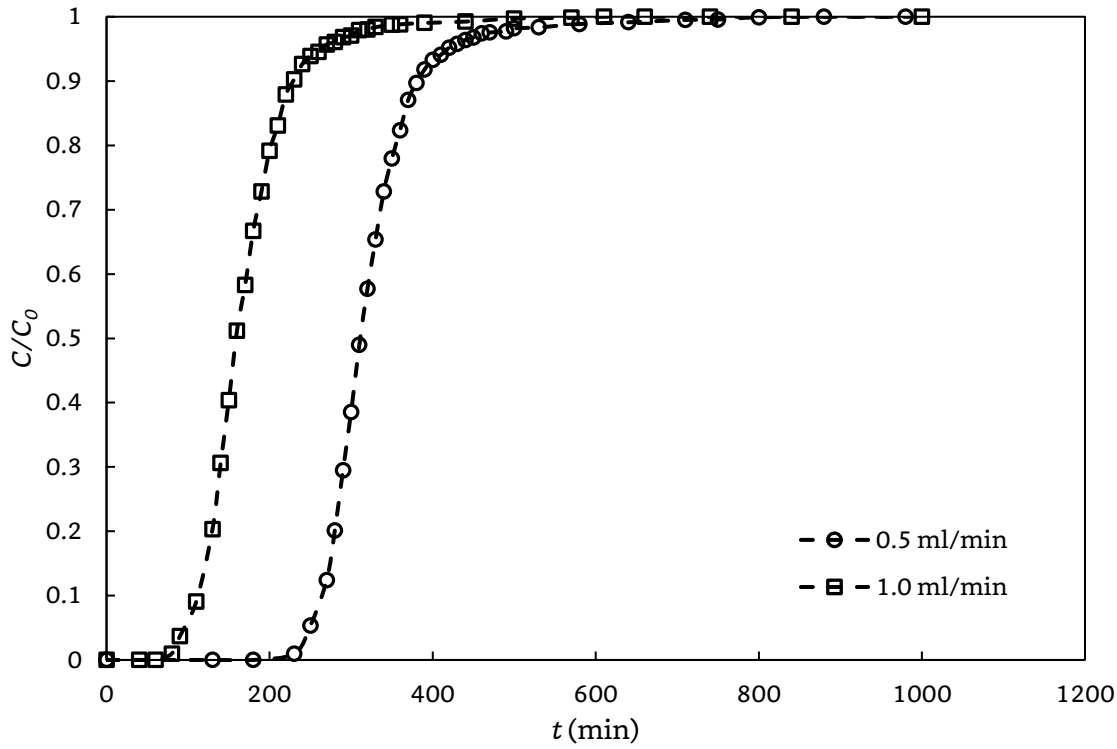

Figure 5.7 Breakthrough curves for the removal of DMAc using hollow fibre module type-II packed with *AC03* in the shell side at different flow rates

Clearly, the performance of module type-II was much better than that of the type-I, but it was still not good enough and there was room for further improvements. It is speculated that the reason for the low DMAc uptake was that the effluent exit of module type-II (opening no.3 in this case) was located at the end of the module, and the DMAc solution had to flow through the entire distance of the module if it had to directly contact the adsorbents packed near the entrance (opening no.1 in this case), which was the path of paramount resistance comparing to those packed near the exit. The liquid streams tended to flow along paths with resistance as low as possible. Consequently, the activated carbon powders packed more than 70mm away from the exit were left almost untouched, and the DMAc adsorption primarily in only the top part (around 20%, suspectedely) of all the *AC03* located around the exit. Also, for the same reason, the adsorbents

located at the opposite side of the exit contribute noticeably less than those packed at the same side with the exit.

To prove these speculations and the explanations discussed above, another set of experiments of “chalk powders and ink” was conducted to study how uniformly the liquid would contact the particles packed in the fibre model.

The entire process was captured by a time-lapse camera at one frame per minute. The whole photo sequence was analysed and re-drawn automatically by the software “Adobe Illustrator”, generating a monochromatic chronologic evolution chart (shown in Figure 5.8).

As illustrated in Figure 5.8, the module started with an all-white looking. Not before long, the black colour appeared at the adjacent areas around the exit. Then the black coloured area began to expand gradually across the module both horizontally and vertically. In local areas that were farther away from the effluent exit, the more delayed that area turned into black colour, which proved the hypothesis mentioned above that the “remote” areas were less favourable by the fluids. After 1h, the rate of the expansion of the black area began to decrease gradually. Around 1.5h since start, the black coloured area stopped expanding completely, and about 20% of the original white area turned black. This supported the speculation that only 20% of the packed powder in module type-II actually contacted with the flowing streams.

Though the “chalk dust and ink” simulation could provide a brief illustration of whether an area of the packed adsorbents was directly contacted with the fluid or not, it was yet uncertain whether that area was saturated (fully utilised for adsorption and reached a equilibrium) by just observing the colour.

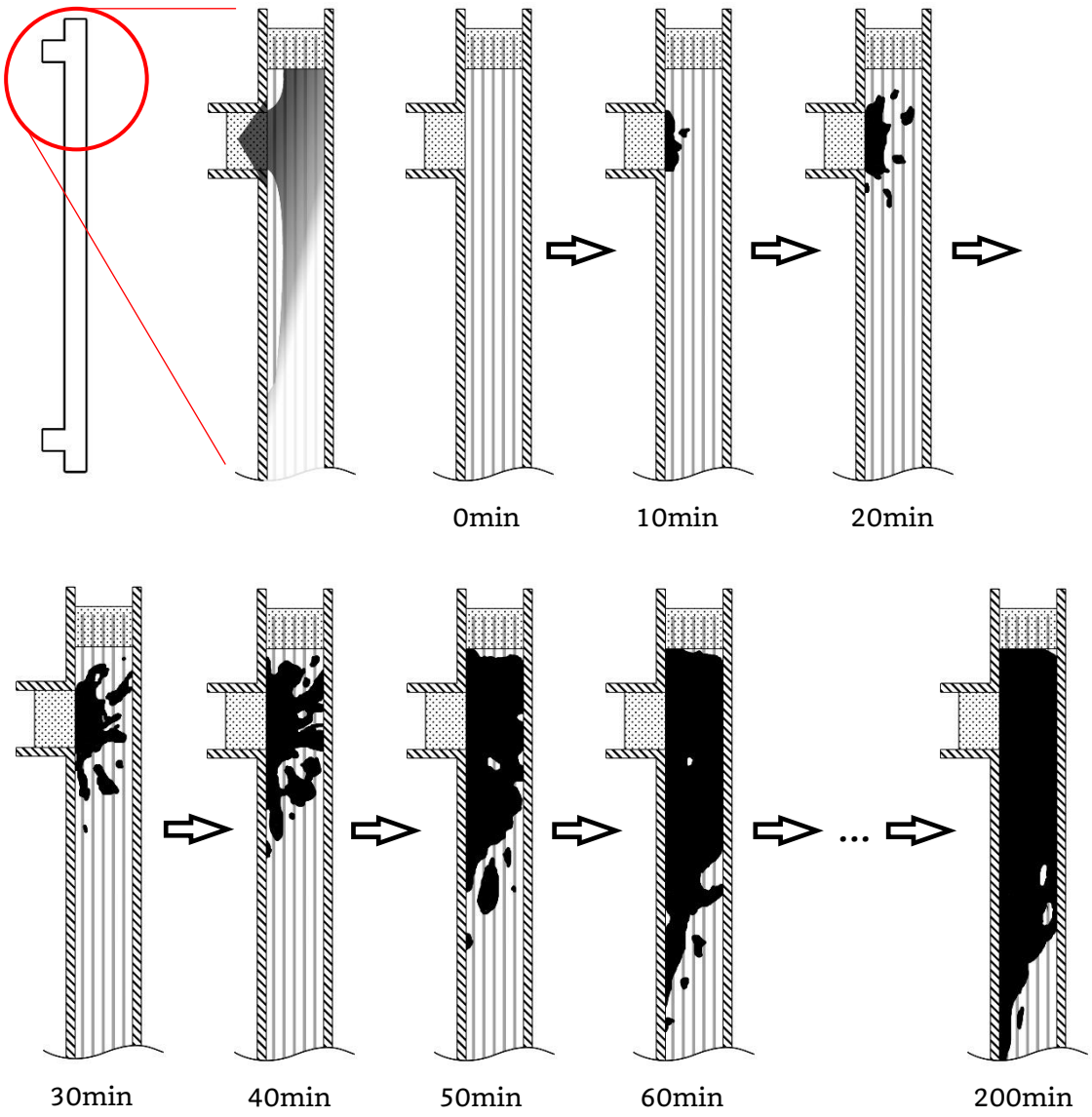

Figure 5.8 Monochromatic chronologic evolution chart showing how the ink flowed through hollow fibre module type-II packed with white chalk powders in the shell side at the flow rate of 1.0ml/min

This issue and the fact that only 20% of the adsorbents packed inside module type-II were exploited were the reasons to add more effluent exits in the module, namely module type-III in subsequent studies. According to the results of the experiment on module type-II, the breakthrough behaviour at the five effluent exits should be similar but with different time delays. The breakthrough curves for effluent exiting the five openings at an overall 1.0ml/min volumetric flow rate are shown in Figure 5.9. It is shown that the effluent leaving openings no.4-6 began to show DMAc breakthrough earlier than the DMAc breakthrough in effluent exiting opening no.5, and DMAc

breakthrough at exit no.6 occurred in the last. Clearly, this indicates that DMAc adsorption in the contactor did not occur uniformly, which is consistent with the findings in the "chalk powder-ink" contact experiments.

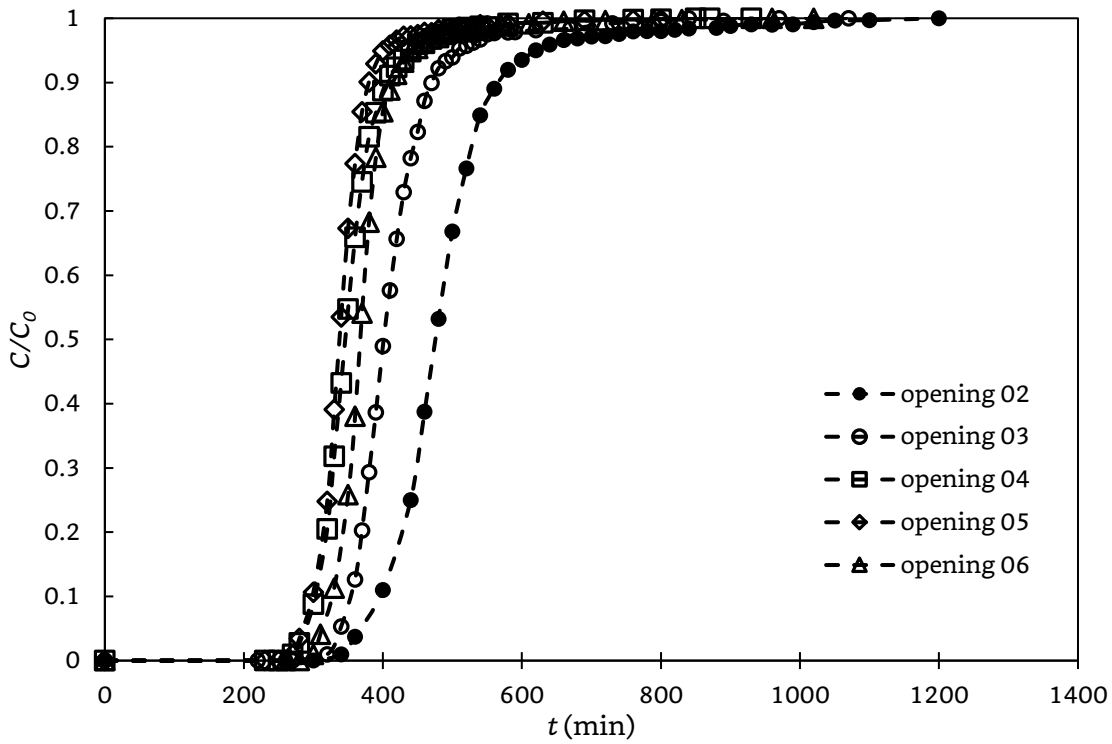

Figure 5.9 Breakthrough curves for the removal of DMAc monitored at the openings no.2, no.3, no.4, no.5 and no.6 of the hollow fibre module type-III packed with *AC03* in the shell side at the overall flow rate of 1.0ml/min

However, the total uptake at full breakthrough of the module type-III did not agree with that of the module type-II at the flow rate of 1.0ml/min. Though the exact flow rate of each individual opening was not measured or monitored (it would take tremendous efforts to do so), the total uptake of each module could be roughly calculated (using equation 4.1). The total uptake at full breakthrough of module type-III (approximately 0.07 mmol/g) was less than the five times of the uptake of type-II (approximately 0.026*5=0.13 mmol/g). They were supposed to be equal if 1/5 (obtained by the "chalk dust and ink" experiment) of the packed adsorbent inside module type-II was directly flowed through by the treated fluid. Furthermore, both type-II and III hollow fibre contactors could not achieve DMAc saturation uptakes anywhere close to that of the traditional columns packed with *AC01* (see Table 4.1 in Chapter 4), regardless the fact that *AC01* and *AC03* showed

the same potential capacity during equilibrium adsorption study (see Chapter 3).

There were three possible explanations (illustrated in Figure 5.10) to those unmatched adsorption uptakes:

- For the hollow fibre contactor modules having effluent exits on the side, it is certain that there would be a decent amount of packed adsorbent left untouched by the fluid even after a full DMAc breakthrough due to the asymmetrical structures of the module, no matter how many side openings added. It is highly likely that the amount of adsorbent that actually adsorbed DMAc near the effluent exit of module type-II is larger than the adsorbent amount near each effluent exit of module type-III, because of the lower effluent flow rate in each exit as compared to the case of type II where all effluent exited the adsorber from a single location. Near neighbouring openings, some portions of adsorbent may contact the liquid flowing towards both exits, resulting in an early exhaust of the adsorbent locally, which decreases the DMAc uptake from liquid leaving both exits.
- *AC03* is a fine powder. When the fluid flows through a densely-packed bed for a long time, fingering will occur in the packed powders and the fluid may tend to gather together into micro-channels, and the flow channelling will lead to nonuniform fluid/particle contacts, thereby lowering the DMAc adsorption efficiency.
- Once channelling occurs, the resistance to liquid flow towards an effluent exit will be remarkably reduced, and the majority of the fluid begins to take the 'short cuts' and no longer flows through the intended area of the adsorbent bed, making that part of the adsorbent be flooded but under saturated till the end, which further diminishes the overall adsorption uptake of the entire module.

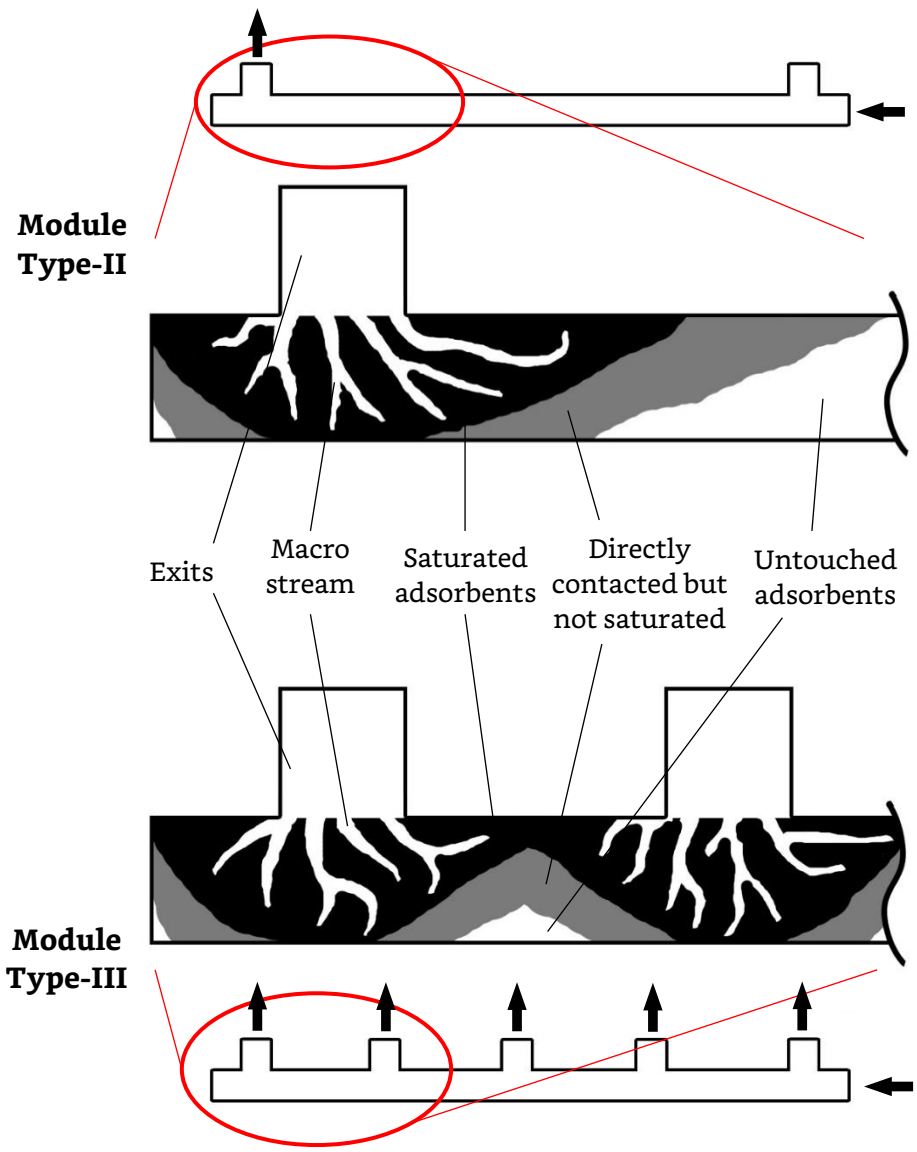

Figure 5.10 Schematics of how the fine carbon powder *AC03* packed inside the hollow fibre contactor module type-II and type-III was not fully utilised and the overall DMAc uptake was low

5.3.3 Asher Configuration

In light of the disadvantages of the former three types of HF contactor modules, Asher configuration was also tested in this project in order to achieve a high uptake. The overall structure was symmetrical, and all the hollow fibres were distributed uniformly in the module. During operation, the fluid flow patterns in each section of the module weere similar along the axial direction, no matter which type of sectional arrangement it has.

At first, three configurations of module type-IV were prepared. This part of the project also attempted to investigate whether the geometric structures of the hollow fibre arrays could notably affect the performance of a contactor. The breakthrough curves of the three configurations of module type-IVs are demonstrated in Figure 5.11.

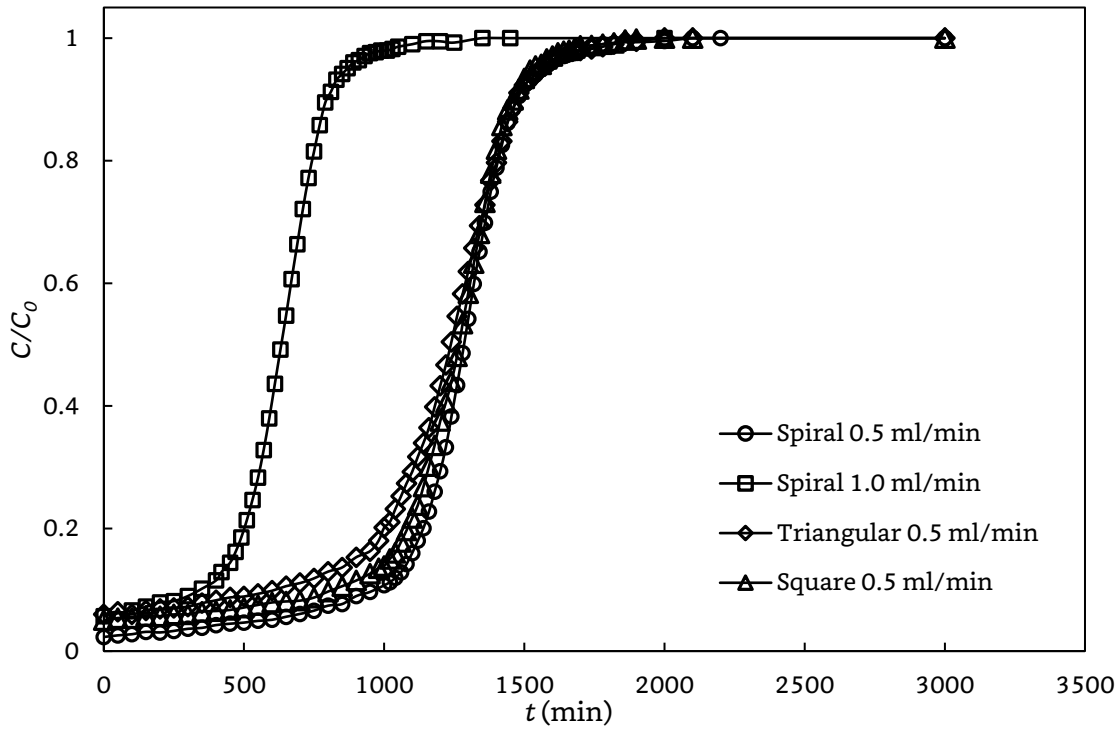

Figure 5.11 Breakthrough curves for DMAc removal using hollow fibre module type-IV (with square, triangular and spiral configuration) packed with *AC03* in the shell side at various flow rates

Using the graph, the DMAc uptakes of each run when reaching breakthrough points were calculated, which turned out to be about the same, averaging 0.135 mmol/g. The comparison of the saturation capacities of different types of contactors is presented in Table 5.2.

Table 5.1 DMAc uptakes at saturation in hollow fibre contactor modules type-II and type-III packed with *AC03* when DMAc in effluent were completely broken through, at inflow rate of 1.0ml/min

Module	Type-II	Type-III	Type-IV	Regular packed columns
Adsorbent	*AC03*	*AC03*	*AC03*	*AC01*
Flow rate (ml/min)	0.5 & 1.0	1.0	0.5 & 1.0	0.5 & 1.0
Overall uptake at complete breakthrough (mmol/g)	0.026	0.069	0.14	0.17
Equilibrium uptake in batch studies (mmol/g)	0.19			0.17

The following observations can be made based on data in Figure 5.11 and Table 5.2:

- At the beginning of each operation, no matter what fibre arrangement, the initial concentration of DMAc outflows from the module was not neglibly low, which means portions of the fluids flowed pass the module without being treated. This was because the manually packed adsorbent bed was not integrally dense and uniform, and there were some voids randomly located in the module between neighbouring hollow fibres. This would lead to some liquid streams traveling from the inlet hollow fibres to the outlet ones without contacting the activated carbon. This issue could be resolved with skilful assembly of the hollow fibre module.
- Though Table 5.2 shows that the saturation uptake of hollow fibre contactor module type-IV was noticeably larger than that obtained with a regular column studied in Chapter 4, the two uptakes should be about the same. It means the hollow fibre module type-IV in this study can be practical which can use *AC03* powders, making the type-IV packed with *AC03* the best contactor of all tested in this project, with the highest efficiency

- When operating at the flow rate of 0.5ml/min, there was little difference in breakthrough profiles among the three fibre arrangements in module type-IV, regardless of some minor inconsistencies among the curves caused by manual production and operation. In the handmade modules, not every hollow fibre was perfectly straight and parallel as designed, and the activated carbon powders may not be homogeneously densely packed.

5.4 Conclusions

In this chapter, adsorption of DMAc in various types of hollow fibre contactors packed with *AC03* powders was studied; the following conclusions can be drawn:

- There were a lot of downsides of earlier versions of hollow fibre contactor module, such as extremely low saturation capacity (uptake at full breakthrough). From type-I to type-IV, the performance of the modules was improved significantly after modifications.
- Due to the lack of precision of the modules produced, there was no significant difference of performance among the type-IV modules with three different fibre arrangements.
- The hollow fibre contactor type-IV filled with *AC03* powders showed a high saturation capacity and high adsorption efficiency, as well as a sharp breakthrough curve.

Chapter 6: General Conclusions and Recommendations

6.1 Conclusions

A thorough Batch adsorption study helped to understand the mechanism involved in the removal of DMAc from aqueous solutions by three types of activated carbons. An accurate evaluation of adsorption thermodynamics and reusability of the adsorbent helped us to see if the adsorption system is feasible or not. Dynamic adsorption studies on adsorption columns allow us to determine the breakthrough of the column. The column design parameters were evaluated based on models fit to experimental data which could be used to scale up the adsorption column. Multiple designs of the hollow fibre contactors were also experimented to seek the most efficient way to utilise the powder form of activated carbons. Based on the thesis work completed in this study, several general conclusions can be drawn.

- The adsorption of DMAc from aqueous solution onto activated carbons followed the Langmuir isotherm. The calculated free energy (ΔG) for DMAc adsorption on activated carbons suggested the adsorption was a physical process that thermo dynamic property changes [i.e., entropy (ΔS) and enthalpy (ΔH)], spontaneously and exothermically. The adsorption kinetic rate constant k_2 was independent of the adsorbate

concentration, but it was different for different types of activated carbons. The kinetic model fitting based on the pseudo-second-order model was modified to correct an oversight that has been neglected in all studies reported in the literature. The DMAc adsorbed in the carbons was desorbed effectively using ethanol, followed by evaporation under heating or vacuum. After regeneration, the activated carbon did not have any change in adsorption uptake capacity and of adsorption rate constant. Thus, these activated carbons can be reused repeatedly as adsorbents for DMAc removal.

- The activated carbons can be packed in columns for dynamic adsorption applications. The influent flow rate affected the column performance and a decrease in breakthrough time was observed with an increased flow rate. The saturated adsorption capacity of the activated carbon bed remained constant regardless of the flow rates. All the three models for dynamic adsorption in packed columns (i.e., Yoon-Nelson model, BDST model and Thomas model) were shown to fit well with the experimental data. The bed depth service time model and Thomas model, which have essentially the same basis, described the adsorption breakthrough equally well. However, when fine powders of activated carbons were used in the packed bed, the resistance to liquid flow was too high to be effective for DMAc removal from waste water.
- Thus, hollow fibre contactors were investigated in order to use powder form of activated carbons efficiently. Four types of hollow fibre adsorber designs were tested with regards to effluent withdrawn from the adsorbers. It was shown that uniform distribution of the liquid flow was critical to DMAc removal. Among the four designs, module type-IV showed the best performance

6.2 Recommendations for Future Studies

Activated carbons have already been used in the field of medical, environmental and chemical industries. The present research is an expansion of using them as a potential adsorbent for DMAc removal from wastewater. The followings are recommended for future studies:

- Competitive adsorption of multiple solute components. When wastewater contains multiple tertiary pollutants, the interactions between these solute components may influence the uptake of individual pollutant on the carbon. The effects of the interactions between the various compounds on the adsorption characteristics of an individual component should be studied to get a full picture of wastewater treatment with activated carbons.
- DMAc recovery. In this study, the carbon adsorbents loaded with DMAc were recovered but the DMAc ended up in the desorbent, which was ethanol in this case. Additional separation should be required to process those wastes (e.g., distillation) so that ethanol could be reused in the adsorbent regeneration.
- During the column adsorption study, only the influence of the flow rate was inspected. The effect of the influent DMAc concentration on the dynamic adsorption behaviour should be investigated as well.
- Besides the three types of activated carbons (made from bamboos) used in this project, there are a great variety activated carbons available. The raw materials used to produce activated carbons and the shape them are expected to affect the adsorption in properties and characteristics. It is thus desirable to screen a variety of the activated carbons for the target application.
- No significant difference among the adsorption behaviour of of the hollow fibre contactor modules filled with the activated carbon powders was observed when the hollow fibres were arranged in

different fashion (e.g., square, triangular, spiral). Additional work is needed to confirm whether this is still valid for larger scale modules.

- The properties of the hollow fibres (e.g., diameters, wall thickness) should also be investigated for optimal design of fibre-modulated adsorbers filled with powder form of adsorbents.

References

[1] activated carbons Compound Database. National Center for Biotechnology Information.

[2] Alt, C., Ullmann's Encyclopedia of Industrial Chemistry. vol: 2006.

[3] Silvia, M.; Vincenzo, L.; Arturo, M.; Giovanni, G. P., Microsomal metabolism of N,N-diethylacetamide and N,N-dimethylacetamide and their effects on drug-metabolizing enzymes of rat liver. *Biochemical Pharmacology* **1994**, 48 (4), 717-726.

[4] Yokozeki, A., Theoretical performances of various refrigerant–absorbent pairs in a vapor-absorption refrigeration cycle by the use of equations of state. *Applied Energy* **2005**, 80 (4), 383-399.

[5] Opinion of the committee for risk assessment on a dossier proposing harmonised classification and labelling at EU level of DMAc. (ECHA), European Chemical Agency. Helsinki, Finland, **2014**; Vol. (EC) No 1272/2014, p 6.

[6] Nomiyama, T.; Omae, K.; Ishizuka, C.; Yamauchi, T.; Kawasumi, Y.; Yamada, K.; Endoh, H.; Sakurai, H., Dermal absorption of N,N-dimethylacetamide in human volunteers. *International Archives of Occupational and Environmental Health* **2000**, 73 (2), 121-126.

[7] Barnes, J. R.; Ranta, K. E., The metabolism of dimethylformamide and dimethylacetamide. *Toxicology and Applied Pharmacology* **1972**, 23 (2), 271-276.

[8] Luo, Y.; Guo, W.; Ngo, H. H.; Nghiem, L. D.; Hai, F. I.; Zhang, J.; Liang, S.; Wang, X. C., A review on the occurrence of micropollutants in the aquatic environment and their fate and removal during wastewater treatment. *Science of the Total Environment* **2014**, 473, 619-641.

[9] Salleh, M. A. M.; Mahmoud, D. K.; Karim, W. A. W. A.; Idris, A., Cationic and anionic dye adsorption by agricultural solid wastes: A comprehensive review. *Desalination* **2011**, 280 (1), 1-13.

[10] Xu, P.; Zeng, G. M.; Huang, D. L.; Feng, C. L.; Hu, S.; Zhao, M. H.; Lai, C.; Wei, Z.; Huang, C.; Xie, G. X., Use of iron oxide nanomaterials in wastewater treatment: a review. *Science of the Total Environment* **2012**, 424, 1-10.

[11] Noll, K. E., Adsorption technology for air and water pollution control. CRC Press: 1991.

[12] Yagub, M. T.; Sen, T. K.; Afroze, S.; Ang, H. M., Dye and its removal from aqueous solution by adsorption: a review. *Advances in Colloid and Interface Science* **2014**, 209, 172-184.

[13] Bansal, R. C.; Goyal, M., Activated Carbon Adsorption. CRC press: 2005.

[14] Mezohegyi, G.; van der Zee, F. P.; Font, J.; Fortuny, A.; Fabregat, A., Towards advanced aqueous dye removal processes: a short review on the versatile role of activated carbon. *Journal of Environmental Management* **2012**, 102, 148-164.

[15] Weber, W. J.; Morris, J. C., Kinetics of adsorption on carbon from solution. *Journal of the Sanitary Engineering Division* **1963**, 89 (2), 31-60.

[16] Wu, F.-C.; Tseng, R.-L.; Juang, R.-S., Initial behavior of intraparticle diffusion model used in the description of adsorption kinetics. *Chemical Engineering Journal* **2009**, 153 (1), 1-8.

[17] Spahn, H.; Schlünder, E., The scale-up of activated carbon columns for water purification, based on results from batch tests—I: Theoretical and experimental determination of adsorption rates of single organic solutes in batch tests. *Chemical Engineering Science* **1975**, 30 (5), 529-537.

[18] Hong, Z.; JinYuan, J.; YueXi, Z.; XueMin, C., Adsorption and photodegradation of N,N-dimethylacetamide on suspended sediment particles in water. *Research of Environmental Sciences* **2009**, 22 (8), 902-906.

[19] Han, R.; Wang, Y.; Zhao, X.; Wang, Y.; Xie, F.; Cheng, J.; Tang, M., Adsorption of methylene blue by phoenix tree leaf powder in a fixed-bed column: experiments and prediction of breakthrough curves. *Desalination* **2009**, 245 (1), 284-297.

[20] Zhang, W.; Dong, L.; Yan, H.; Li, H.; Jiang, Z.; Kan, X.; Yang, H.; Li, A.; Cheng, R., Removal of methylene blue from aqueous solutions by straw based adsorbent in a fixed-bed column. *Chemical Engineering Journal* **2011**, 173 (2), 429-436.

[21] Li, Y.; Du, Q.; Liu, T.; Peng, X.; Wang, J.; Sun, J.; Wang, Y.; Wu, S.; Wang, Z.; Xia, Y., Comparative study of methylene blue dye adsorption onto

activated carbon, graphene oxide, and carbon nanotubes. *Chemical Engineering Research and Design* **2013**, 91 (2), 361-368.

[22] Leenheer, J.; Noyes, T. A filtration and column-adsorption system for onsite concentration and fractionation of organic substances from large volumes of water; United States Government Publication Office (USGPO): 1984.

[23] Shafeeyan, M. S.; Daud, W. M. A. W.; Shamiri, A., A review of mathematical modeling of fixed-bed columns for carbon dioxide adsorption. *Chemical Engineering Research and Design* **2014**, 92 (5), 961-988.

[24] Li, A.; Zhang, Q.; Zhang, G.; Chen, J.; Fei, Z.; Liu, F., Adsorption of phenolic compounds from aqueous solutions by a water-compatible hypercrosslinked polymeric adsorbent. *Chemosphere* **2002**, 47 (9), 981-989.

[25] Worch, E., Fixed-bed adsorption in drinking water treatment: a critical review on models and parameter estimation. *Journal of Water Supply: Research and Technology-Aqua* **2008**, 57 (3), 171-183.

[26] Thomas, H. C., Heterogeneous ion exchange in a flowing system. *Journal of the American Chemical Society* **1944**, 66 (10), 1664-1666.

[27] Wolborska, A., Adsorption on activated carbon of p-nitrophenol from aqueous solution. *Water Research* **1989**, 23 (1), 85-91.

[28] Schneider, R.; Cavalin, C.; Barros, M.; Tavares, C., Adsorption of chromium ions in activated carbon. *Chemical Engineering Journal* **2007**, 132 (1), 355-362.

[29] Bohart, G.; Adams, E., Some aspects of the behavior of charcoal with respect to chlorine. 1. *Journal of the American Chemical Society* **1920**, 42 (3), 523-544.

[30] Hutchins, R., New method simplifies design of activated-carbon systems. *Chemical Engineering* **1973**, 80 (19), 133-138.

[31] Yoon, Y. H.; NELSON, J. H., Application of gas adsorption kinetics I. A theoretical model for respirator cartridge service life. *The American Industrial Hygiene Association Journal* **1984**, 45 (8), 509-516.

[32] Lively, R. P.; Chance, R. R.; Kelley, B.; Deckman, H. W.; Drese, J. H.; Jones, C. W.; Koros, W. J., Hollow fiber adsorbents for CO2 removal from flue gas. *Industrial & Engineering Chemistry Research* **2009**, 48 (15), 7314-7324.

[33] Prasad, R.; Sirkar, K., Dispersion - free solvent extraction with microporous hollow - fiber modules. *AIChE journal* **1988**, 34 (2), 177-188.

[34] Labreche, Y.; Fan, Y.; Lively, R.; Jones, C. W.; Koros, W. J., Direct dual layer spinning of aminosilica/Torlon? hollow fiber sorbents with a lumen layer for CO2 separation by rapid temperature swing adsorption. *Journal of Applied Polymer Science* **2015**, 132 (17).

[35] Wickramasinghe, S.; Semmens, M. J.; Cussler, E., Mass transfer in various hollow fiber geometries. *Journal of Membrane Science* **1992**, 69 (3), 235-250.

[36] Gabelman, A.; Hwang, S.-T., Hollow fiber membrane contactors. *Journal of Membrane Science* **1999**, 159 (1), 61-106.

[37] Yang, M. C.; Cussler, E., Designing hollow - fiber contactors. *AIChE Journal* **1986**, 32 (11), 1910-1916.

[38] Feng, X.; Ivory, J., Hollow fiber and spiral wound contactors for fluid/particle contact and interaction. *Chemical Engineering Communications* **2002**, 189 (2), 247-267.

[39] Cunha, G. d. C.; Rom?o, L.; Santos, M.; Araújo, B.; Navickiene, S.; De Pádua, V., Adsorption of trihalomethanes by humin: Batch and fixed bed column studies. *Bioresource Technology* **2010**, 101 (10), 3345-3354.

[40] Bunluesin, S.; Kruatrachue, M.; Pokethitiyook, P.; Upatham, S.; Lanza, G. R., Batch and continuous packed column studies of cadmium biosorption by Hydrilla verticillata biomass. *Journal of Bioscience and Bioengineering* **2007**, 103 (6), 509-513.

[41] Liu, Y., Is the free energy change of adsorption correctly calculated? *Journal of Chemical & Engineering Data* **2009**, 54 (7), 1981-1985.

[42] Ho, Y.-S.; McKay, G., Sorption of dye from aqueous solution by peat. *Chemical Engineering Journal* **1998**, 70 (2), 115-124.

[43] Hameed, B.; Din, A. M.; Ahmad, A., Adsorption of methylene blue onto bamboo-based activated carbon: kinetics and equilibrium studies. *Journal of Hazardous Materials* **2007**, 141 (3), 819-825.

[44] Mittal, A.; Jhare, D.; Mittal, J., Adsorption of hazardous dye Eosin Yellow from aqueous solution onto waste material De-oiled Soya: Isotherm, kinetics and bulk removal. *Journal of Molecular Liquids* **2013**, 179, 133-140.

[45] Langmuir, I., The adsorption of gases on plane surfaces of glass, mica and platinum. *Journal of the American Chemical Society* **1918**, 40 (9), 1361-1403.

[46] Graham, D., The characterization of physical adsorption systems. I. The equilibrium function and standard free energy of adsorption. *The journal of Physical Chemistry* **1953**, 57 (7), 665-669.

[47] Annadurai, G.; Juang, R.-S.; Lee, D.-J., Use of cellulose-based wastes for adsorption of dyes from aqueous solutions. *Journal of Hazardous Materials* **2002**, 92 (3), 263-274.

[48] Moreno-Castilla, C., Adsorption of organic molecules from aqueous solutions on carbon materials. *Carbon* **2004**, 42 (1), 83-94.

[49] Yang, R. T., Gas separation by adsorption processes. Butterworth-Heinemann: 2013.

[50] Manning, G. S., Limiting laws and counterion condensation in polyelectrolyte solutions I. Colligative properties. *The Journal of Chemical Physics* **1969**, 51 (3), 924-933.

[51] AmiN,N. K., Removal of reactive dye from aqueous solutions by adsorption onto activated carbons prepared from sugarcane bagasse pith. *Desalination* **2008**, 223 (1), 152-161.

[52] Vidali, G.; Ihm, G.; Kim, H.-Y.; Cole, M. W., Potentials of physical adsorption. *Surface Science Reports* **1991**, 12 (4), 135-181.

[53] Freundlich, H.; Hatfield, H. S., Colloid and capillary chemistry. 1926.

[54] Qiu, H.; Lv, L.; Pan, B.-c.; Zhang, Q.-j.; Zhang, W.-m.; Zhang, Q.-x., Critical review in adsorption kinetic models. *Journal of Zhejiang University Science A* **2009**, 10 (5), 716-724.

[55] Taylor, H. S., The activation energy of adsorption processes. *Journal of the American Chemical Society* **1931**, 53 (2), 578-597.

[56] Ho, Y.-S., Review of second-order models for adsorption systems. *Journal of hazardous materials* **2006**, 136 (3), 681-689.

[57] Malik, P., Dye removal from wastewater using activated carbon developed from sawdust: adsorption equilibrium and kinetics. *Journal of Hazardous Materials* **2004**, 113 (1), 81-88.

[58] Kavitha, D.; Namasivayam, C., Experimental and kinetic studies on methylene blue adsorption by coir pith carbon. *Bioresource Technology* **2007**, 98 (1), 14-21.

[59] Tanthapanichakoon, W.; Ariyadejwanich, P.; Japthong, P.; Nakagawa, K.; Mukai, S.; Tamon, H., Adsorption–desorption characteristics of phenol and reactive dyes from aqueous solution on mesoporous activated carbon prepared from waste tires. *Water Research* **2005**, 39 (7), 1347-1353.

[60] Suzuki, M., Role of adsorption in water environment processes. *Water Science and Technology* **1997**, 35 (7), 1-11.

[61] Xu, X.; Gao, B.; Wang, W.; Yue, Q.; Wang, Y.; Ni, S., Adsorption of phosphate from aqueous solutions onto modified wheat residue: characteristics, kinetic and column studies. *Colloids and Surfaces B: Biointerfaces* **2009**, 70 (1), 46-52.

[62] Pushnov, A., Calculation of average bed porosity. *Chemical and Petroleum Engineering* **2006**, 42 (1-2), 14-17.

[63] Ahmad, A.; Hameed, B., Fixed-bed adsorption of reactive azo dye onto granular activated carbon prepared from waste. *Journal of Hazardous Materials* **2010**, 175 (1), 298-303.

[64] Pan, C. Y.; McMinis, C. W., Hollow fiber bundle element. US Patents: 1992.

[65] Asher, W. J., Hollow fiber contactor and process. US Patents: 1997.

Appendix A

TOC calibration line for DMAc concentration

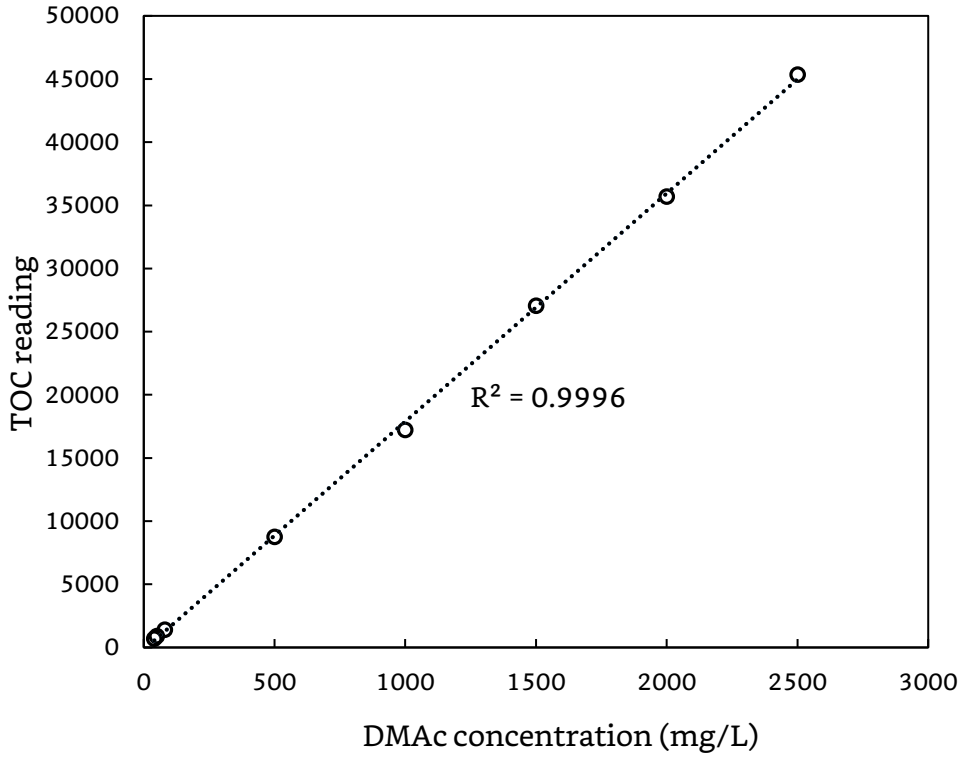

Figure A.1 Calibration curve used to determine DMAc concentration in water

Appendix B

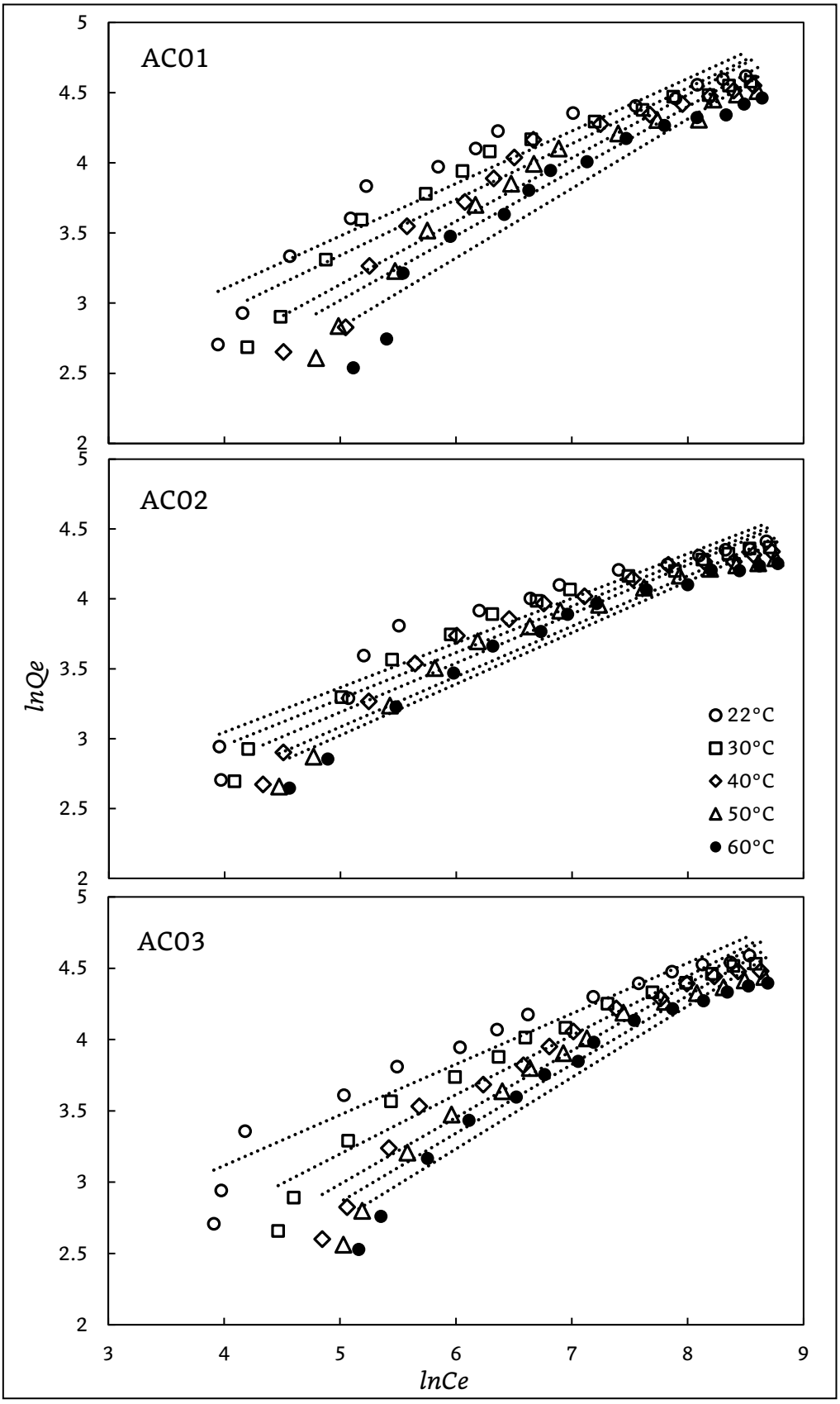

Figure B.1 Data fitting with the linearized form of the Freundlich equilibrium adsorption model for DMAc adsorption on *AC01*, *AC02* and *AC03* at different temperatures

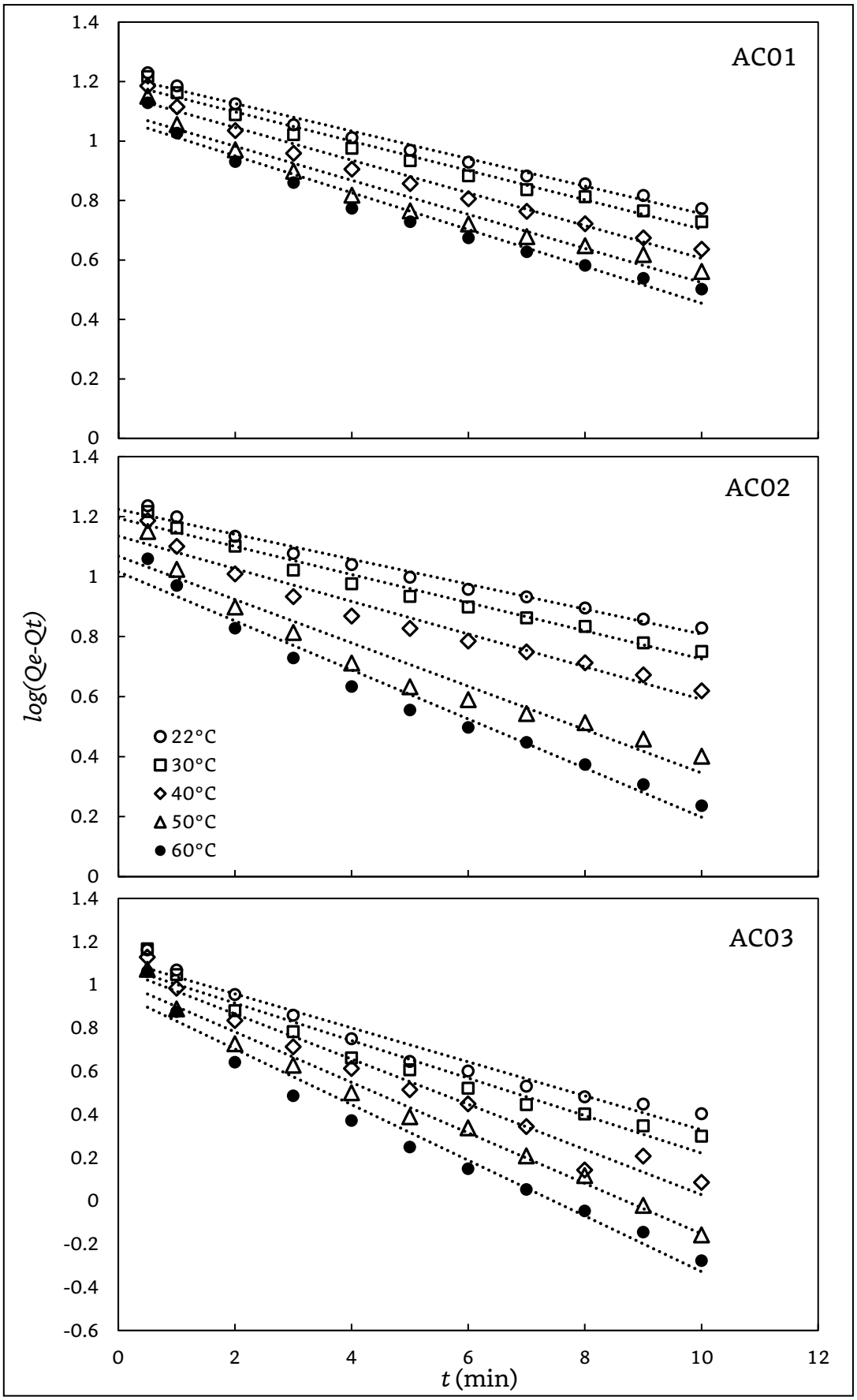

Figure B.2 Data fitting with the linearized form of the pseudo-first order kinetic model for DMAc adsorption on *AC01*, *AC02* and *AC03* at different temperatures

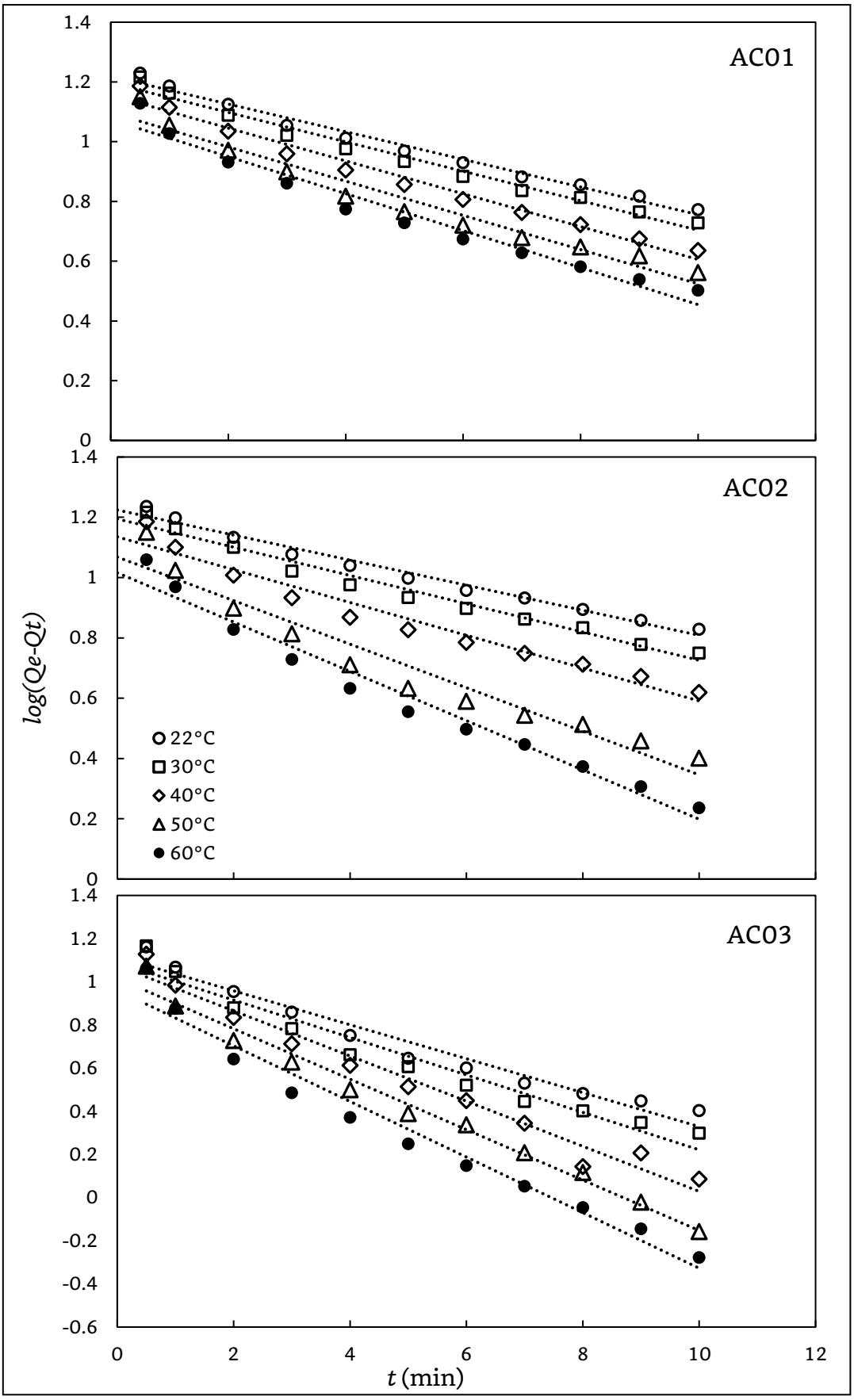

Figure B.3 Data fitted to the linear form of the intraparticle diffusion kinetic model for DMAc adsorption on *AC01*, *AC02* and *AC03* at different temperatures

Table B.1 Correlation coefficients R^2 of the fitting kinetic experimental data with the pseudo-first order model

	R^2				
	Operating Temperature				
Adsorbent	20°C	30°C	40°C	50°C	60°C
AC01	0.984	0.979	0.976	0.954	0.961
AC02	0.981	0.974	0.956	0.940	0.972
AC03	0.959	0.951	0.97	0.980	0.967

Table B.2 Correlation coefficients R^2 of the fitting kinetic experimental data with the intraparticle diffusion model

	R^2				
	Operating Temperature				
Adsorbent	20°C	30°C	40°C	50°C	60°C
AC01	0.929	0.914	0.894	0.851	0.849
AC02	0.991	0.981	0.952	0.911	0.940
AC03	0.927	0.886	0.891	0.873	0.810

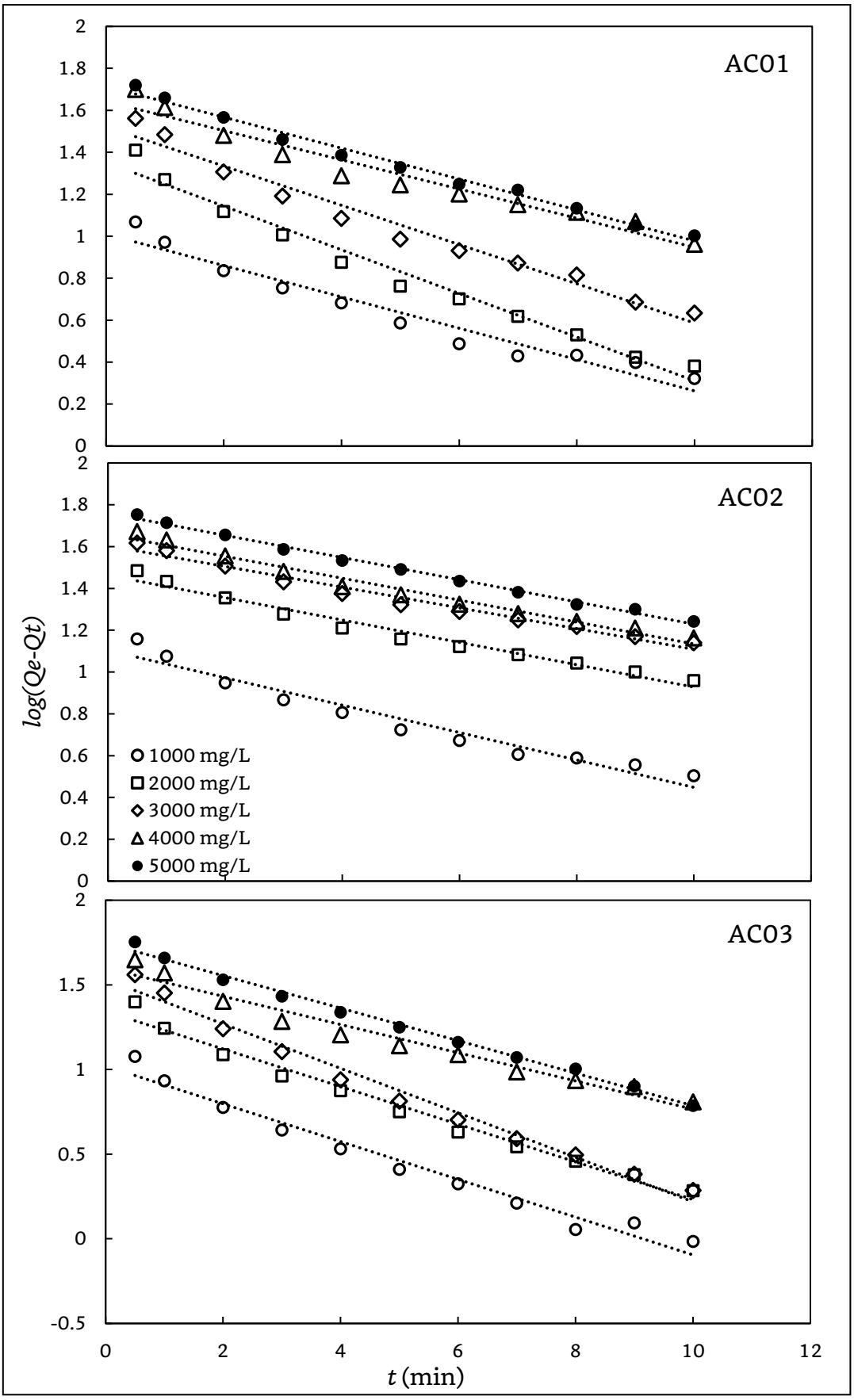

Figure B.4 Data fitting with the linearized form of the pseudo-first order kinetic model for *AC01*, *AC02* and *AC03* adsorbing DMAc solution of different initial concentrations at 40°C

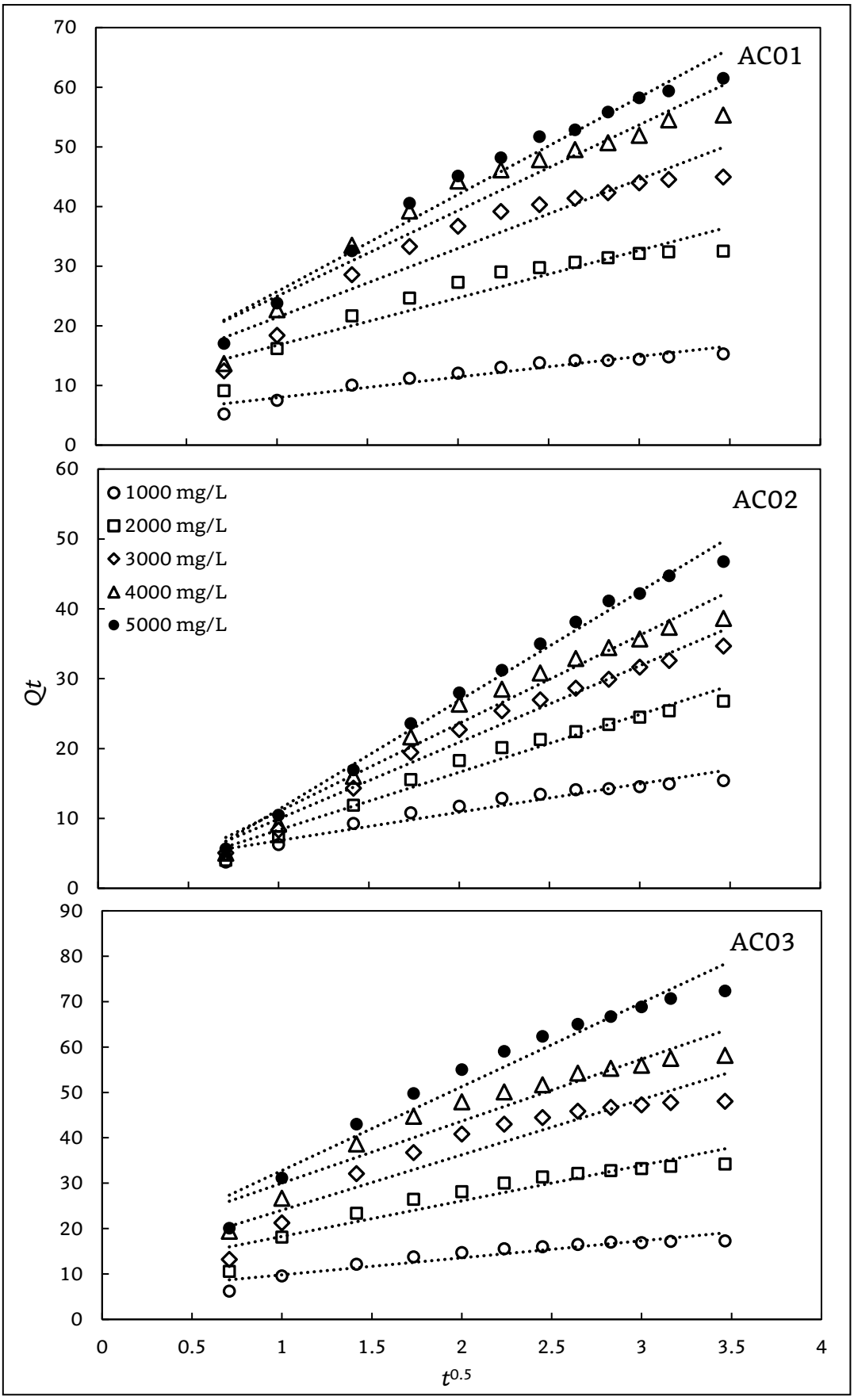

Figure B.5 Data fitting with the linearized form of the intraparticle diffusion kinetic model for *AC01*, *AC02* and *AC03* adsorbing DMAc solution of different initial concentrations at 40°C

Table B.3 Correlation coefficients R^2 of the fitting kinetic experimental data with the pseudo-first order model

	R^2				
	Initial DMAc Concentration (mg/L)				
Adsorbent	1000	2000	3000	4000	5000
AC01	0.949	0.975	0.971	0.950	0.982
AC02	0.951	0.973	0.977	0.976	0.995
AC03	0.971	0.981	0.988	0.964	0.993

Table B.4 Correlation coefficients R^2 of the fitting kinetic experimental data with the intraparticle diffusion model

	R^2				
	Initial DMAc Concentration (mg/L)				
Adsorbent	1000	2000	3000	4000	5000
AC01	0.922	0.886	0.905	0.921	0.970
AC02	0.928	0.971	0.978	0.972	0.991
AC03	0.882	0.887	0.876	0.908	0.950

Appendix C

Table C.1 Checklist of the coefficients for calculating superficial velocity ε in packed bed column operations [62]

Shape of granules	Coefficients*		
	A	*B*	*n*
Spheres	1.0	0.375	2
Cylinders	0.9198	0.3414	2
Lumps of irregulars	1.5	0.35	1
Rashing rings	0.349	0.5293	1
* The values are for uncharged granules only			

The Matlab® software code for fitting the experimental kinetic data with equation 3.30

File 01 "SolveODEL.m":

```
%% Estimating Coefficients of ODEs to Fit Given Experimental Data
clear all
clc
clf

filename = 'data_C.xlsx';
data = xlsread(filename);
dataGroup = 1; % dataGroup could be any number, corresponding to
the experimental results
K2_0 = 0.000001; % guess of initial value of K2
Q_0 = 0.00000001; % guess of initial value of Q

exp_t = data(α:β,1); % α and β are the starting and ending data roll
number of the selected period
exp_Q = data(α:β, γ); % γ is the corresponding data sequence number
const = data(δ:ε, γ); % δ and ε are the starting and ending roll number
of the preliminary constants that are already known
Qm = const(1);
Kl = const(2);
C0 = const(3);
```

```
M = const(4);
V = const(5);

options1 = optimset('TolX', 1e-8);
K2_estimate = fminsearch(@(K2)odefitL(exp_t, exp_Q, K2, const,
Q_0), K2_0, options1);

%% Data comparison
K2 = K2_estimate;
t = linspace(0, max(exp_t), 50);
odefun = @(t, Q) K2 * (Qm*Kl*(C0-Q*M/V)/(1+Kl*(C0-Q*M/V)) - Q)^2;
options2 = odeset('RelTol',1e-9);
[t, Q] = ode113(odefun, t, Q_0, options2);
figure(1)
plot(t, Q, 'r-', exp_t, exp_Q, 'b+-')
xlabel('t (s)');
ylabel('Q (mg/g)');
legend('Estimated results', 'Experimental results',
'Location','northwest')
```

File 02 “odefitL.m”:

```
function err = odefitL(exp_t, exp_Q, K2, const, Q_0)

Qm = const(1);
Kl = const(2);
C0 = const(3);
M = const(4);
V = const(5);
odefun = @(t, Q) K2 * (Qm*Kl*(C0-Q*M/V)/(1+Kl*(C0-Q*M/V)) -
Q)^2;
options = odeset('RelTol',1e-6);
[t, Q] = ode113(odefun, exp_t, Q_0, options);
err = sum((Q - exp_Q).^2);      % compute error between
experimental Q and fitted Q
end
```

Appendix D

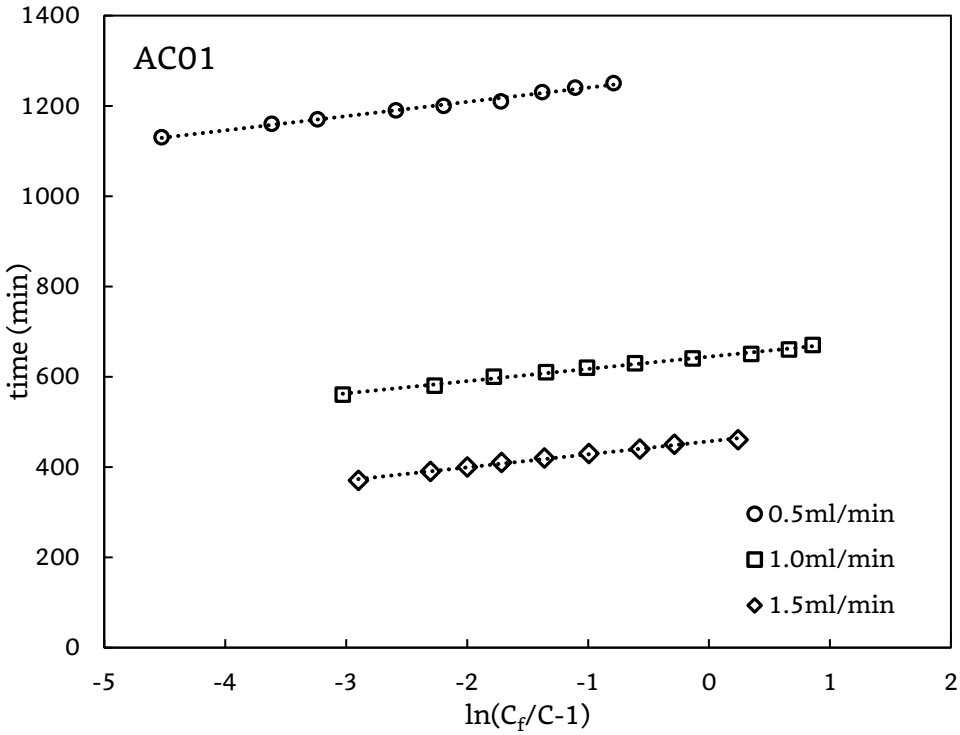

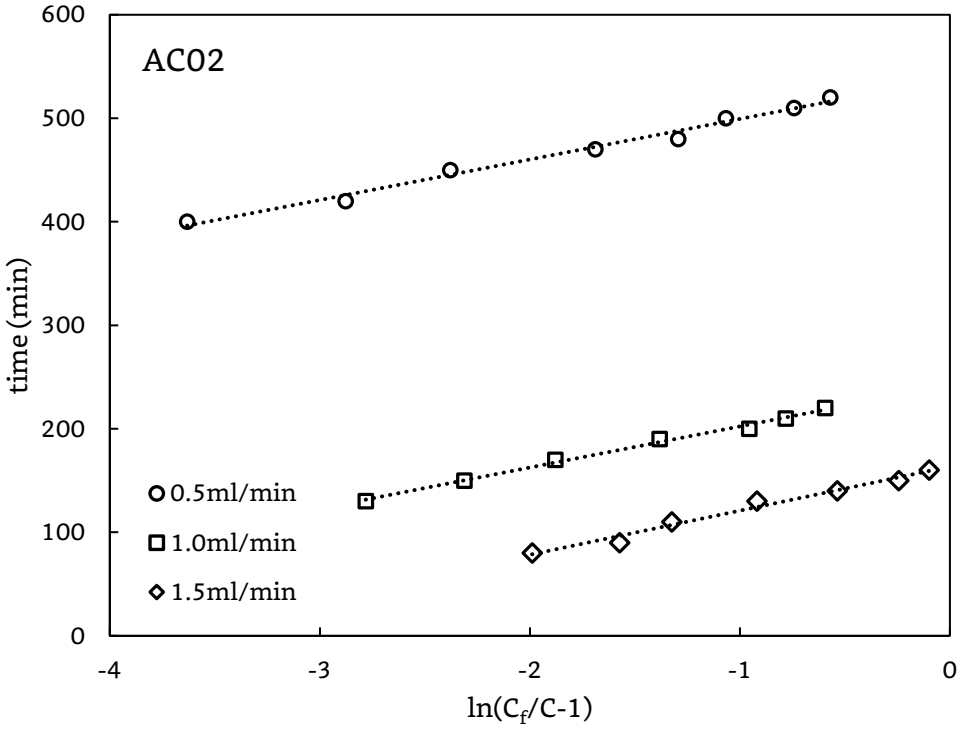

Figure D.1 Breakthrough data fitting to BDST model for removing DMAc from effluent exiting the packed bed columns of *AC01* and *AC02* at different flow rates

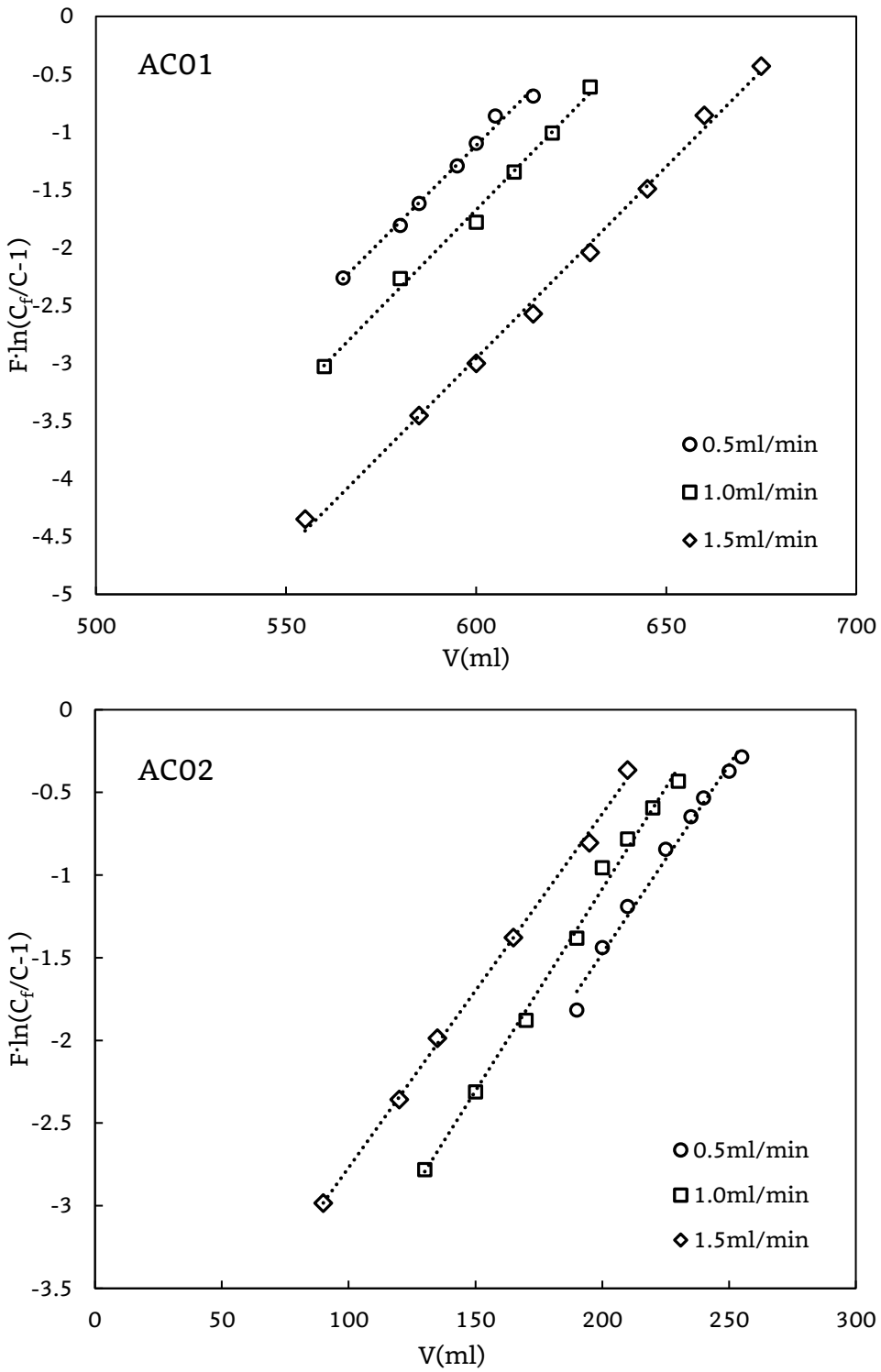

Figure D.2 Breakthrough data fitting to Thomas model for removing DMAc from effluent exiting the packed bed columns of *AC01* and *AC02* at different flow rates.

Appendix E

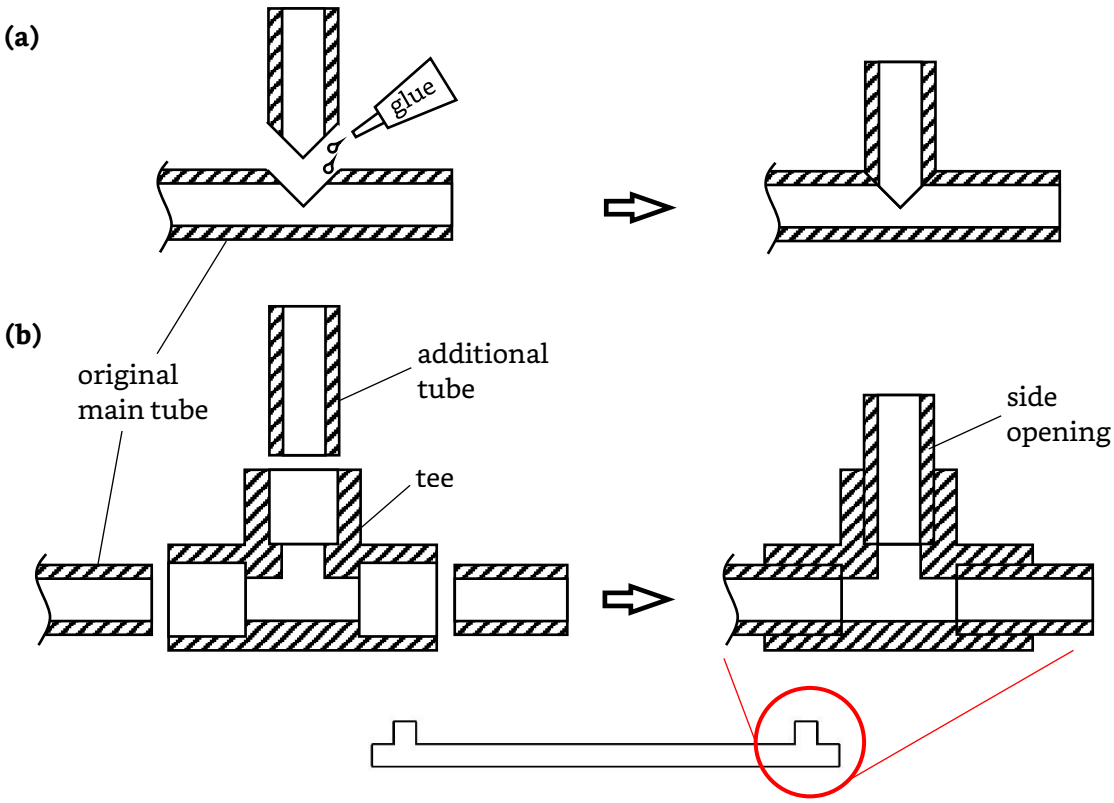

Figure E.1 Illustration of how the hollow fibre contactor modules were constructed, (a) using adhesives, (b) using tees.